AD-A251 949

NASA CONTRACTOR REPORT 189131

# SPACE STORABLE

# ROCKET TECHNOLOGY PROGRAM

# SSRT

FINAL REPORT - BASIC PROGRAM

MAY 12, 1992

Prepared by:
M.L. Chazen, T. Mueller, A.R. Casillas, D. Huang
TRW Applied Technology Division
Redondo Beach, California 90278

**NASA**

National Aeronautics and
Space Administration

92-14861

NASA CONTRACTOR REPORT 189131

# SPACE STORABLE

# ROCKET TECHNOLOGY PROGRAM

# SSRT

FINAL REPORT – BASIC PROGRAM

MAY 12, 1992

Prepared by:
M.L. Chazen, T. Mueller, A.R. Casillas, D. Huang
TRW Applied Technology Division
Redondo Beach, California 90278

Prepared for:
NASA–LeRC
Cleveland, Ohio 44135
Contract NAS 3–26246

**NASA**

National Aeronautics and
Space Administration

92-14778

NASA CONTRACTOR REPORT 189131

# SPACE STORABLE

# ROCKET TECHNOLOGY PROGRAM

# SSRT

## FINAL REPORT – BASIC PROGRAM

## MAY 1992

Prepared for:
NASA–LeRC
Cleveland, Ohio 44135
Contract NAS 3–26246

Prepared by:
M.L. Chazen, T. Mueller, A.R. Casillas, D. Huang
TRW Applied Technology Division
Redondo Beach, California 90278

Approval:

*Melvin L. Chazen*

Melvin Chazen
Program Manager

*Albert Solbes*

Albert Solbes, Manager
Combustion and Energy Technology Department

# TABLE OF CONTENTS

# LIST OF TABLES

# LIST OF FIGURES

## ABSTRACT

The Space Storable Rocket Technology Program (SSRT) was conducted for NASA-LeRC by TRW to establish a technology base for a new class of high performance and long-life bipropellant engines using space storable propellants. The results of the initial phase of this systematic multi-year program are described. Task 1 evaluated several characteristics for a number of fuels to determine the best space storable fuel for use with $LO_2$. The results of this task indicated that $LO_2$-$N_2H_4$ is the best propellant combination and provides the maximum mission/system capability-maximum payload into GEO of satellites. Task 2, Preliminary Design, developed two models-performance and thermal. The performance model indicated the performance goal of specific impulse $\geq$ 340 seconds ($\epsilon$ = 204) could be achieved. The thermal model was developed and anchored to hot fire test data. Task 3, Exploratory Test, consisted of design, fabrication and testing of a 200 lbf thrust test engine operating at a chamber pressure of 200 psia using $LO_2$-$N_2H_4$. A total of 76 hot fire tests were conducted demonstrating performance > 340 seconds ($\epsilon$ = 204) which is a 25 second specific impulse improvement over the existing highest performance flight apogee type engines.

# 1.0 SUMMARY

The Space Storable Rocket Technology (SSRT) Basic Program was initiated in mid February 1991 and completed on schedule in mid October 1991. The program was very successful in achieving its overall objectives.

The Applications Evaluation task (Task 1) evaluated several characteristics for a number of fuels to determine the best space storable fuel for use with $LO_2$ oxidizer. These evaluation factors included mission usage, propulsion system configuration and space storable fuel properties to achieve payload maximization. The evaluation task also established preliminary system and engine requirements. The maximum mission potential usage for the Space Storable engine is placement into GEO of NASA, military and commercial communication, surveillance, tracking, earth observation and meteorological satellites. The system analyses and fuels evaluation indicated that $LO_2$-$N_2H_4$ is the best propellant combination and provides the maximum mission/system capability-maximum payload into GEO. The nominal engine design based on preliminary system/engine requirements is presented as follows:

| | |
|---|---|
| Propellants | $LO_2$-$N_2H_4$ |
| Thrust ($F_\infty$) | 200 lbf |
| Chamber Pressure ($P_C$) | 200 psia |
| Specific Impulse ($Isp_\infty$) | 340 lbf-sec/lbm |

The Preliminary Design task (Task 2) developed a performance model which indicated the performance goal could be achieved. A thermal model was developed and anchored to the test data obtained in the Exploratory Test task so it would be a useful tool. The thermal model indicated that additional injector dome cooling is required to operate for long duration at high engine performance. Therefore, overall engine dome concepts have been identified which will be evaluated in Option 1.

The Exploratory Test task (Task 3) consisted of design, manufacturing, testing and analysis of the test data. Two series of tests were conducted evaluating six configurations indicating high performance could be attained. A total of 76 tests was conducted. Performance of 95% $C^*$ which projects to > 340 lbf-sec/lbm vacuum specific impulse ($\epsilon = 204$) was achieved with thermal characteristics indicating that operation with a columbium thrust chamber is feasible. The use of a rhenium thrust chamber is another alternative which would allow performance approaching 350 lbf-sec/lbm.

1

## 2.0  INTRODUCTION

The increasingly demanding spacecraft missions and their associated requirements for increased payloads over the last 30 years have been successfully achieved by the steadily improving capabilities of spacecraft propulsion systems. These systems have used earth storable propellants, principally either hydrazine as a monopropellant or nitrogen tetroxide/amine fuels as bipropellant.  The technology level of these propellants and their systems have been repeatedly improved as mission demands have grown.

Space storable propellant usage offers the advantage of using higher performance propellants to achieve increased payload weight into orbit.  The results of TRW studies are in concert with NASA-LeRC's conclusion that liquid oxygen ($LO_2$) is the best space storable oxidizer.  The space storable fuels are defined as those fuels that can be passively stored, within mission constraints, without active cooling or refrigeration. Figure 2-1 shows the overall propulsion scheme of propellant development (Isp levels with respect to time) and where space storable fuels fit into this overall scheme which indicates the need for space storable rocket development.  Space storable propellants provide the link between upgraded earth storable and an integrated H/O system.  Among the categories evaluated were alcohols, amines, cryogens and hydrocarbons. In order to adequately evaluate the propellants, selection criteria were established and system analyses conducted based on representative missions and engine performance.  The results of this Task 1 study provided the following:

- Evaluation of mission usage

- Propulsion systems and fuels evaluation to achieve payload maximization

- Evaluation and selection of fuels

- Preliminary system and engine requirements

The space storable rocket technology (SSRT) program consists of four phases (Basic program + three options).  The first phase (Basic Program) consisted of three tasks:

- Applications Evaluation as discussed above

- Preliminary Design

    - Performance analyses
    - Thermal analyses
    - Overall engine concepts

2
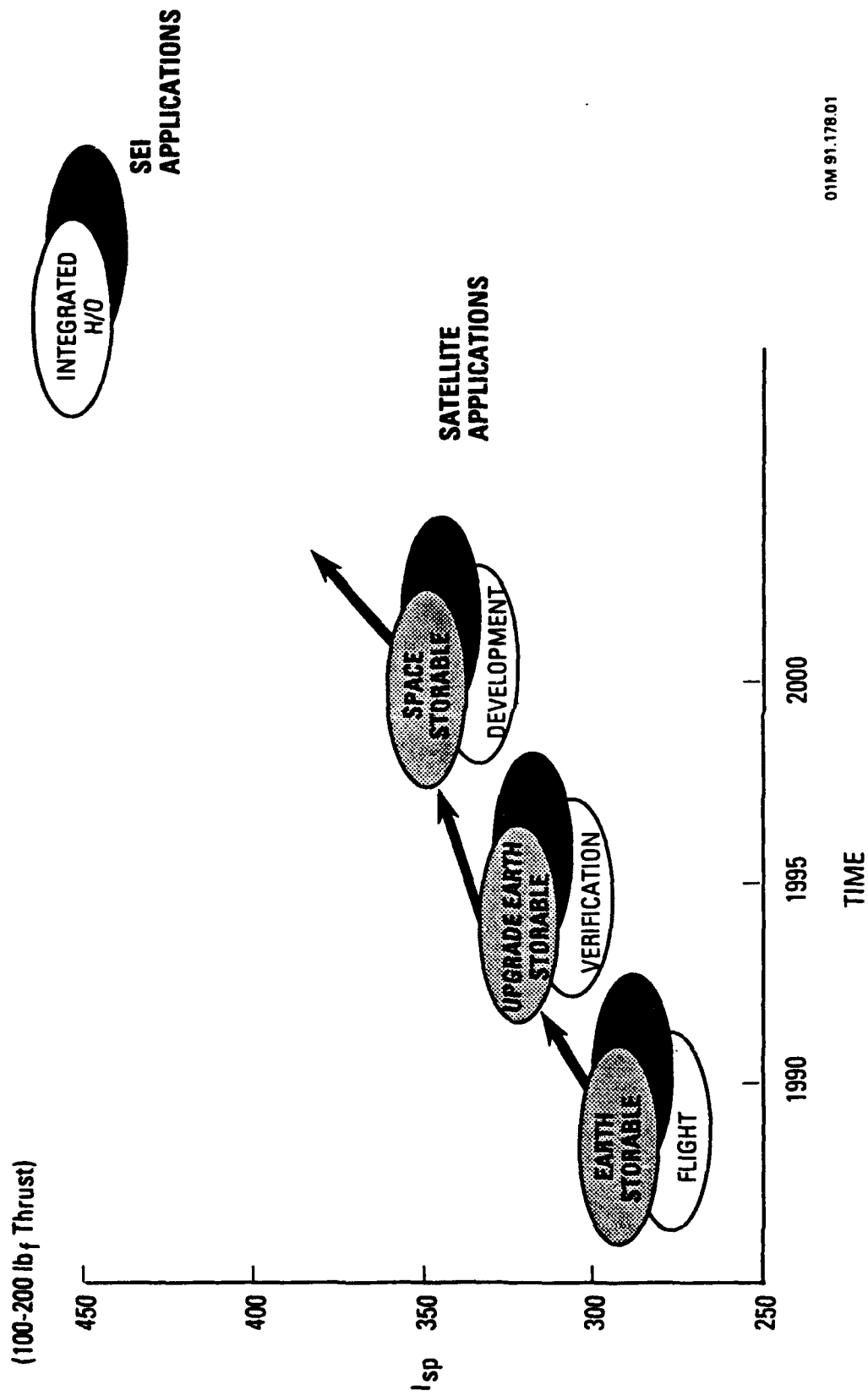
Figure 2-1. Apogee Engine Applications

01M 91.178.01

3

● Exploratory Tests

     – Initial tests with $LO_2$
     – Modify hardware based on initial test results
     – Retest with modified hardware

This report will discuss the results of the three tasks of the Basic program phase.

## 3.0 APPLICATIONS EVALUATION

Space storable propellants offer the advantage of providing higher performance to achieve greater payload weight into orbit. The applications evaluation studied the following areas:

- Mission evaluation usage of advanced propulsion technology

- Propulsion systems and fuels evaluation to achieve payload maximization

- Evaluation and selection of fuels

- Preliminary system and engine requirements

- Conclusions

## 3.1 Missions

Three representative missions were investigated to utilize advanced propulsion technology. These three types of missions are defined as follows:

- Perigee/apogee integral propulsion systems are used to place satellites into geosynchronous earth orbit (GEO) utilizing expendable launch vehicles (i.e., Atlas, Delta, etc.). These missions include NASA, military and commercial applications for communication, surveillance, tracking, earth observation and meteorology. These missions constitute the greatest quantity and frequency of mission applications and are shown in Table 3-1 which average 30-40 yearly not including classified military missions.

- Low earth orbit is another mission application. One application uses the Orbit Maneuvering Vehicle (OMV) or another similar vehicle to go from shuttle cargo bay to Space Station or from Space Station to the required mission. Table 3-2 shows the typical OMV missions and their requirements. Figure 3-1 shows the representative mission selected for the system study since it utilizes the greatest $\Delta V$ requirement.

- The planetary application is another representative mission. The Comet Rendezvous Asteroid Flyby (CRAF) was selected as the typical planetary application. The mission is shown in Figure 3-2 and the $\Delta V$ requirements are shown in Table 3-3.

5
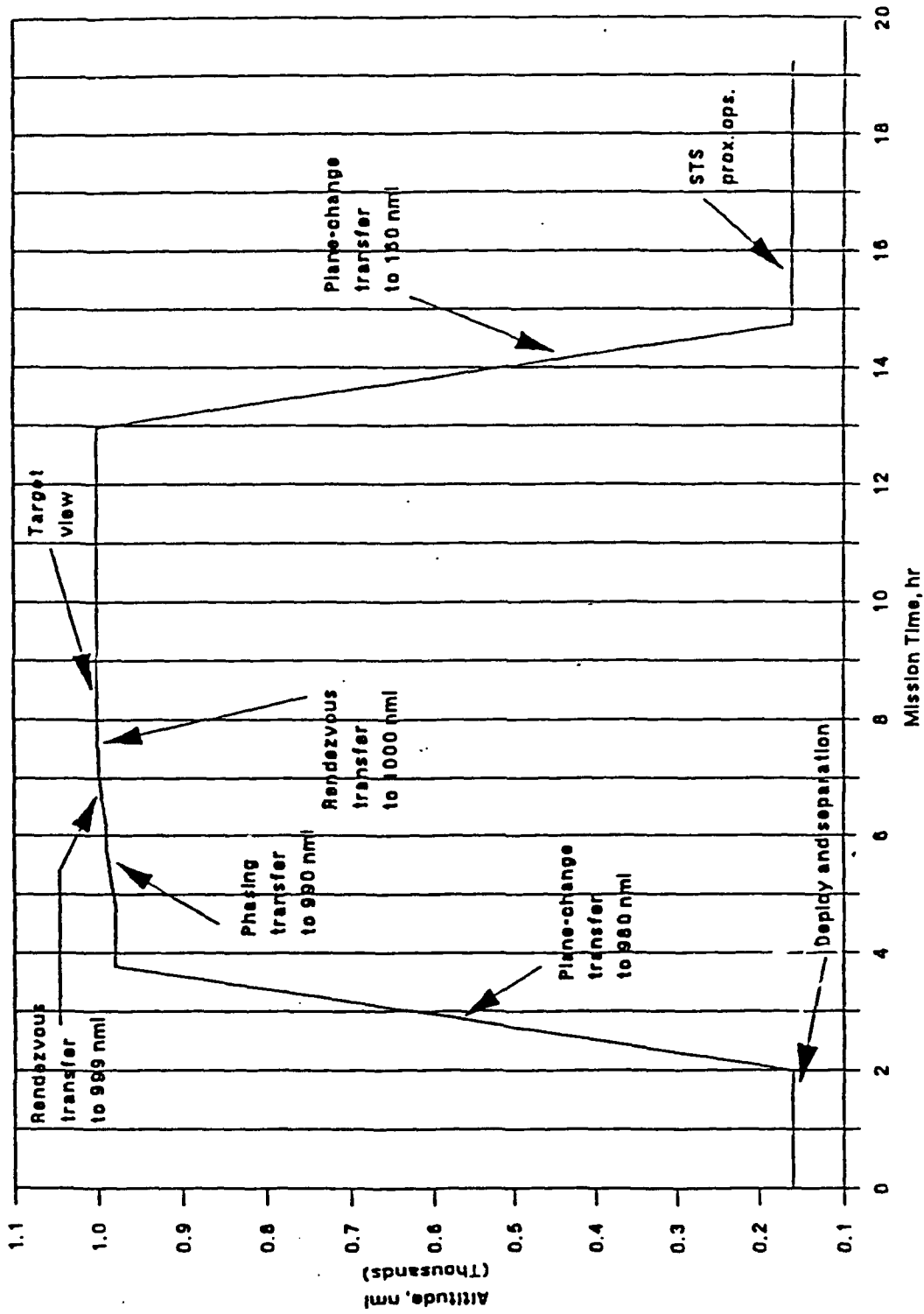
Figure 3-1.  DRM-6/STS Altitude Profile

6
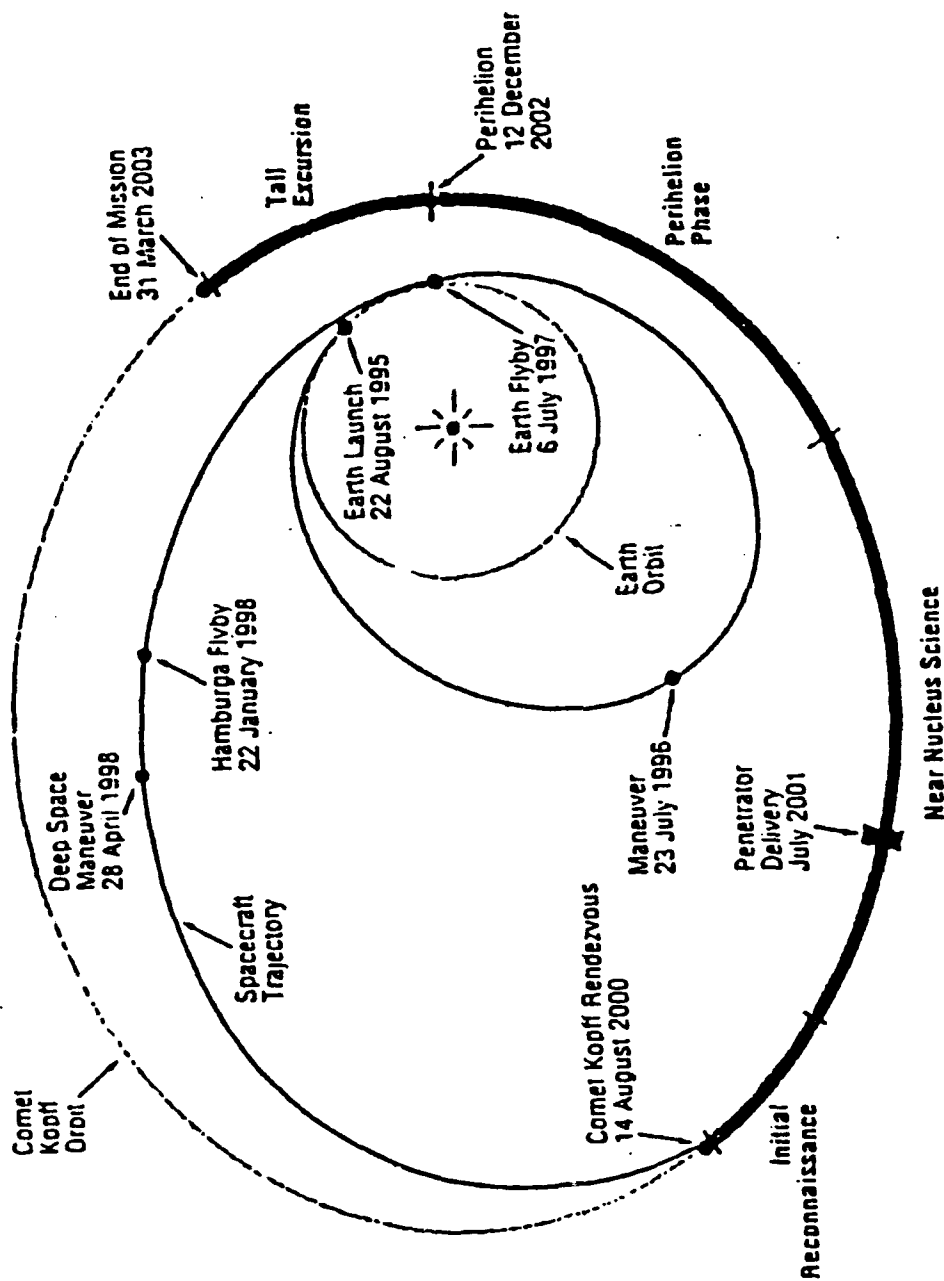
CRAF spacecraft would be launched in 1995 and make one Earth-return orbit before reaching Comet Kopff in 2000. CRAF would orbit Kopff for about 2.5 years as it becomes more active.

Figure 3-2. CRAF Mission Benefits Using Advanced Propulsion

7

TABLE 3-1
MISSION PLANNING

| LAUNCH VEHICLE | 1992 | 1993 | 1994 | 1995 | 1996 | 1997 |
|---|---|---|---|---|---|---|
| Arianespace | Insat 2A | Intelsat VII F4 | Astra 1D | | | |
| | Telecon 2 F1 | Galaxy 7 | Brazilsat B2 | | | |
| | Intelsat VI F4 | Telecom 2 F2 | | | | |
| | Intelsat VII F1 | Astra 1 C | | | | |
| | Satcom C3 | Brazilsat B1 | | | | |
| | Topex/Poseidon | ESA Infraved Space OBS | | | | |
| | Hispasat 1 | | | | | |
| | Hispasat 2 | | | | | |
| | Galazy 4 | | | | | |
| | | | | | | |
| Long March | Aussat B1 | Aussat B2 | | | | |
| | | | | | | |
| Shuttle | USML-01 | SL-D2 | IML-02 | USML-02 | SRL-03 | |
| | LAGEOS II | SLS-02 | SPTN-04 | SL-D3 | GEOSTAR-03 | |
| | EURECA-1R | TDRS-F | ISEM-02 | SPACEHAB-06 | SPACEHAB-07 | |
| | ASP | DEE | CXM-02 | SPTN-05 | OAET-03 | |
| | DOD | CTM | SFU-RETR | CXH-10 | ATLAS-05 | |
| | TSS-01 | SPACEHAB-02 | CXM-03 | USMP-04 | SSBUV-A-04 | |
| | EURECA-1L | OAET-01 | CMSE-02 | WSF-03 | CONE | |
| | 1MAX-06 | CAPL | XTE | SSF/MB-02 | SSF/MB-04 | |
| | E01-III/TEMP 2A-03 | FLOATZONE-01 | EUVE RETR | SPACEHAB-05 | SSF/MB-03 | |
| | ATLAS-01 | SRAD/TP1TS | GEOSTAR-01 | GEOSTAR-02 | SSF/MB-05 | |
| | SSBUV-04 | WSF-01 | SPACEHAB-03 | EURECA-2R | SLS-03 | |
| | ACTS | 1EH | FROZEPIPE | CMSE-03 | USMP-05 | |
| | CANEX-02 | 1SEM-01 | HPE | ATLAS-04 | WSF-04 | |
| | DXS | SPACEHAB-01 | MICROWAVE-01 | W1SP | DCWS | |
| | INTELSAT VI-R | OREFUS-SPAS | USMP-03 | SSBUV-A-03 | | |
| | CVTE-01 | GAS BRIDGE | OAET-FLYER | AAFE | | |
| | ASEM | SHOOT | SRL-02 | OAET-02 | | |
| | SL-J | | CRISTA-SPAS | SSF/MB-01 | | |
| | GAS BRIDGE | | ATLAS-03 | | | |
| | | | SSBUV-A-02 | | | |
| | | | WSF-02 | | | |
| | | | SPACEHAB-04 | | | |
| | | | EURECA-2L | | | |
| | | | CXM-04 | | | |
| | | | | | | |
| MEDIUM CLASS | GEOTAIL (D) | POLAR (D) | RADARSAT (D) | GPS III (D) | LIFESAT 1 (D) | ACE (D) |
| Atlas (A) | WIND (D) | NOAA-J (A) | LAGEOS III (D) | GPS III (D) | LIFESAT 2 (D) | LIFESAT-3 (D) |
| Delta (D) | GPS II (D) | GPS II (D) | NOAA-K (T-11) | GPS III (D) | NOAA-L (T-11) | NOAA-M (T-11) |
| Titan II (T-11) | GPS II (D) | GPS II (D) | GPS II (D) | DMSP 5D2 (T-11) | GPS III (D) | GPS III (D) |
| | GPS II (D) | GPS II (D) | GPS II (D) | | GPS III (D) | GPS III (D) |
| | GPS II (D) | GPS II (D) | GPS II (D) | | GPS III (D) | GPS III (D) |
| | GPS II (D) | GPS II (D) | GPS II (D) | | GPS III (D) | GPS III (D) |
| | DMSP 5D2 (T-11) | | DMSP 5D2 (T-11) | | GPS III (D) | GPS III (D) |
| | | | | | DMSP 5D2 (T-11) | GPS III (D) |

8

TABLE 3-1
MISSION PLANNING CONTINUED

| LAUNCH VEHICLE | 1992 | 1993 | 1994 | 1995 | 1996 | 1997 |
|---|---|---|---|---|---|---|
| INTERMEDIATE CLASS | GOES-I (A-1) | Intelsat VII F2 (11AS) | MSAT (1C) | SOHO (11AS) | DSCS 5D3 (11) | ATDRS-1 (1C) |
| Titan III / Atlas I/II AS | M0 (T-111) | Intelsat VII F3 (11AS) | Telstar 4 F2 (11AS) | TDRS-G (1C) | UHF FO (A-1) | GOES-L (A-1) |
| | GOES-J (A-1) | UHF-2 (A-1) | SAX (A-1) | GOES-K (A-1) | UHF FO (A-1) | SSF |
| | GALAXY-1R (A-1) | Telstar 4 F1 (11AS) | ORION-2 (11A) | MARS OBS | UHF FO (A-1) | DSCS 5D3 (11) |
| | UHF-1 (A-1) | ORION-1 (11A) | DSCS 5D3 (11) | SSF | | UHF FO (A-1) |
| | DSCS 5D3 (A-11) | DSCS 5D3 (11) | UHF FO (A-1) | UHF FO (A-1) | | |
| | | DSCS 5D3 (11) | UHF FO (A-1) | UHF FO (A-1) | | |
| | | | | UHF FO (A-1) | | |
| | | | | | | |
| LARGE CLASS | MILITARY SURV | MILITARY SURV | MILITARY SURV | MILITARY SURV | MILITARY SURV | MILITARY SURV |
| Titan IV | | MILITARY SURV | MILITARY COMM | MILITARY COMM | MILITARY SURV | MILITARY COMM |
| | | | | CASSINI CRAF | CASSINI CRAF | MILITARY COMM |
| | | | | | SSF | SURV |
| | | | | | | SURV |
| | | | | | | SSF |
| | | | | | | |
| SECONDARY P/LS | PMG | SEDS-2 | HETE | NGL | | |
| Delta | EUV | SAC-B | | 1CDC | | |
| | SEDS-1 | | | | | |

Table 3-2. OMV Key Mission Requirements

| Mission | Payload (lbm) | Altitude (nmi) | STS Mission ΔV (fps) | Total Impulse ($10^6$ lbf-sec) |
|---|---|---|---|---|
| DRM-1 Observatory Servicing | 25,000 | 130 | 1207.9 | 2.5 |
| DRM-2 Payload Placement | 3,500 | 340 | 2967.4 | 1.6 |
| DRM-3 Payload Retrieval | 11,000 | 220 | 2318.9 | 1.3 |
| DRM-4 Payload Reboost | 25,000 | 100/220 | 1685.4 | 1.0 |
| DRM-5 Payload Deboost | 75,000 | 0 | 1153.3 | 1.2 |
| DRM-6 Payload Viewing | 200 | 840 | 5738.8 | 2.5 |
| DRM-7 Subsatellite | 5,000 | 0 | 2919.9 | 1.7 |
| DRM-8 Multiple PL | 5,000/ 10,000 | 85/110 | 1893.7 | 1.0 |
| DRM-9 In-Situ Servicing | 5,000 | 400 | 2947.0 | 1.7 |
| DRM-10 Module Transfer | 50,000 | 110 | 1250.7 | 2.6 |

*Bipropellant Engine Mission ΔV Requirements

| Elapsed Time (hr) | | ΔV (fps) |
|---|---|---|
| 1.43 | Transfer burn (plane change transfer to 980 nmi) | 2804.1 |
| 1.0 | Transfer burn (phasing transfer to 990 nmi) | 28.9 |
| 0.93 | Rendezvous burn (rendezvous transfer to 1000 nmi) | 28.5 |
| 1.47 | Transfer burn (plane change transfer to 160 nmi) | 2877.3 |
| | | 5738.8 |

10

TABLE 3-3. CRAF MISSION ΔV REQUIREMENTS.

| Maneuver | Days After Launch | ΔV (fps) | Total Impulse (It) $10^6$ lbf-sec |
|---|---|---|---|
| Post launch (8-22-95) | 10-30 | 164.05 | 0.06 |
| Maneuver (7-23-96) | 306-366 | 1933.06 | 0.61 |
| Aimpoint biasing reserve | 510 | 32.81 | 0.01 |
| Earth flyby (7-6-97) | 654-714 | 29.52 | 0.01 |
| Hamburga flyby (1-22-98) | 854-894 | 32.8 | 0.01 |
| Maneuver (4-28-98) | 950-1010 | 539.06 | 0.15 |
| Comet rendezvous (8-14-00) | 1799-1895 | 6978.99 | 1.33 |
| Nucleus approach (reserve) | 1829-1903 | 98.82 | 0.01 |
| Initial flybys and navigation reserve | 1903-1958 | 26.24 | 0.003 |
| Near encounter and navigation reserve | 1958-2456 | 19.68 | 0.003 |
| Perihelion flybys | 2456-2678 | 245.09 | 0.03 |
| Active comet reserve | 2456-2768 | 95.15 | 0.01 |
| Comet tail excursion | 2678-2768 | 279.21 | 0.03 |
| Comet exploratory contingency | 2456-2778 | 127.30 | 0.01 |
| Totals | | 10601.83 | 2.4 |

## 3.2 System Analyses

System analyses were conducted for each of the three missions of 3.1. The fuels considered and selected typical for these missions are shown in Table 3-4.

### 3.2.1 Engine Performance

The engine configuration utilized for this study consisted of 100-400 lbf thrust radiation cooled engines operating at 100-400 psia chamber pressure. This selection was based on the use of multiple liquid bipropellant engines to avoid single point failures. Rhenium thrust chambers were used to achieve the high performance (4000°F wall temperatures). A high thrust version was investigated using 1000 lbf thrust regeneratively cooled engines operating at 400 psia chamber pressure. The engine performance used is presented in Table 3-5 and was anchored to the TRW dual mode engine which is qualified and successfully flying.

### 3.2.2 System Configuration

The baseline system to be used for evaluation which is presently flying on communication satellite applications to GEO is shown in Figure 3-3. This configuration was based on evaluation of the various system options and includes the following:

- Pressurization - regulated pressure-fed system using $GH_e$ at 7500 psia in spherical graphite/epoxy overwrapped tank with aluminum liner.

- Propellant storage - two oxidizer and two fuel tanks which are cylindrical with elliptical heads and are graphite/epoxy overwrapped with aluminum liner. MLI is used for the cryogenic tanks.

- Perigee/apogee engines - radiation cooled as discussed in 3.2.1. The low thrust version used a total thrust of 400 lbf (1, 2 or 4 engines) while the high thrust version used a total thrust of 2000 lbf (2 engines).

- Reaction control system - decomposed hydrazine system per Figure 3-4. For $LO_2$-$N_2H_4$ system, the hydrazine is fed from main hydrazine tanks.

The ground rules used to analyze the various applications and fuels are:

- Residual - 1% of total propellant was considered unusable for all applications including OMV and CRAF.

12

LEGEND

- 100 LBF LAE
- EHT
- 5 LBF ROCKET ENGINE ASSY (REA)
- 1 LBF ROCKET ENGINE ASSY (REA)
- FILTER
- LATCH VALVE
- SERVICE VALVE
- $P_1$ BOL PRESSURE TRANDUCER
- $P_2$ EOL PRESSURE TRANDUCER
- PARALLEL REDUNDENT CHECK VALVE
- NC-PYROVALVE NORMALLY CLOSED
- NO-PYROVALVE NORMALLY OPEN
- REDUNDANT REGULATOR

HIGH-PRESSURE TRANSDUCER

HIGH-PRESSURE LATCHING VALVE

EVEN SIDE

ODD SIDE

$N_2H_4$

$N_2O_4$

NC

NO
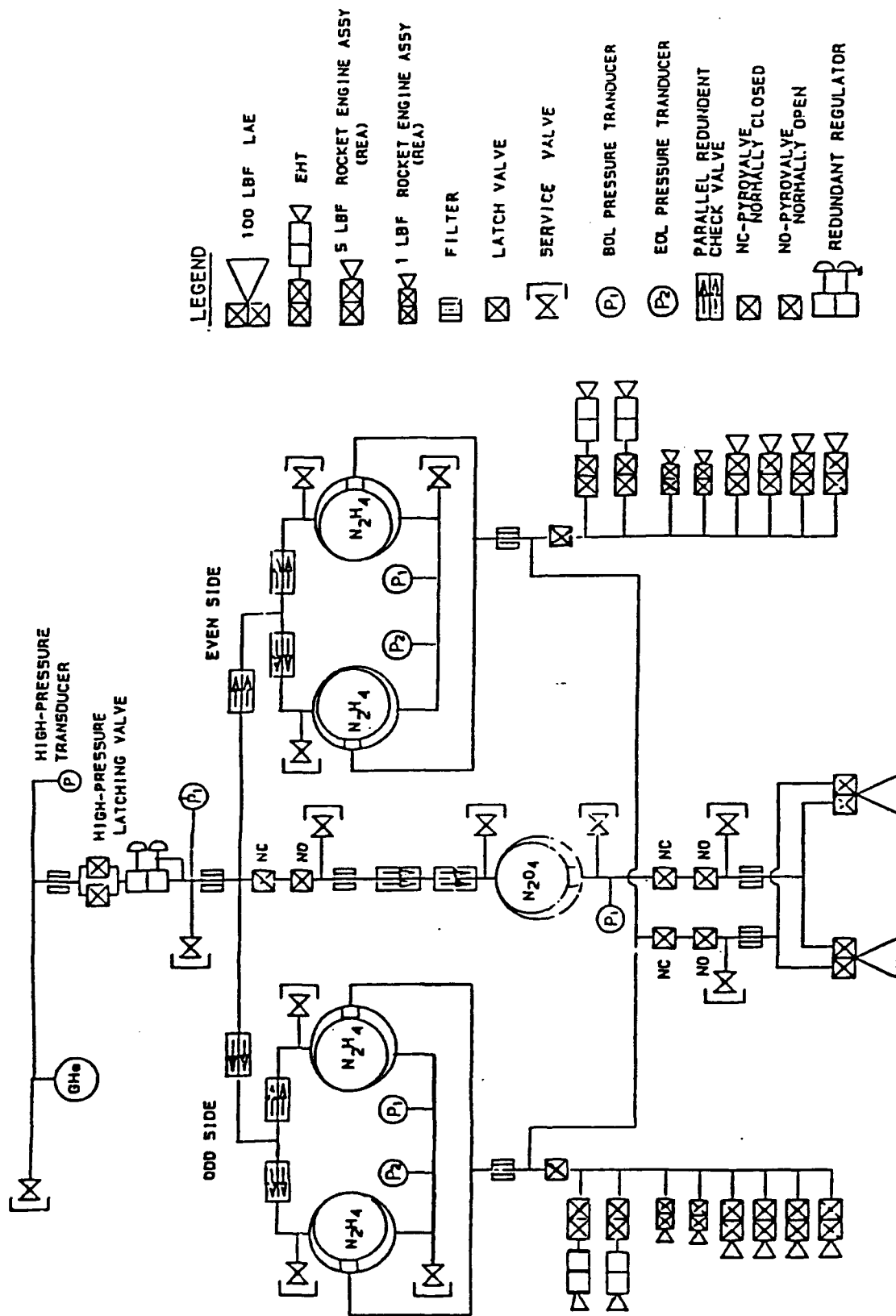
Figure 3-3.    Representative Integral Dual Mode Propulsion System for GEO Satellites.

13

HELIUM
PRESSURANT
TANK

PRESSURE
TRANSDUCER

FILL & DRAIN
VALVE

N/C SQUIB
VALVE

FILTER

REGULATOR

N/O SQUIB VALVE

$N_2H_4$
PROPELLANT
TANK

$N_2H_4$

filter

Line heater
(typical)

Isolation
valve

A SIDE
5.0 lb$_f$
THRUSTER
ASSEMBLY
(6 REQUIRED)

+RA  -RA  +PA  -PA  -Z1A  +Z2A

B SIDE
5.0 lb$_f$
THRUSTER
ASSEMBLY
(6 REQUIRED)

+RA  -RA  +PA  -PA  -Z1A  +Z2A
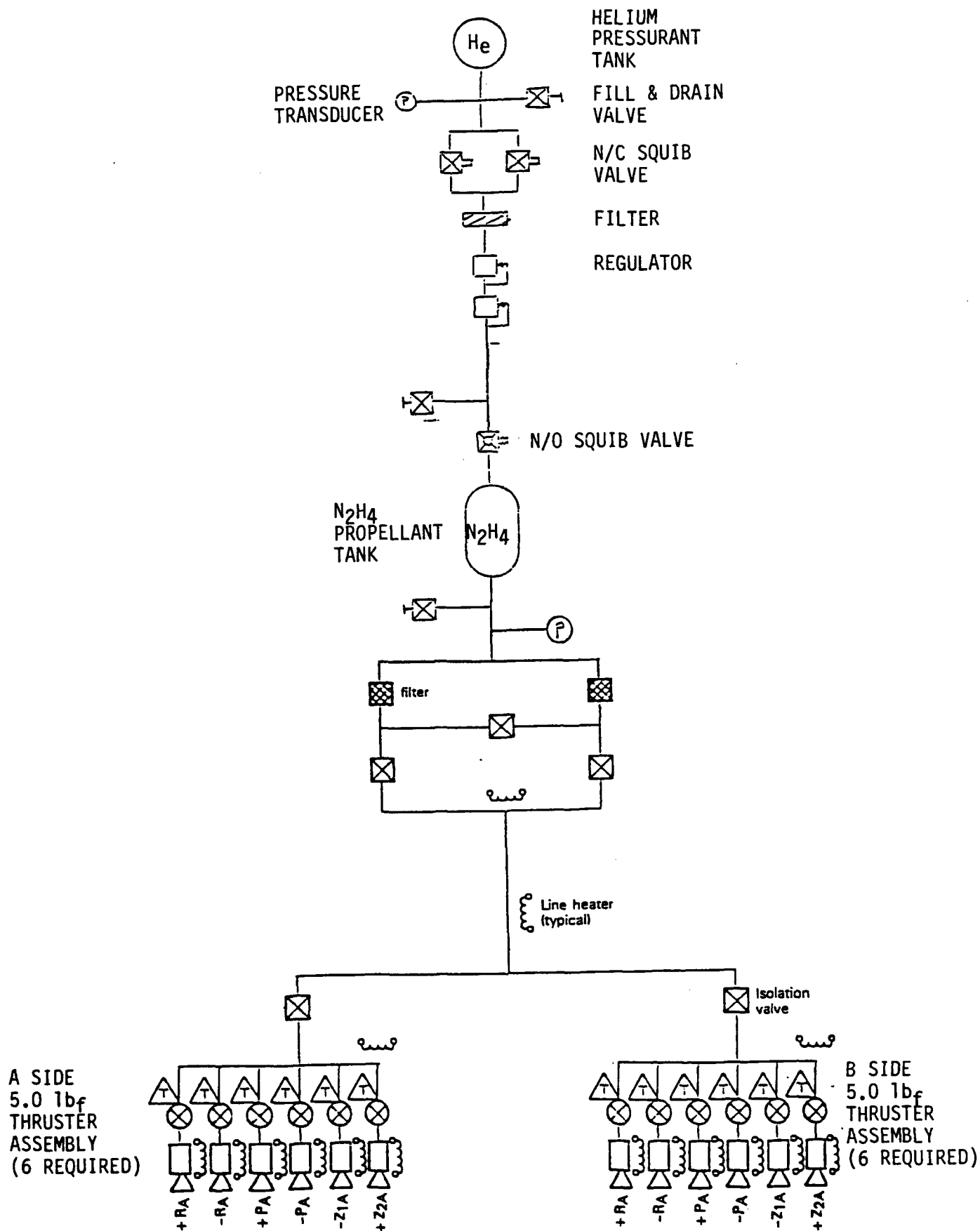
Figure 3-4.   Hydrazine RCS System

Table 3-4.  Fuels Selection for System Studies.

| Fuel Category | Fuels | Selected Fuel | Rationale |
|---|---|---|---|
| Alcohols | CH₃OH<br>C₂H₅OH<br>C₃H₇OH | C₂H₅OH | Selected as the alcohol considered for rocket applications by other contractors |
| Amines | MMH<br>N₂H₄<br>UDMH<br>50% N₂H₄/50% UDMH | MMH<br>N₂H₄ | Selected as the highest performing amine fuels which are flight usable presently |
| Borons | B₂H₆<br>B₅H₉ | Not selected | Due to toxicity and previously experienced performance problems |
| Cryogenic | LH₂ | LH₂ | Selected as the highest performing fuel |
| Gels with AL | MMH gel with aluminum | Not selected | Not competitive for subject space engine considerations Lower in performance and worse exhaust products. |
| Hydrocarbons | CH₄<br>C₂H₆<br>C₃H₈<br>RP-1 | CH₄<br>C₃H₈<br>RP-1 | Selected as fuels considered by various agencies/ contractors for potential space engine considerations |

15

**Table 3-5. Engine performance**

provides input into system analyses

| Propellants | Thrust $F_\infty$ ~lbf (N) | Chamber Pressure Pc ~psia (N/cm$^2$) | Mixture Ratio O/F | Specific Impulse $Isp_\infty$ ~lbf-sec/lbm (Nsec/kg) |
|---|---|---|---|---|
| LO$_2$-LH$_2$ | 100 (445)<br>200 (890)<br>400 (1779)<br>1000 (4448) | 100 (69)<br>200 (138)<br>400 (276)<br>400 (276) | 3.95<br>4.35<br>4.74<br>5.0 | 435.8 (4274)<br>439.4 (4309)<br>442.6 (4340)<br>444.6 (4360) |
| LO$_2$-RP-1 | 100 (445)<br>200 (890)<br>400 (1779)<br>1000 (4448) | 100 (69)<br>200 (138)<br>400 (276)<br>400 (276) | 2.34<br>2.34<br>2.34<br>2.5 | 325.2 (3189)<br>331.8 (3254)<br>338.2 (3316)<br>346.9 (3402) |
| LO$_2$-C$_3$H$_8$ | 100 (445)<br>200 (890)<br>400 (1779)<br>1000 (4448) | 100 (69)<br>200 (138)<br>400 (276)<br>400 (276) | 2.36<br>2.56<br>2.75<br>3.0 | 331.3 (3249)<br>338.2 (3316)<br>343.3 (3366)<br>353.2 (3464) |
| LO$_2$-C$_2$H$_5$OH | 100 (445)<br>200 (890)<br>400 (1779)<br>1000 (4448) | 100 (69)<br>200 (138)<br>400 (276)<br>400 (276) | 1.45<br>1.65<br>1.69<br>1.8 | 316.8 (3106)<br>323.2 (3169)<br>329.8 (3234)<br>336.5 (3300) |
| LO$_2$-MMH | 100 (445)<br>200 (890)<br>400 (1779)<br>1000 (4448) | 100 (69)<br>200 (138)<br>400 (276)<br>400 (276) | 1.16<br>1.16<br>1.36<br>1.50 | 338 (3314)<br>343.5 (3368)<br>348.7 (3419)<br>355.3 (3484) |
| N$_2$O$_4$-N$_2$H$_4$ (TRW DM-LAE) | 100 (445) | 100 (69) | 1.07 | 314.5 (3084) |
| LO$_2$-N$_2$H$_4$ | 100 (445)<br>200 (890)<br>400 (1779)<br>1000 (4448) | 100 (69)<br>200 (138)<br>400 (276)<br>400 (276) | 0.75<br>0.75<br>0.75<br>0.75 | 340.3 (3337)<br>345 (3383)<br>348.9 (3421)<br>353 (3462) |
| LO$_2$-CH$_4$ | 100 (445)<br>200 (890)<br>400 (1779) | 100 (69)<br>200 (138)<br>400 (276) | 2.81<br>2.81<br>2.81 | 336 (3295)<br>343.8 (3371)<br>346.6 (3399) |

- Boil-off - 0.4% of the cryogenic propellant was considered boil-off except for high thrust condition which used 0.25%. These losses were used for all applications including OMV and CRAF. $LH_2$ losses were established at 6.1% (based on AFRPL-TR-86-045).

- Startup/Shutdown - 0.5% of total propellant used for all applications. For $LH_2$, 2% was used.

- Thermodynamic vent system cooling - 2% total of $LH_2$.


## 3.2.3 Results of System Analyses

System analyses were conducted to evaluate their weights to orbit for the three types of missions (GEO, OMV, CRAF) defined in 3.1.


## 3.2.3.1 Perigee/Apogee Applications

The investigation of mission applications indicates perigee/ apogee applications have the greatest usage potential in the foreseeable future. Therefore, the system analyses for these applications are most important and the results have the greatest impact. The analyses used the Delta 7925 (6000 lbm into LEO) and Atlas IIA (14,750 lbm into LEO) as typical launch vehicles. The results of the analyses are presented in Table 3-6 which indicates $LO_2-N_2H_4$ is the best propellant combination to achieve the greatest weight into GEO. These weights consider the major subsystems except for the RCS system and system components (regulators, valves, lines, heaters).

The hydrogen tank volumes ($\sim$ 450% of amine tank volume) are so great that $LH_2$ could only be integrated into the vehicle using toroidal tanks necessitating aluminum toroidal tanks due to unavailable overwrapping toroidal tank technology. This results in non-competitive weights into GEO.

The impact of the RCS subsystem was investigated. Figure 3-4 shows the system used to assess RCS impact based on a $\Delta V$ = 1465 ft/sec for RCS and stationkeeping. Figure 3-5 shows the RCS weight impact on payload into GEO.


## 3.2.3.2 OMV Type Applications

System analyses were conducted to determine the best propellant combination for a typical low earth orbit application and the OMV viewing mission (DRM-6) was selected. The four best fuels (amines and hydrocarbons) were selected for the analyses including $N_2H_4$, MMH, $CH_4$ and $C_3H_8$. The propulsion system was similar to Figure 3-3 except four

Figure 3-5.

WEIGHT OF PAYLOAD INTO GEO
is impacted by RCS
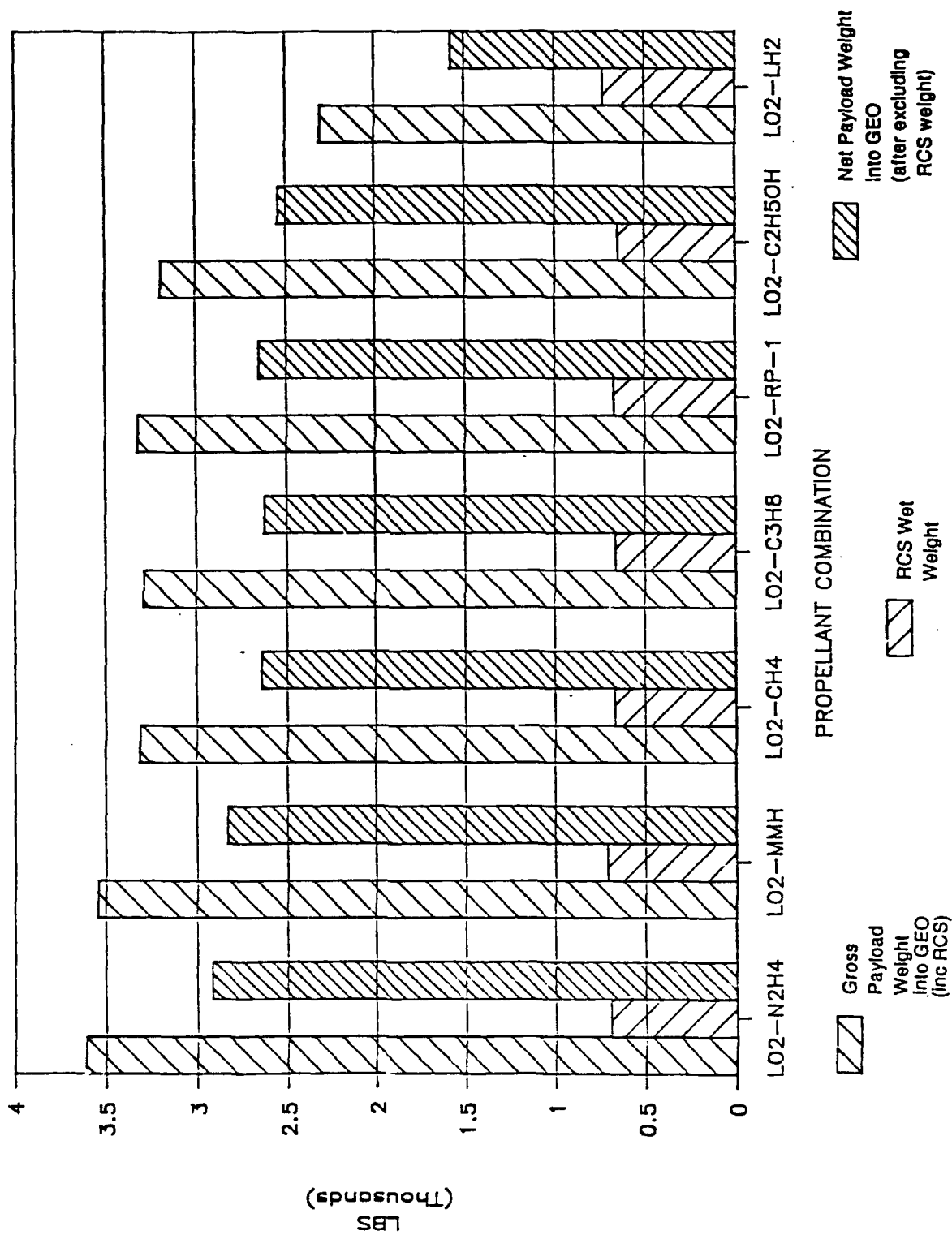
Table 3-6. Weight into GEO.

Is Maximized Using $N_2H_4$

| Weight into LEO (lbm) | Thrust ($F_\infty \sim$ lbf) | $P_c$ (psia) | Weight into GEO | | | | | | | |
|---|---|---|---|---|---|---|---|---|---|---|
| | | | $N_2O_4$-$N_2H_4$ (B/L) | $LO_2$-$N_2H_4$ | $LO_2$-MMH | $LO_2$-$CH_4$ | $LO_2$-$C_3H_8$ | $LO_2$-RP-1 | $LO_2$-$C_2H_5OH$ | $LO_2$-$LH_2$* |
| 6000 | 100 | 100 | 1307 | 1425 | 1395 | 1289 | 1280 | 1295 | 1245 | 924 |
| 6000 | 200 | 200 | | 1442 | 1415 | 1320 | 1311 | 1324 | 1271 | 905 |
| 6000 | 400 | 400 | | 1436 | 1414 | 1294 | 1309 | 1332 | 1280 | 783 |
| 6000 | 1000 | 400 | | 1416 | 1409 | - | 1332 | 1344 | 1278 | 775 |
| 14,750 | 100 | 100 | 3290 | 3581 | 3506 | 3246 | 3225 | 3261 | 3138 | 2330 |
| 14,750 | 200 | 200 | | 3613 | 3549 | 3315 | 3293 | 3324 | 3194 | 2308 |
| 14,750 | 400 | 400 | | 3588 | 3534 | 3239 | 3277 | 3333 | 3205 | 1973 |
| 14,750 | 1000 | 400 | | 3583 | 3567 | - | 3378 | 3406 | 3245 | 1999 |

*These payload weights are based on aluminum toroidal tanks for $LH_2$ with MLI and graphite/epoxy cylindrical (with elliptical heads) $LO_2$ tanks using aluminum liners with MLI to integrate into vehicle due to excessive volumes of $LH_2$.

19

engines of 100 lbf thrust (operating at 100 psia chamber pressure) were utilized for this application. Two engines operate simultaneously for each maneuver and the other two engines provide redundancy. The results of the system analyses are presented in Table 3-7 and indicate $LO_2-N_2H_4$ is the system of choice as it provides the lightest initial vehicle/system weight and highest bulk density and mass fraction over the other candidates.

## 3.2.3.3  CRAF Application

System analyses were conducted to determine the best propellant combination for a typical planetary mission and the CRAF mission was selected - current plans show the use of a typical bipropellant system similar to our system studies. The four best fuels were evaluated using the same regulated pressure-fed configuration of Figure 3-3 but using only one 100 lbf thrust radiation cooled engine operating at 100 psia chamber pressure. The initial spacecraft weight is 11,305 lbm. The results of the system analyses are presented in Table 3-8 and indicate $LO_2-N_2H_4$ is the best system as it provides the maximum payload weight with the lightest system and maximum bulk density and mass fraction over the other candidates.

## 3.2.3.4  Summary/Conclusion

Based on the system analyses, the overall mission/system capability is summarized in Table 3-9. Using the Figure of merit defined and presented in Table 3-9, $LO_2-N_2H_4$ is the best propellant combination.

## 3.3  Fuels Evaluation

The seven selected fuels were evaluated to select the best engine and system to achieve the mission applications. Eight evaluation factors were considered in the evaluation.

- Mission/System Capability

    The evaluation factor considered weight and volume considerations of engine and system. The figure of merit and evaluation of Table 3-9 were the basis of evaluation of this factor.

- Safety Considerations

    The safety considerations included three factors-- flammability, explosive potential and system safety were the major considerations.

Table 3-7. Summary of OMV Type System Capabilities

Indicates $LO_2$-$N_2H_4$ is Best Overall System

| Parameter | $LO_2$-$N_2H_4$ | $LO_2$-MMH | $LO_2$-$CH_4$ | $LO_2$-$C_3H_8$ |
|---|---|---|---|---|
| ΔV-ft/s | 5739 | 5739 | 5739 | 5739 |
| Total impulse - $10^6$ lbf-s | 2.500 | 2.505 | 2.519 | 2.509 |
| Propulsion system wet weight-lbm | 7714 | 7806 | 8024 | 8130 |
| Initial OMV weight (inc payload)-lbm | 18,106 | 18,170 | 18,227 | 18,364 |
| Mass fraction | 0.95 | 0.95 | 0.93 | 0.94 |
| Bulk density | 66.4 | 62.6 | 51.8 | 55.6 |

$$\text{Mass fraction} = \frac{\text{Usable propellant weight}}{\text{Propulsion system wet weight}}$$

$$\text{Bulk density} = \frac{1 + O/F}{\left(\frac{1}{\rho_f} + \frac{O/F}{\rho_{ox}}\right)}$$

Table 3-8. CRAF Mission System Capabilities

Are Best Achieved Using $LO_2$-$N_2H_4$ System

| Parameter | $LO_2$-$N_2H_4$ | $LO_2$-MMH | $LO_2$-$CH_4$ | $LO_2$-$C_3H_8$ |
|---|---|---|---|---|
| ΔV-ft/s | 10,602 | 10,602 | 10,602 | 10,602 |
| Total impulse - $10^6$ lbf-s | 2.378 | 2.372 | 2.366 | 2.352 |
| Propulsion system wet weight-lbm | 7315 | 7368 | 7543 | 7567 |
| Payload weight-lbm | 3990 | 3937 | 3762 | 3738 |
| Mass fraction | 0.96 | 0.95 | 0.93 | 0.94 |
| Bulk density | 66.4 | 62.6 | 51.8 | 55.6 |

$$\text{Mass fraction} = \frac{\text{Usable propellant weight}}{\text{Propulsion system wet weight}}$$

$$\text{Bulk density} = \frac{1 + O/F}{\left(\frac{1}{\rho_f} + \frac{O/F}{\rho_{OX}}\right)}$$

22

Table 3-9. Mission/System Capability.

| Parameter | LO2-N2H4 | LO2-MMH | LO2-LH2 | LO2-CH4 | LO2-C3H8 |
|---|---|---|---|---|---|
| Weight into GEO (Atlas IIA)-lbm (kg) | 3613 (1642) | 3549 (1613) | 2308 (1049) | 3315 (1507) | 3293 (1497) |
| Net weight into GEO (inc. RCS)-lbm (kg) | 2919 (1327) | 2837 (1290) | 1577 (717) | 2646 (1203) | 2628 (1194) |
| Mass fraction (w/o RCS) | 0.95 | 0.94 | 0.75 | 0.92 | 0.93 |
| Bulk density-lbm/ft$^3$ (kg/m$^3$) | 66.4 (1066) | 62.6 (1005) | 18.6 (299) | 51.8 (831) | 56.3 (904) |
| OMV initial weight (inc payload)-lbm (kg) | 18,106 (8230) | 18,170 (8259) | Not considered due to excessive volumes LH2 | 18,227 (8285) | 18,364 (8347) |
| Mass fraction | 0.95 | 0.95 | | 0.93 | 0.94 |
| Bulk density-lbm/ft$^3$ (kg/m$^3$) | 66.4 (1066) | 62.6 (1005) | | 51.8 (831) | 55.6 (892) |
| CRAF mission payload-lbm (kg) | 3990 (1814) | 3937 (1790) | | 3762 (1710) | 3738 (1699) |
| Mass fraction | 0.96 | 0.95 | | 0.93 | 0.94 |
| Bulk density-lbm/ft$^3$ (kg/m$^3$) | 66.4 (1066) | 62.6 (1005) | | 51.8 (831) | 55.6 (892) |
| Overall mission/system capability ranking* | 1 | 2 | 5 | 4 | 3 |

*Figure of merit for ranking = $\frac{\text{Net wt into GEO (inc RCS)}}{\text{Max net wt into GEO (inc RCS)}} + \frac{\text{Mass fraction}}{\text{Max mass fraction}} + \frac{\text{Bulk density}}{\text{Max bulk density}}$

- **System Integration**

    System integration considered two primary considerations--RCS and fuel integration. The RCS must be integrated to achieve minimum weight and complexity while achieving high reliability with the necessary control. In all cases, hydrazine RCS was used as the system due to its high reliability and demonstrated flight data base. Fuel integration considered insulation of cryogenic tanks and lines and design of regulators and valves.

- **Plume Contamination**

    The exhaust products at the nozzle exit were evaluated based on the engine operating conditions. The major toxic constituent was determined to be CO although the amine fuels had traces of NO. The exhaust products are summarized in Table 3-10.

- **Logistics**

    The logistics considerations were based on the use of the fuel for flight at the launch facilities. This factor considered shipping, storage, availability of fuel, ground support at the launch facilities and validated operating procedures at the launch facilities.

- **Materials Compatibility**

    This factor considered seals and materials that are compatible with the fuels.

- **Cost of System**

    The cost assessment included development, recurring and life cycle cost of system/engine.

- **System Risk**

    The risk assessment included development and recurring cost and schedule risk.

The evaluation of the eight factors is presented in Table 3-11. The results indicated that $LO_2$-$N_2H_4$ is the best propellant combination of the eight evaluated. Therefore, TRW recommends the use of $LO_2$-$N_2H_4$ in the development of the Space Storable Test Bed Rocket Engine.

Table 3-10. Exhaust Product Constituents

| Propellant Combination | Toxic Constituents | Significant Exhaust Constituents (>1%-mole) | | | | | | | Trace* Constituents | Rating (10-max) |
|---|---|---|---|---|---|---|---|---|---|---|
| | | H | $H_2$ | $H_2O$ | CO | $CO_2$ | $O_2$ | $N_2$ | | |
| $LO_2$-$LH_2$ | - | 2.1 | 43.7 | 54.2 | | | | | | 10 |
| $LO_2$-$CH_4$ | CO | 4.2 | 15.1 | 48.9 | 21.7 | 10.8 | | | $O_2$-0.2% | 5 |
| $LO_2$-$C_3H_8$ | CO | 5.9 | 11.7 | 40.4 | 27.1 | 14.2 | | | 0-0.2%; $O_2$-0.5% | 4** |
| $LO_2$-RP-1 | CO | 6.4 | 10.6 | 33.5 | 32.8 | 15.9 | | | 0-0.2%; $O_2$-0.6% | 4** |
| $LO_2$-$C_2H_5OH$ | CO | 4.5 | 6.7 | 48.6 | 18.4 | 20.0 | 1.5 | | 0-0.3%; OH-0.1% | 4 |
| $LO_2$-MMH | CO | 3.9 | 16.8 | 39.8 | 14.3 | 5.3 | | 19.3 | NO-0.4% | 4 |
| $LO_2$-$N_2H_4$ | - | 2.9 | 15.5 | 48.5 | | | | 32.5 | NO-0.4% | 8 |

*Trace - 0.1-0.5% (mole)

**Industry has found significant carbon formation.

25

Table 3-11. Fuels Evaluation

Indicates Hydrazine is the Best Overall

| Evaluation Factors | Maximum Points | $N_2H_4$ Hydrazine | MMH Monomethyl-hydrazine | $LH_2$ Liquid Hydrogen | $CH_4$ Liquid Methane | $C_3H_8$ Liquid Propane | RP-1 Rocket Fuel | $C_2H_5OH$ Ethyl Alcohol |
|---|---|---|---|---|---|---|---|---|
| Mission/system capability | 25 | 25 | 24 | 14 | 22 | 22 | 22 | 21 |
| Safety considerations | 10 | 9 | 9 | 5 | 10 | 10 | 10 | 10 |
| System integration | 10 | 10 | 8 | 2 | 6 | 6 | 6 | 6 |
| Plume contamination | 10 | 8 | 4 | 10 | 5 | 4 | 4 | 4 |
| Logistics | 10 | 10 | 10 | 6 | 6 | 6 | 8 | 6 |
| Materials compatibility | 5 | 5 | 5 | 3 | 5 | 5 | 5 | 5 |
| Cost of system | 15 | 15 | 12 | 8 | 9 | 9 | 10 | 10 |
| System risk | 15 | 15 | 12 | 8 | 10 | 10 | 10 | 10 |
| Total points | 100 | 97 | 84 | 56 | 73 | 72 | 75 | 72 |

## 3.4 System Requirements

A preliminary set of system and engine requirements have been established based on the system studies and TRW experience with systems and engines. The system analyses indicated that the payload to orbit optimized at 200 lbf thrust and 200 psia chamber pressure. Therefore, this was the recommended design point pending further testing. The preliminary system requirements are shown in Table 3-12. The engine preliminary requirements are shown in Table 3-13. These requirements will be updated as test results necessitating change become available.

## 3.5 Applications Evaluation Conclusions

The maximum mission potential usage for the Space Storable engine is placement of satellites into GEO for NASA, military and commercial applications for communication, surveillance, tracking, earth observation and meteorology.

To achieve this mission potential, an evaluation of the various candidate fuels indicated that $LO_2$-$N_2H_4$ is the best propellant combination and provides the maximum mission/ system capability. The preliminary system and engine requirements provided the basis for the preliminary design and indicated the nominal engine design as follows:

| | |
|---|---|
| Propellants | $LO_2$-$N_2H_4$ |
| Thrust ($F_\infty$) | 200 lbf |
| Chamber Pressure ($P_C$) | 200 psia |
| Specific Impulse ($Isp_\infty$) | 340 lbf-sec/lbm |

Table 3-12.  Propulsion System Requirements.

**System Definition:**

**Integral Propulsion System**

Dual Mode Orbit Boost Subsystem - necessary impulse to place satellite into geosynchronous orbit from the parking orbit established by the expendable launch vehicle (i.e., Atlas IIA)

**Reaction Control subsystem ($N_2H_4$)**

Attitude Control - necessary torques to control spacecraft attitude about all three axes
Stationkeeping (inclination control) - provide necessary impulse to accomplish 0.1-degree inclination limit for 10 years (N-S + E-W)

Disposal - provide impulse to move the spacecraft into a disposal orbit at the end of its operational life

**Configuration - See Attachment**

**Major Components**

Pressurization:  GHe - 7500 psia storage pressure regulated to propellant tank pressure
Graphite/epoxy spherical overwrapped tank with aluminum liner

**Propellant Tanks:**

Oxidizer ($LO_2$) - Cylindrical tanks with elliptical heads - graphite/epoxy overwrapped with aluminum liner - MLI with foam
Two tanks required

Fuel ($N_2H_4$) - Cylindrical tanks with elliptical heads - graphite/epoxy overwrapped with aluminum liner - Two tanks required

**Apogee Engines:**

Thrust - 400 lbf total - two 200 lbf thrust engines - nongimballed - single seat valves
Operation - steady state with maximum firing duration of 3000 seconds
Life - 10,000 seconds (Qualification - 15,000 seconds)
Specific impulse ($Isp_{ss}$) - 340 lbf-s/lbm
Inlet pressure to engine - 350 psia
Engine weight - 11 lbm maximum each

28

Table 3-12. Propulsion System Requirements (Continued)

Heaters required to prevent $N_2H_4$ from freezing
Mixture ratio (O/F) - 0.75 (orifice to $\pm 0.03$)

System:

Total perigee/apogee impulse - $3.7 \times 10^6$ lbf-s (Atlas IIA - 14,750 lbm to LEO)
$\Delta V$ - 14,043 ft/s
RCS $\Delta V$ - 1465 ft/s (N-S + E-W) + 650 lbm usable propellant
Losses: Boil-off = 0.4% $LO_2$; residuals - 1% total propellant; startup/shutdown - 0.5% total propellant
Cleanliness - PR2-2-12

Requirements:

Electrical Interface:

Voltage - 24-34 Vdc nominal using electrical harness to components - valves, heaters, system components
Pigtails shall be used for all electrical components

Mechanical Interface:

Engines - three point mount
Engine length - 29 inches maximum
Valve inlets - pigtails for welding to system manifold

Environments:

Thermal Interface

Interior of spacecraft - 50-80°F
Exterior boundary conditions

Worst case solar inputs; worst case cold - exposure to deep space with no solar inputs

29

Table 3-12. Propulsion System Requirements

**Dynamic-random vibration**

Qualification:
    20 Hz   - 0.026 $g^2$/Hz
    20-50 Hz   - +6 dB/oct
    50-800 Hz   - 0.16 $g^2$/Hz
    800-2000 Hz   - -6 dB/oct
    2000 Hz   - 0.026 $g^2$/Hz

    14.1 g-rms

A/T:
    20 Hz   - 0.01 $g^2$/Hz
    20-160 Hz   - +3 dB/oct
    160-250 Hz   - 0.08 $g^2$/Hz
    250-2000 Hz   - -3 dB/oct
    2000 Hz   - 0.01 $g^2$/Hz

    10.0 g-rms

**Characteristics:**

External leakage (exclusive of engine/thruster valves) - 15 scc/hr GHe
Engine/thruster valve leakage - 5 scc/hr GHe per valve (each propellant)
Propellant tank pressure - fuel pressure +5 psia of oxidizer pressure
Apogee engine alignment - 0.5 degree
Mixture ratio control 0.75 ±0.08 over operational requirements of temperature and pressure including engine O/F tolerance

**Reliability:**

Operating life - 10 years; storage life - 4 years; useful life - 14 years
Reliability of system - 0.955 - no single point failures of active components

**System weight:** Dry weight - TBD lbm

Table 3-13. Engine Requirements

| | |
|---|---|
| Thrust $(F_\infty)$-lbf | $200 \pm 10$ $(890 \pm 45$ N) |
| Mixture ratio (O/F) | $0.75 \pm 0.03$ |
| Specific impulse $(Isp_\infty)$-lbf-s/lbm | $\geq 340$ nominal $(\geq 3334$ N-sec/kg) |
| Inlet pressure - psia | $350^{+0}_{-10}$ $(241^{+0}_{-14}$ N/cm$^2$) |
| Fuel inlet temperature - °F | $70 \pm 10$ (excluding heat soakback) $(21 \pm 6$°C) |
| Oxidizer inlet temperature - °F | -285 (excluding heat soakback) (- 176°C) |
| System mixture ratio | $0.75 \pm 0.08$ (includes pressure and temperature variations) |
| Life - sec | 10,000 (qual - 15,000) |
| Maximum continuous firing - sec | 3000 |
| Operation | Steady state (performance at $>$30 s) |
| Operating voltage - Vdc | 24-34 |
| Engine length - inches | 29 maximum (74 cm) |
| Engine diameter - inches | 12 maximum (30.5 cm) |
| Heaters | Required to prevent fuel from freezing |
| Valve seat leakage (scc/hr GHe) | 5 per valve seat |

Random vibration

| | |
|---|---|
| Qual - 14.1 g-rms | A/T - 10.0 g-rms |
| 20 Hz - 0.026 g$^2$/Hz | 20 Hz - 0.01 g$^2$/Hz |
| 20-50 Hz - +6 dB/oct | 20-160 Hz - +3 dB/oct |
| 50-800 Hz - 0.16 g$^2$/Hz | 160-250 Hz - 0.08 g$^2$/Hz |
| 800-2000 Hz - -6 dB/oct | 250-2000 Hz - -3 dB/oct |
| 2000 Hz - 0.026 g$^2$/Hz | 2000 Hz - 0.01 g$^2$/Hz |

| | |
|---|---|
| Oxidizer-fuel inlet pressure variation | Fuel = $\pm 5$ psia of oxidizer pressure |
| Alignment | $\pm 0.5$ degree |
| Engine weight - lbm | 11 maximum (5 kg) |
| Contamination control | PR2-2-12 Valve must have 25 micron inlet filters |

Table 3-13. Engine Requirements (Continued)

Valve characteristics

| | |
|---|---|
| Pull-in voltage (Vdc) | 19 maximum |
| Dropout voltage (Vdc) | ≥2 |
| Open response (ms) | ≤30 |
| Close response (ms) | ≤30 |
| Maximum pressure (psia) | 400 |

| | |
|---|---|
| Engine starts (cold) | 25 |
| Engine roughness | ±12% |
| Gas ingestion | 2 in$^3$  (33 cm$^3$) |
| Oxidizer depletion | Must have capability |
| Heat shield | Minimum impact on engine temperatures |

## 4.0 ANALYSES

The two major categories of analyses emphasized during the Basic program were performance and thermal. The performance analysis objectives were to establish a model to predict sensitivity to design variables and assess ability to meet performance goals. The thermal analyses objectives were to establish a model to assess thermal operating characteristics of the injector and thrust chamber.

## 4.1 Performance Analyses

### 4.1.1 Analysis of Injector

A model of the coaxial pintle injector was developed by Dr. Richard Priem to calculate the performance based on combustion characteristics using $LO_2$-$N_2H_4$. The prime consideration was the model should predict sensitivity of various combustion parameters to design variables. The model for the fuel centered injector incorporates the following elements:

- Injection velocity – treat fluids as columns that intersect each other. First spray is caused by slots of fuel impinging with oxidizer. Second spray is caused by fuel gap flow between slots impinging on oxidizer.

- Jet size and drop size – jet size of each stream is calculated on the basis of a round jet having the same area as the impinging streams. Drop size is calculated using impinging jet correlation curve of TR 67.

- Vaporization

   - Prior to impingement of first spray

      Assume a gas velocity of flow out of the dome through the spray.
      Using assumed velocity calculate momentum balance to determine radial gas velocity of this flow that would balance a decrease in liquid velocity of the first spray to the point where the radial gas velocity equals the resultant spray velocity.
      Then calculate drag and deceleration of the spray along with the amount vaporized of the fuel and oxidizer as a function of radial position.

   - Vaporization of second spray – determine amount vaporized before spray impinges on wall

33

- Vaporization in chamber

> Assumes spray bounces off chamber wall with average angle
> Break spray into five sections having varying mass and bounce angle
> Calculate the amount vaporized in ten annular sections of the chamber
> With the angle, calculate the length prior to movement out of the annular section
> Use this length to determine effective length
> Mass average all the different parts of the spray and sum each for the various annuli

- Mixing in the chamber - simulate mixing by transferring 10% of each flow from adjacent annuli into each other. This is done on a flux difference basis and area of smaller annuli.

- Final performance - based on O/F in each annuli and mass flow, sum the mass averaged $C^*$ to obtain engine $C^*$ and resultant combustion efficiency.

The results of this model were used to predict the trends for combustion efficiencies ($C^*$) of the various elements. The model was established based on the results obtained on the first element tested (-3) with $LO_2$-$N_2H_4$. These results were used to anchor the model. The model was then used on subsequent elements to predict the performance. Table 4-1 shows the results of the analyses and test results. Increasing the number of slots is the most effective way of increasing combustion efficiency ($C^*$).

## 4.1.2 Nozzle Performance

A two dimensional kinetic analysis was conducted to assess the thrust coefficient and potential vacuum specific impulse achievable for the $LO_2$-$N_2H_4$ engine. The analysis was based on a two zone model operating at mixture ratios (O/F) of 0.875 in the core and 0.5 at the wall to produce an overall engine mixture ratio (O/F) of 0.8. The overall engine characteristics are as summarized follows:

| | |
|---|---|
| Thrust ($F_\infty$) | 200 lbf |
| Chamber Pressure ($P_c$) | 200 psia |
| Nozzle Expansion ($\epsilon$) | 204 |
| Mixture Ratio (O/F) | 0.8 |

The results indicated a vacuum thrust coefficient ($C_{f_\infty}$) including boundary layer losses of 1.89. Based on 94.6% combustion efficiency, the vacuum specific impulse ($Isp_\infty$) would be 340 seconds. The effect of combustion efficiency on specific impulse for the two zone TDK analysis is shown in Figure 4-1.

Figure 4-1.

Effect of Combustion Efficiency on Specific Impulse.

$\varepsilon = 204$
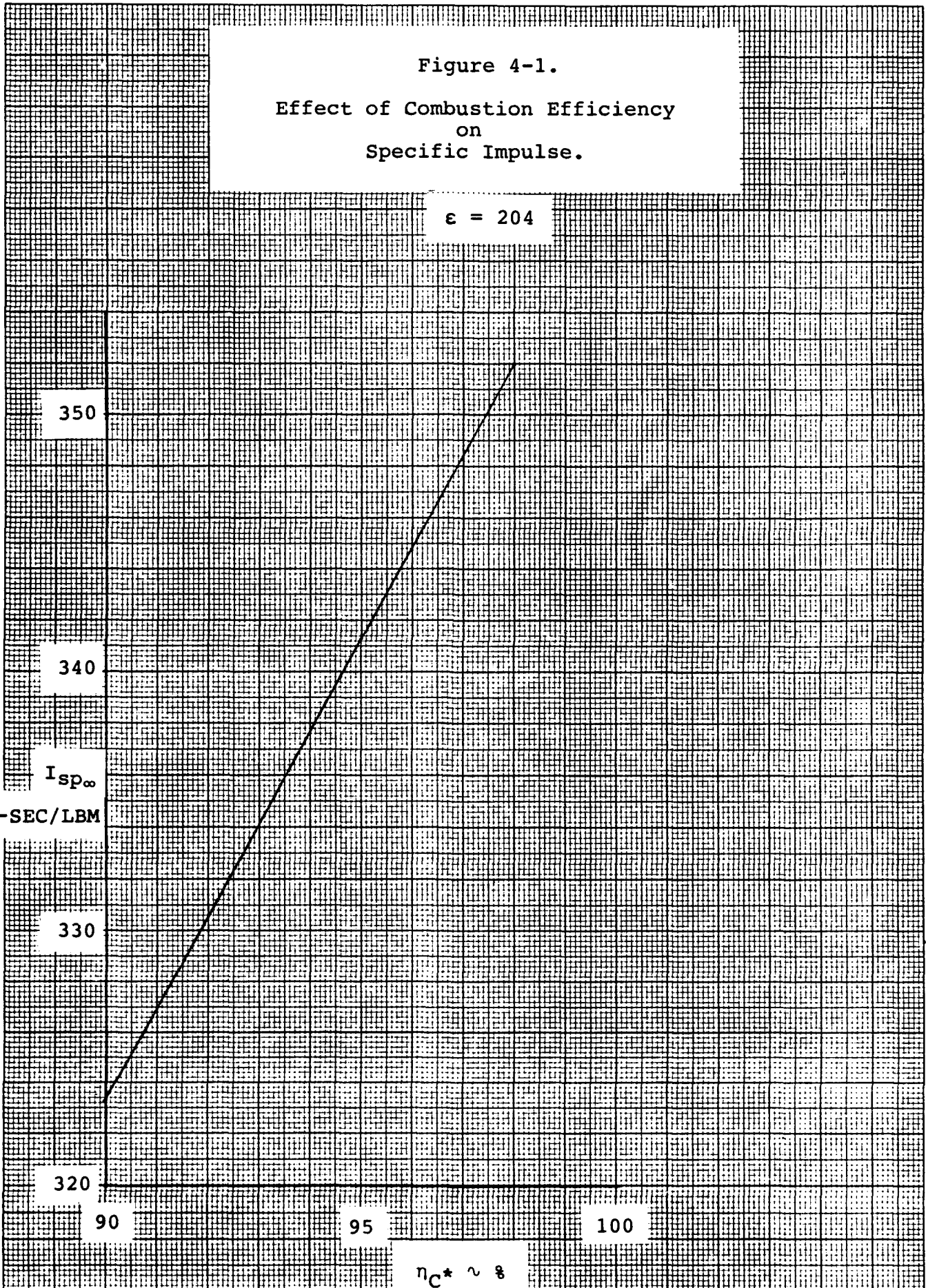
Table 4-1

**Summary of Injector Performance Analyses**
(Fuel Centered Injector)

| ELEMENT CONFIGURATION | NUMBER SLOTS | ASPECT RATIO | $\eta_c^*$ ANALYSIS | $\eta_c^*$ TEST | $Isp_a$(PROTECTED FOR $\epsilon$ = 204) (LBF-SEC/LBM) |
|---|---|---|---|---|---|
| -3 | 30 | 1.6 | 87-90 | 87 | 312 |
| -8 | 36 | 0.7 | 91.8-92.7 | 83.3 | 301 |
| -7 | 40 | 2.2 | 90-92.8 | 91.7 | 331 |
| -9 | 48 | 2.7 | 91.5-94.0 | 91.7 | 331 |
| -10 | 48 | 4.8 | 92.1-94.3 | 91.2 | 329 |
| -11 | 60 | 3.4 | 93-95.3 | 93.3 | 337 |

36

## 4.2 Thermal Analyses

Thermal analyses of the injector and thrust chamber which are shown in Figures 5-1 and 5-2 were conducted to assess areas requiring modifications to the initial design. Thermal models were developed and anchored to test data prior to assessing design capabilities.

### 4.2.1 Injector Thermal Analyses

A SINDA model of the injector dome/neck region was developed to assess combustion gas heating loads from test data. Figure 4-2 shows the locations of the injector thermocouples utilized in test and Figure 4-3 shows a sketch of the model with the thermocouple locations indicated.

The general approach used is presented as follows:

- Film coefficients for the liquid oxygen in the annulus and cone passages were calculated for the forced convection, nucleate boiling, transitional, and film boiling regions using published empirical relations (e.g., Sieder & Tate, Rohsenow, Gambill, and Rocketdyne cryogenic data).

- A heating load was applied from the combustion gases such that the resulting temperatures agreed with measured values.

Results for three cases - low, moderate, and high performance - are presented in the following paragraphs. Higher performance was accompanied by higher heating loads as expected.

- Low Performance. The correlation between measured and predicted dome temperatures for test number, HA2A-4000 (80% $c^*$) is shown in Figure 4-4. The calculated curves were applied to the noted mode numbers of the SINDA model of Figure 4-3. Injector neck temperatures are shown in Figure 4-5. The imposed gas temperature for all zones are shown in Figure 4-6. The higher initial gas temperature ($1650^{\circ}$F) resulted due to the $N_2O_4$-$N_2H_4$ ignition; it then decreased to $450^{\circ}$F at 6.5 seconds when chamber pressure stabilized. The local film coefficients required for the outer zone (Zone 1 in Figure 4-3) was significantly higher than for the other zones. However, Figure 4-7 which shows the transient heat flows, indicated that the $LO_2$ heat absorption requirement at steady-state was only 0.5 Btu/sec.

- Moderate Performance. The correlation of dome and neck temperatures for test number HA4-3999 (87% $c^*$) is shown in Figures 4-8 and 4-9, respectively. The
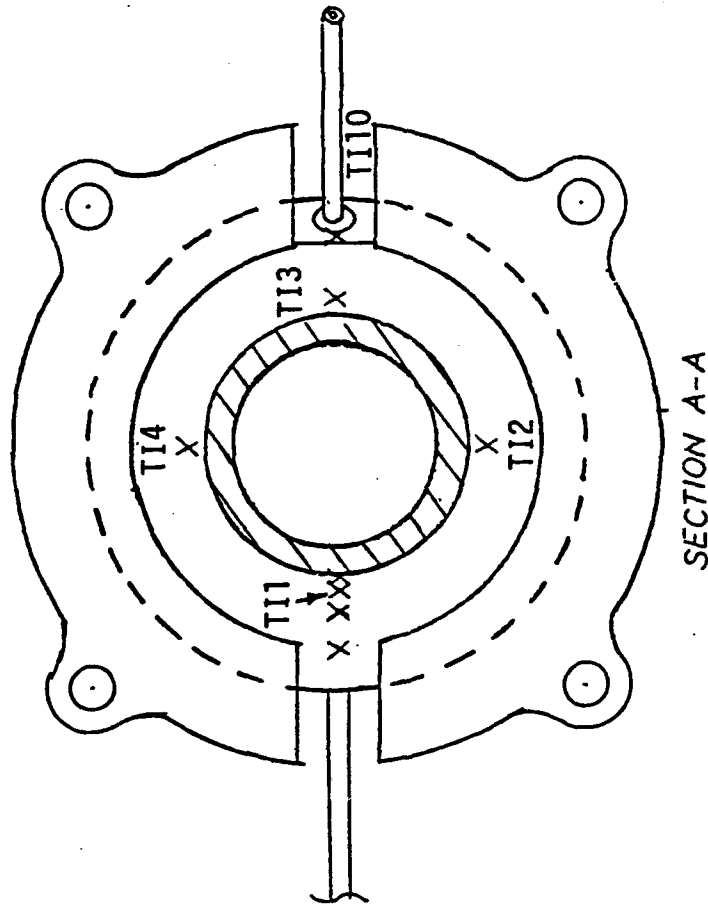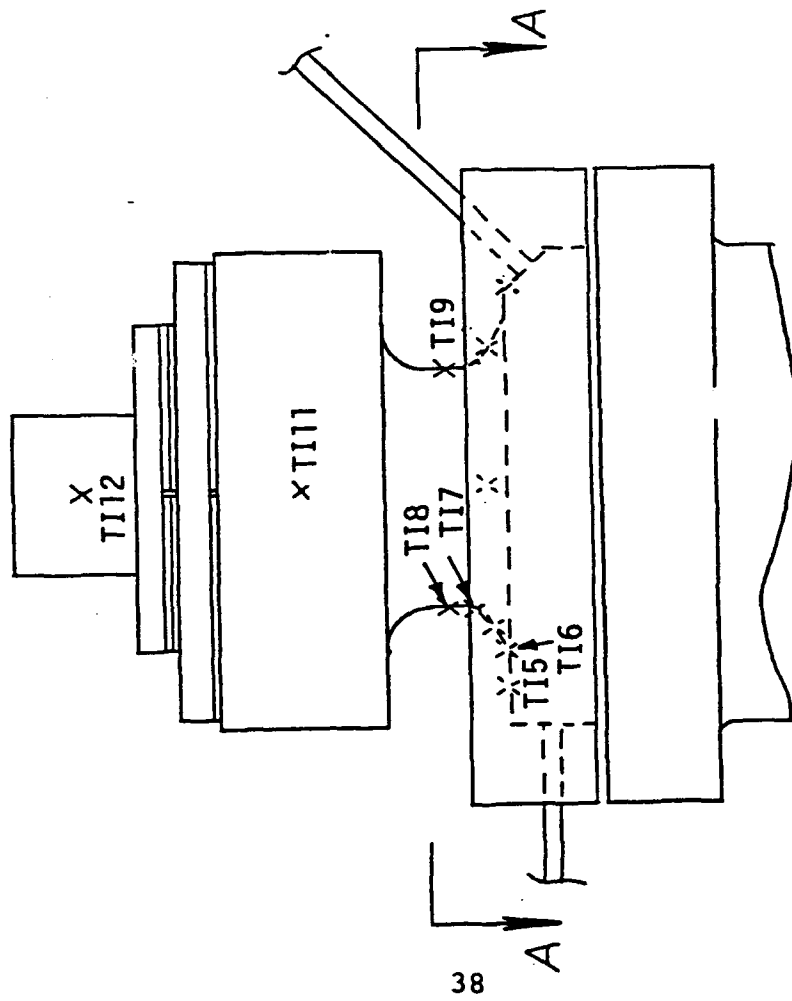
Figure 4-2. SSRT Engine Injector Housing Thermocouple Locations

SECTION A-A

Figure 4-3. SSRT Engine Dome/Neck SINDA Model

39

Figure 4-4. Measured vs Calculated Dome Temperatures - Test HA2A-4000.

Legend:
T211 - Node 211 of SINDA Model of Figure 4-3.
T212 - Node 212 of SINDA Model of Figure 4-3.
⊠ Average Dome Temperature
■ Thermocouple T11 of Figure 4-2.
□ Thermocouple T13 of Figure 4-3.
▲ Thermocouple T14 of Figure 4-3.

40
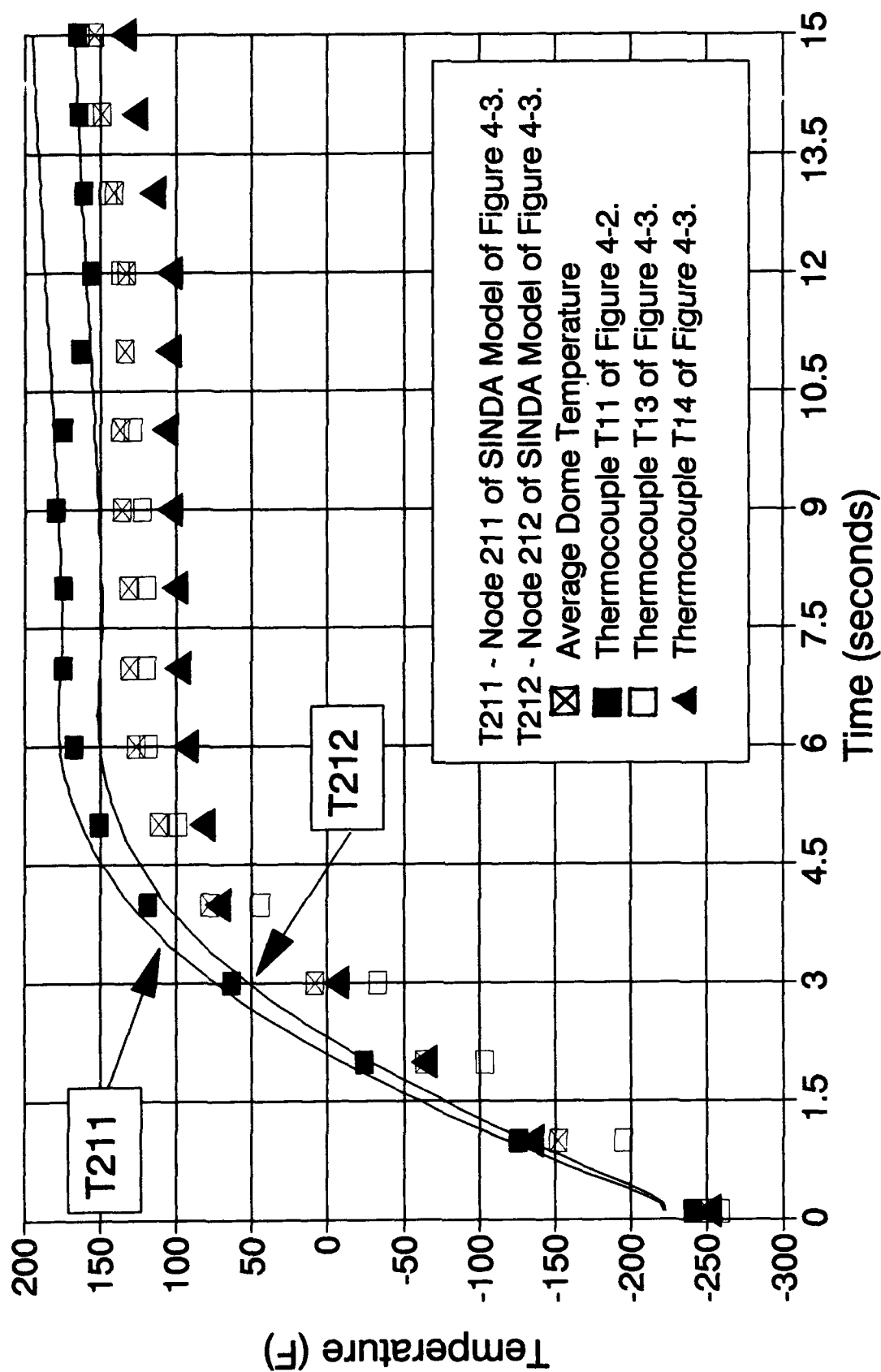
Figure 4-5. Measured vs Calculated Neck Temperatures - Test HA2A-4000.

Legend:
- T74 - Node 74 of SINDA Model of Figure 4-3.
- T84 - Node 84 of SINDA Model of Figure 4-3.
- Average Neck Temperature
- T18 Thermocouple of Figure 4-2.
- T19 Thermocouple of Figure 4-2.
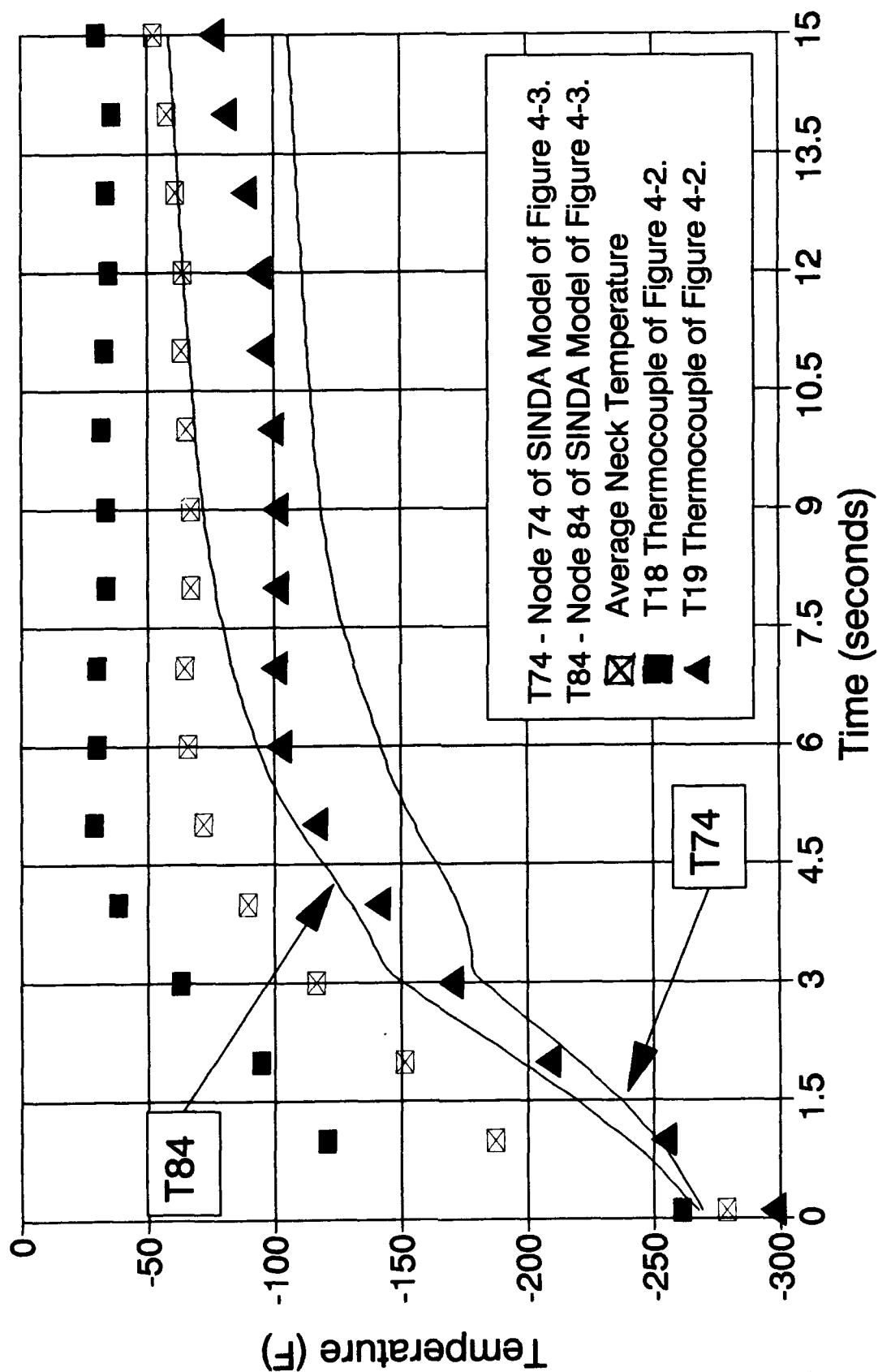
Figure 4-6. Run 4000 Boundary Temp's.

■ ROW 1 MEASURED  ▲ TI11 MEASURED

Hot Gas

Chamber Interface

Head End Interface

Temperature (F)

Time (seconds)
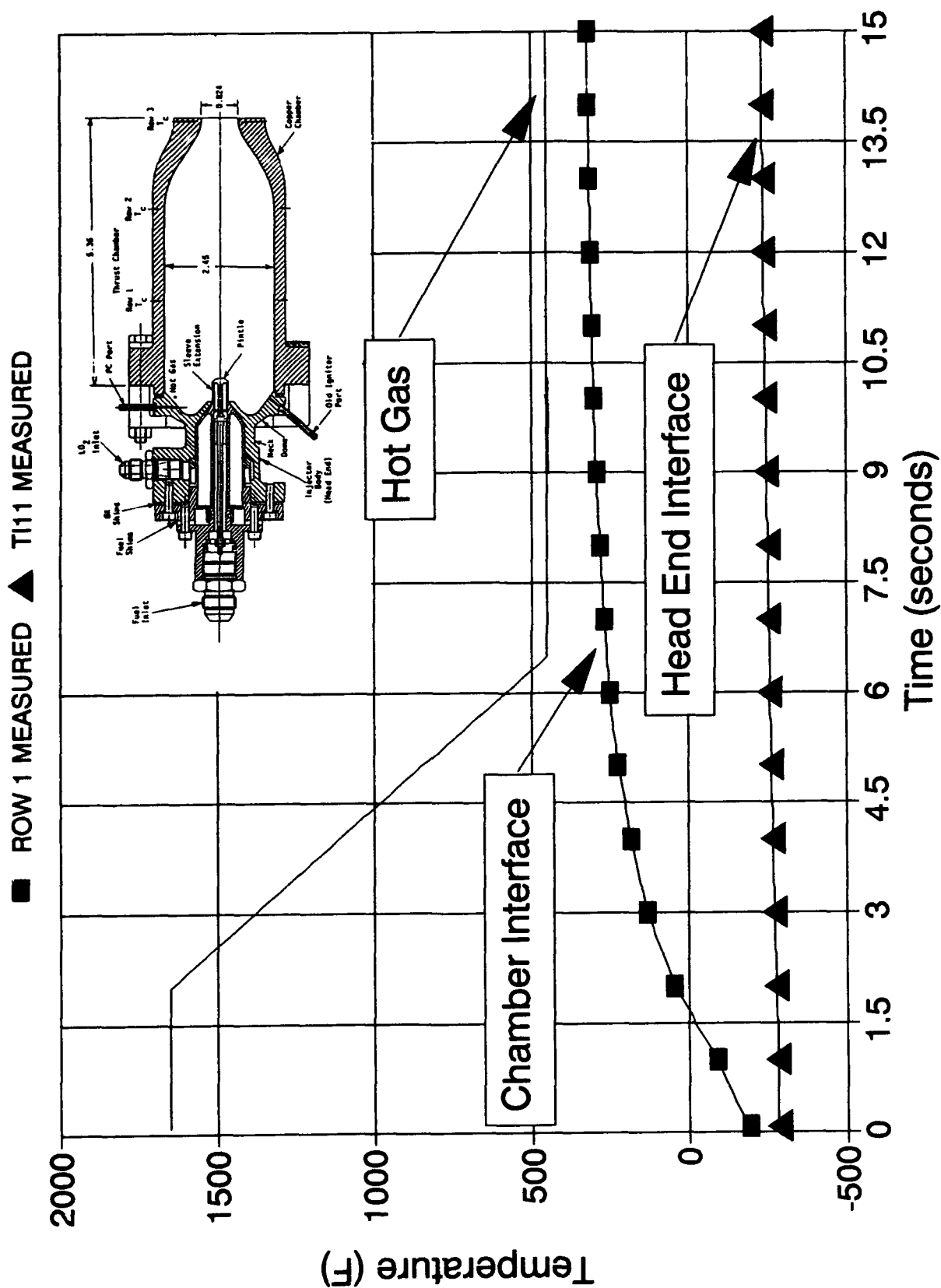
Figure 4-7. Heat Flows - Run HA2A-4000.
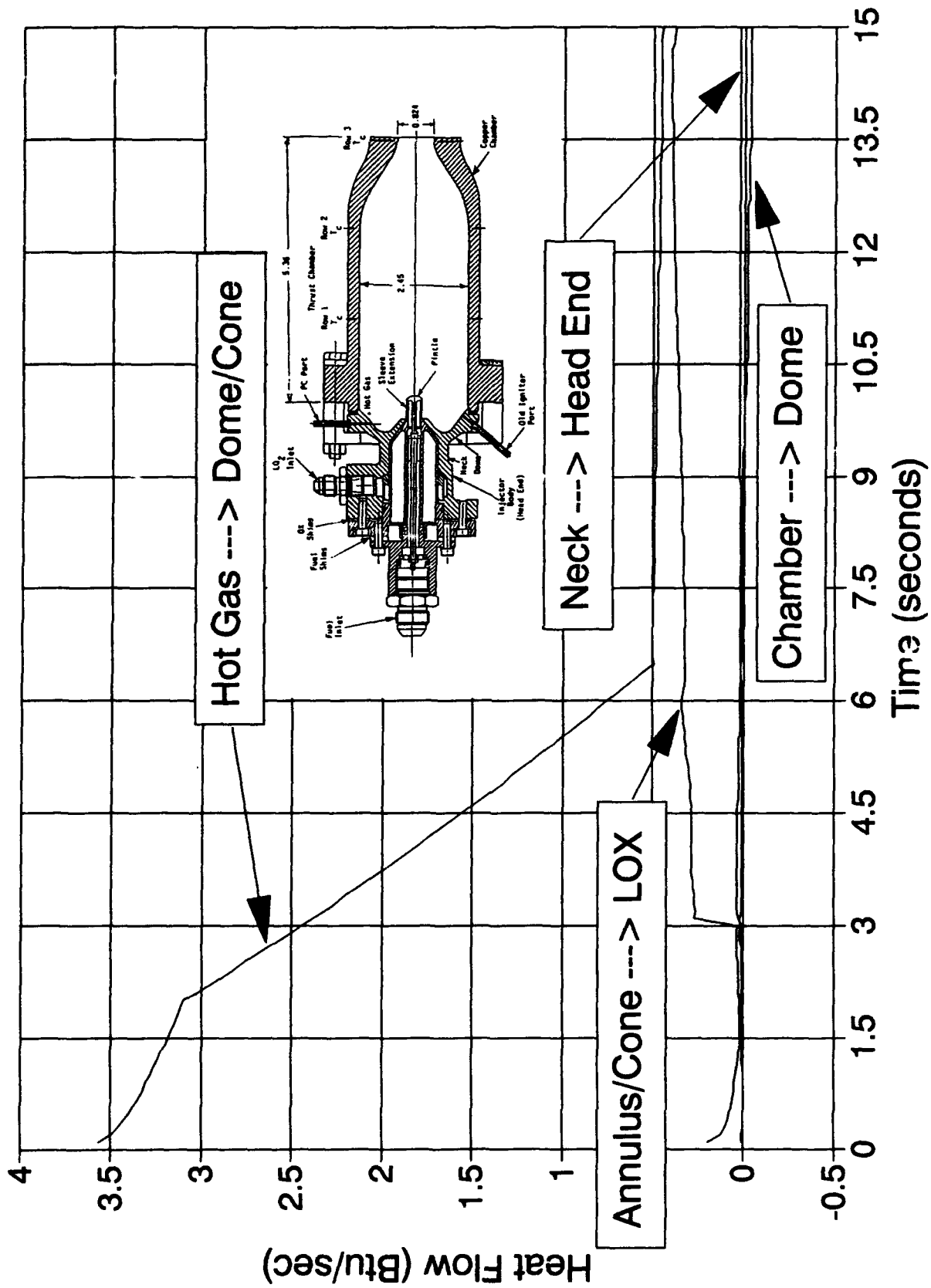
Figure 4-8. Measured vs Calculated Dome Temperatures - Test HA2A-3999

44
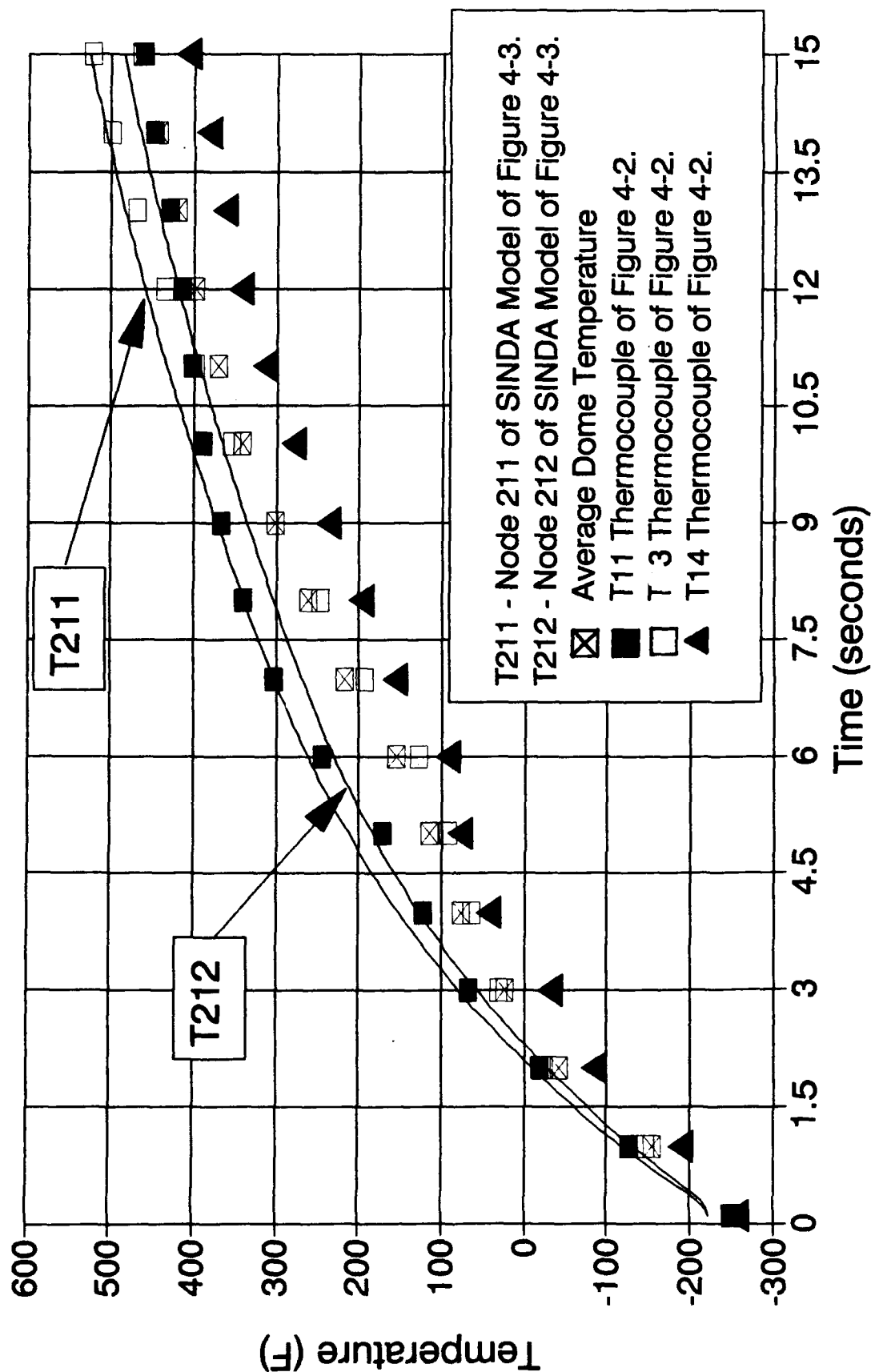
Figure 4-9. Measured vs Calculated Neck Temperatures - Test HA2A-3999.

45
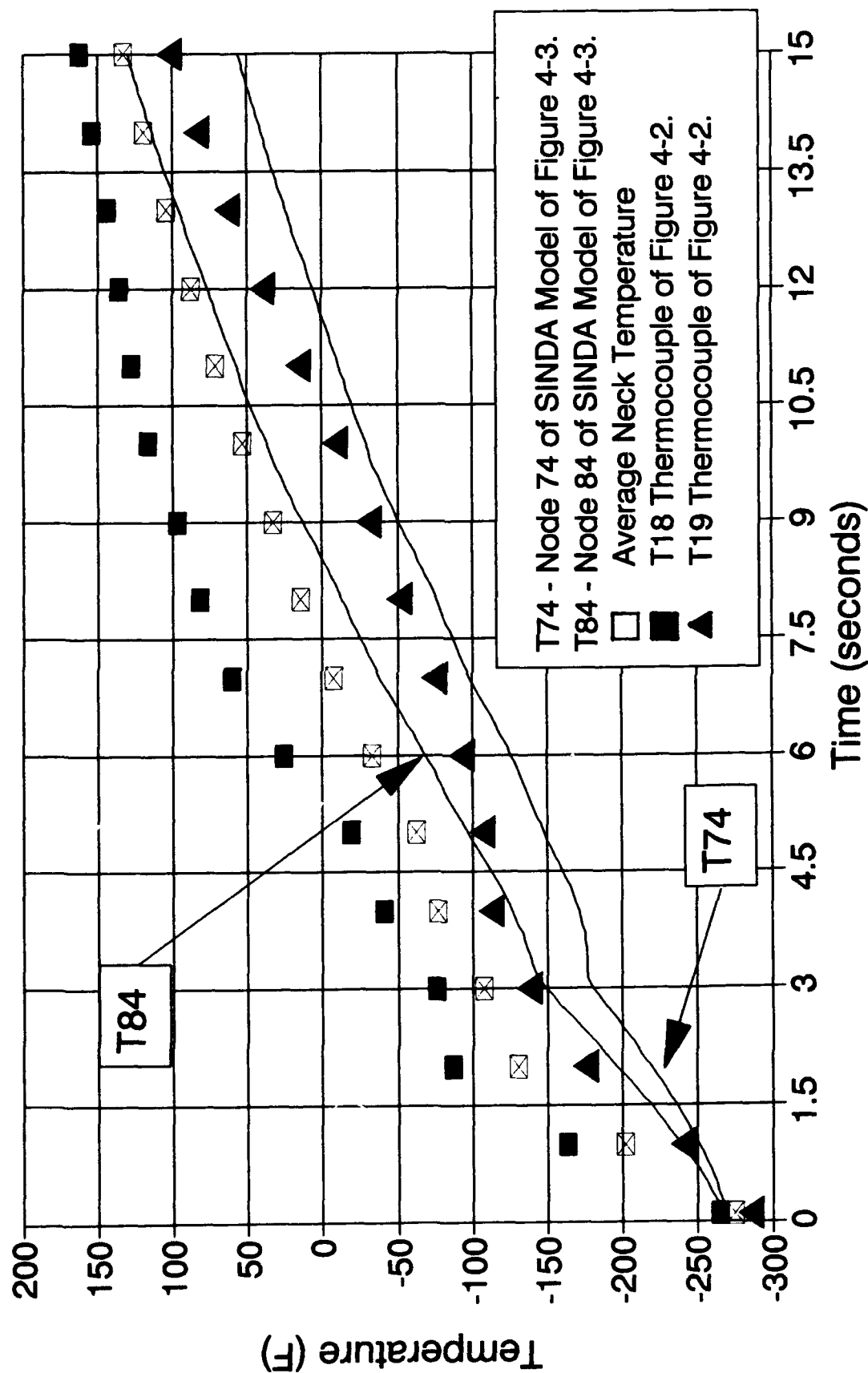
Figure 4-10. Run 3999 Boundary Temp's.

Figure 4-11. Heat Flows - Run HA2A-3999

Hot Gas ---> Dome/Cone

Neck ---> Head End

Annulus/Cone ---> LOX

Chamber ---> Dome

Heat Flow (Btu/sec)

Time (seconds)

47

Figure 4-12. Measured v Calculated Dome Temperatures - Test HA2A-4061

T211

T212

T211 - Node 211 of SINDA Model of Figure 4-3.
T212 - Node 212 of SINDA Model of Figure 4-3.
⊠    Average Dome Temperature
■    Maximum Measured Dome Temperature
▲    Minimum Measured Dome Temperature

Time (seconds)
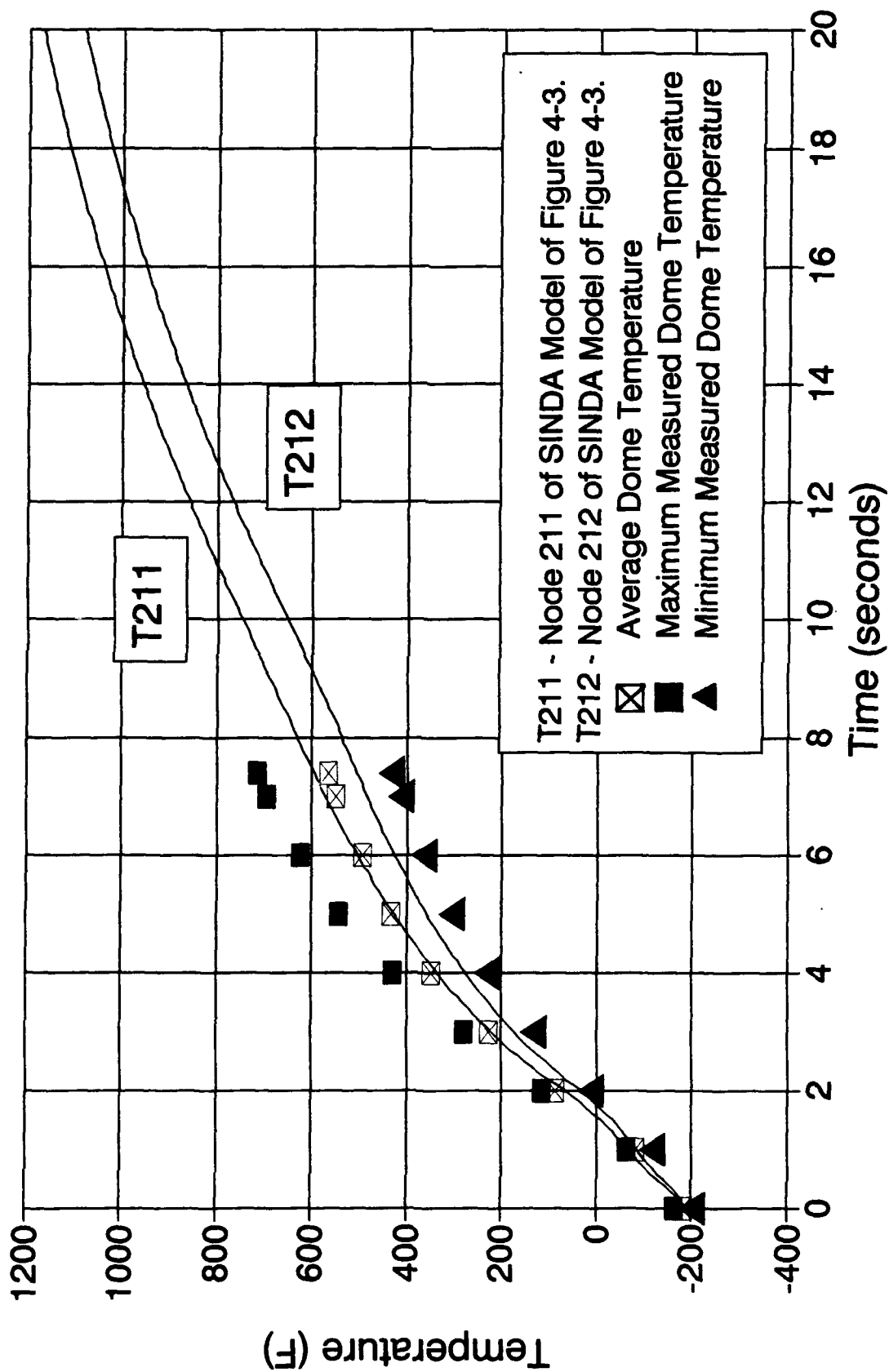
Temperature (F)

Figure 4-13. Measured v Calculated Neck Temperatures - Test HA2A-4061.

Legend:
T74 - Node 74 of SINDA Model of Figure 4-3.
T84 - Node 84 of SINDA Model of Figure 4-3.
⊠  Average Neck Temperature
■  T18 Thermocouple of Figure 4-2.
▲  T19 Thermocouple of Figure 4-2.
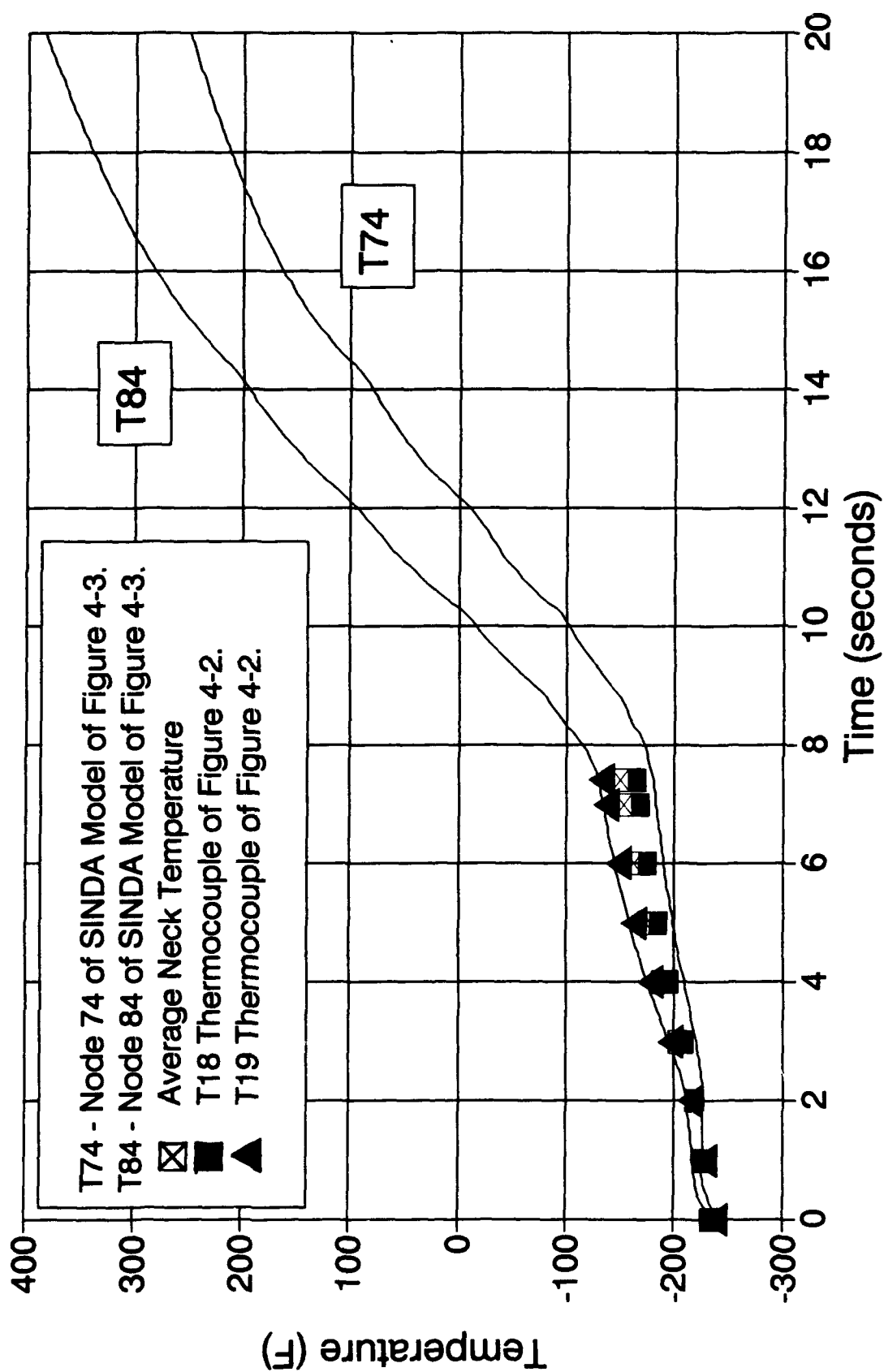
Figure 4-14. Run 4061 Boundary Temp's.
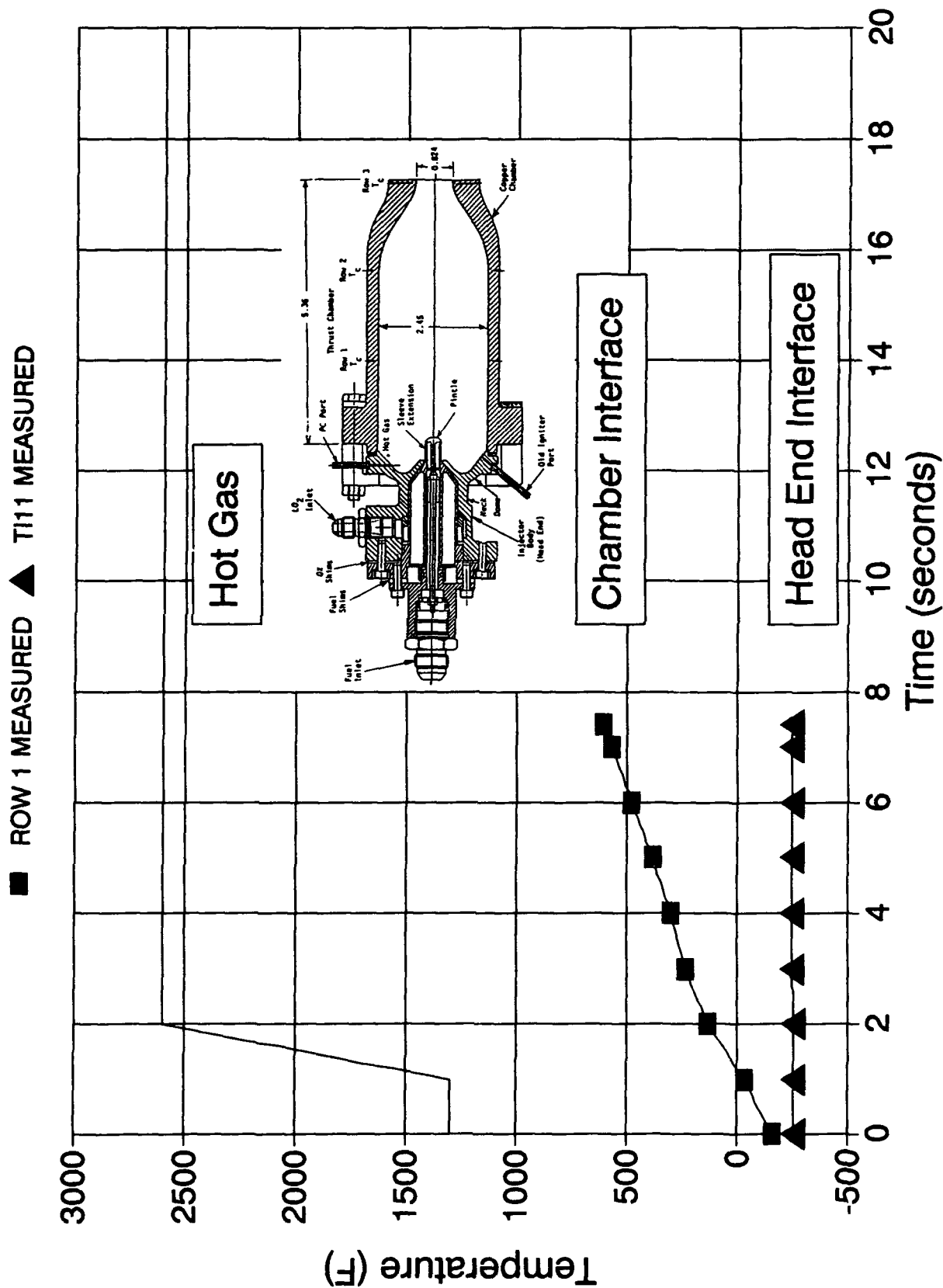
■ ROW 1 MEASURED  ▲ TI11 MEASURED

Hot Gas

Chamber Interface

Head End Interface

50

Figure 4-15. Heat Flows - Run HA2A-4061

51
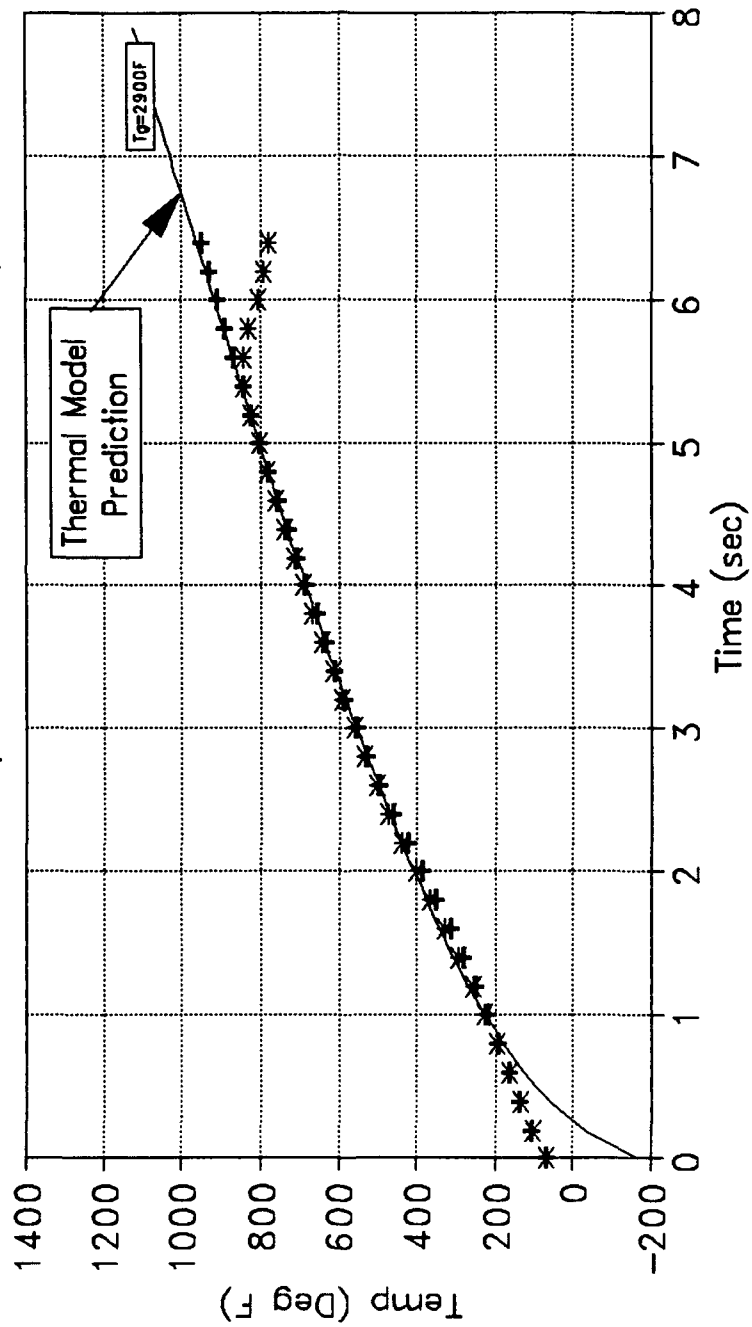
Figure 4-16. Test Data Compared to Thermal Model Result
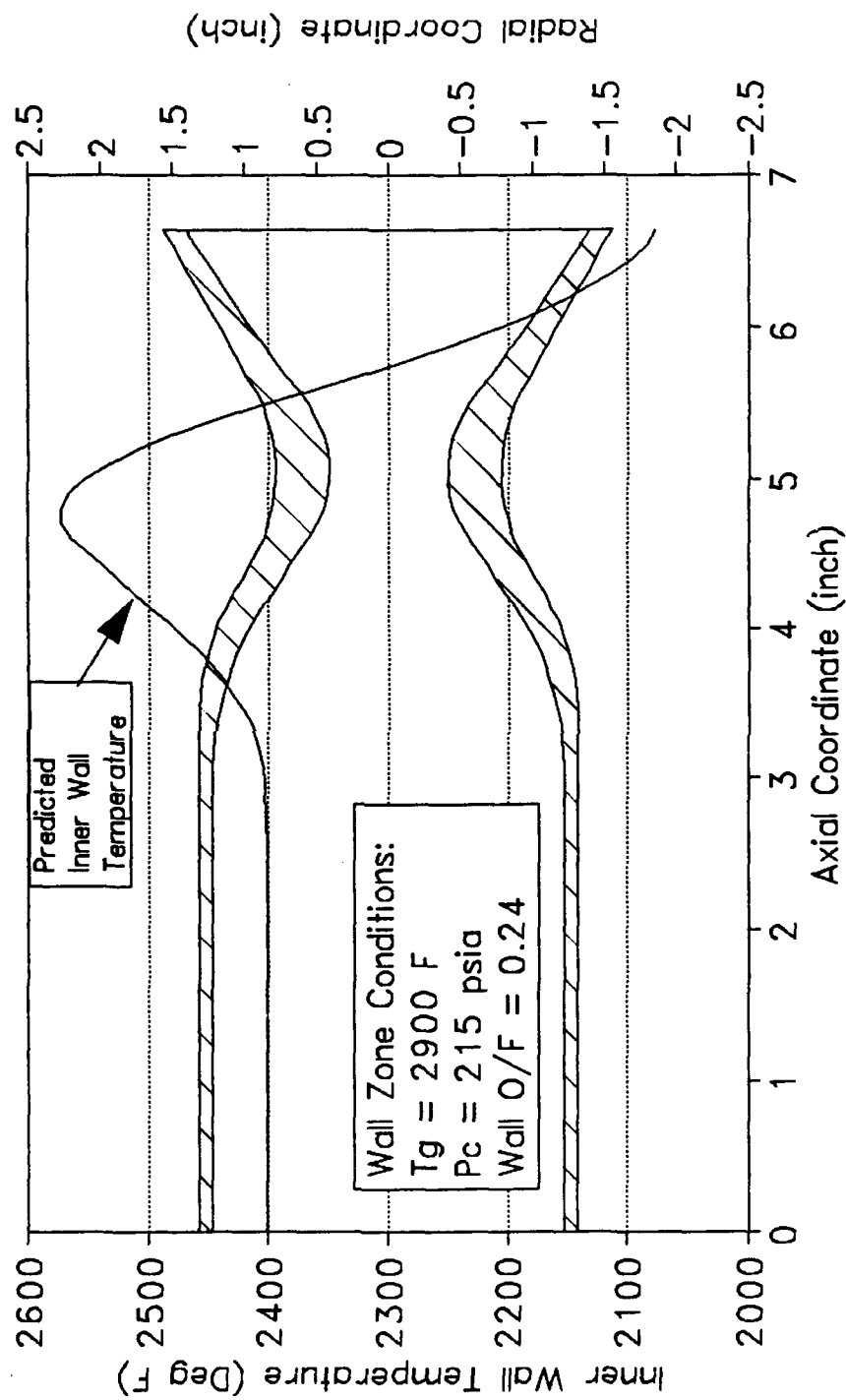
Figure 4-17. Predicted Steady State Columbium Chamber Wall Temperature

53

**Table 4-2**

**Dome Cooling Concepts**

| CONCEPTS | ADVANTAGES | DISADVANTAGES/CONCERNS |
|---|---|---|
| Subcooled LO$_2$ (to-290°F) and maintaining single phase cooling | No injector changes required | Insufficient capability to allow adequate operating margin.<br><br>Adds complexity, weight and cost to system |
| Spiral passage<br>By-passed LO$_2$ cooling | None after investigation | Marginal increase in heat removal capability<br>- Adds significant pressure drop<br>- Wall temperatures operate very close to critical temperature (end point of nucleate boiling prior to entering film boiling)<br>Difficult two-phase flow control<br>Complex design<br>Unknown impact on performance |
| Film cooling | Large margin for cooling<br>Easily adjusted for cooling flowrate<br>Good heat blockage to injector | Adds complexity to design<br>Potential performance impact<br>Concern with fuel migration into cooling orifices |
| Transpiration cooling<br>(Porous type materials/multiples holes) | Large margin for cooling<br>Easily adjusted for cooling flowrate<br>Good heat blockage to injector | Complex design<br>Potential performance impact<br>Materials joining issues |
| Thermal isolation dome | Simple design<br>No performance impact | Hotter dome-outer periphery<br>Material selection issues |
| Thermal blockage<br>(ablative, ceramic, etc.) | Simple design<br>Significant reduction in thermal input | Attachment issues/joint(propellant migration)<br>Issues associated with thermal shock for ceramic and insulative char layer remaining intact for ablative |

54

(inside) and 2410$^O$F (outside).  Therefore, the columbium
thrust chamber is the primary approach.  Rhenium (iridium
coated internally) is the backup approach to the thrust
chamber design which may allow even higher performance.

## 5.0 EXPLORATORY TESTS

### 5.1 Design Approach

The engine design approach was to maximize design and operational flexibility to allow cost effective evaluation of the range of engine parameters. The injector was designed to offer flexibility in test to evaluate the changes necessary to achieve high performance. The goal was to maximize test information for minimum cost. The TRW coaxial injector was ideal for these evaluations as it allowed variations in velocity and geometry of the basic design to be readily tested and assessed.

The exploratory test engine utilized an injector which allowed shimming of the oxidizer and fuel gaps to change velocities and replaceable extensions to change fuel geometry. The thrust chamber for this engine was a robust copper heatsink thrust chamber using thermocouple instrumentation. The injector and thrust chamber were bolted together for ease of testing. Test stand valves were used at this point in the program to eliminate the valve development prior to understanding the specific requirements and interfaces. Pre and post test $GN_2$ purges were used on all propellants. Since the propellants were non-hypergolic, an igniter was required. The igniter used was $N_2O_4$ injected through a port in the injector to ignite with the fuel prior to introduction of $LO_2$. This concept was selected based on ease of design and test.

### 5.2 Engine Design Point

The applications evaluation as discussed in 3.0 evaluated the various fuels and system requirements to maximize payload into orbit. The results indicated the system should be designed to the preliminary requirements of Table 3-12. Based on these preliminary requirements, the engine preliminary requirements of Table 3-13 were developed and provided the design point for the exploratory tests. These requirements also provided the design for the test bed engine as modified based on the exploratory test results.

### 5.3 Design Description and Fabrication

The TRW coaxial injector for the SSRT program was based on the DM-LAE qualified and flying successfully on ANIK satellites (E-1 and E-2). These engines produce an average specific impulse of 314.5 lbf-sec/lbm ($\epsilon$ = 204) and have demonstrated almost 25,000 seconds operating life during qualification with $N_2O_4$-$N_2H_4$.

56

The SSRT injector consisted of the following elements:

- Body of columbium with aluminide coated face (oxidation protection)
- Sleeve of 15-5 pH incorporating thermal isolation of $LO_2$ and $N_2H_4$
- Pintle of 15-5 PH
- Extensions of 15-5 PH incorporating various slot geometries
- Igniter to inject $N_2O_4$ to react with $N_2H_4$ prior to $LO_2$ injection.

The injector in the copper heatsink thrust chamber is shown in Figure 5-1 and photographs of hardware are shown in Figure 5-2. Injector configurations are changed by replacing sleeve extensions to assess variations in fuel slot geometry. Additionally velocity changes can be varied by independently shimming the oxidizer and fuel gaps. Six fuel geometries were evaluated using five different configuration sleeve extensions with the standard pintle. The highest performance sleeve with a pintle incorporating three doublets (designated hybrid) which bleeds fuel into the center of the engine was tested to enhance performance. The slot configurations varied from 36-60 slots with slot widths of 8-16 thousands of an inch and aspect ratios (slot depth/slot width) of 0.67-4.8. These wide variations in fuel geometry along with variations in fuel gaps and oxidizer gaps provided the ability to test over a range of large variations to assess performance characteristics. This flexibility provided a method to obtain affordable test costs with major geometry changes in the injector.

The thrust chamber used during this basic program was a robust heatsink copper chamber with type K thermocouples brazed into the wall at three axial locations and four thermocouples at each station ($90^\circ$ apart). This instrumentation allowed an assessment of the thermal conditions of the thrust chamber.


## 5.4 Test Summary

### 5.4.1 Test Plan

As part of the SSRT basic program, exploratory hot fire tests were defined to provide input to the engine design. These tests were performed using the TRW IR&D hardware that was tested in 1990.

The exploratory tests performed in the basic program were structured to provide basic engineering information relating to the performance and thermal aspects of the design. Some of the issues addressed were:

57
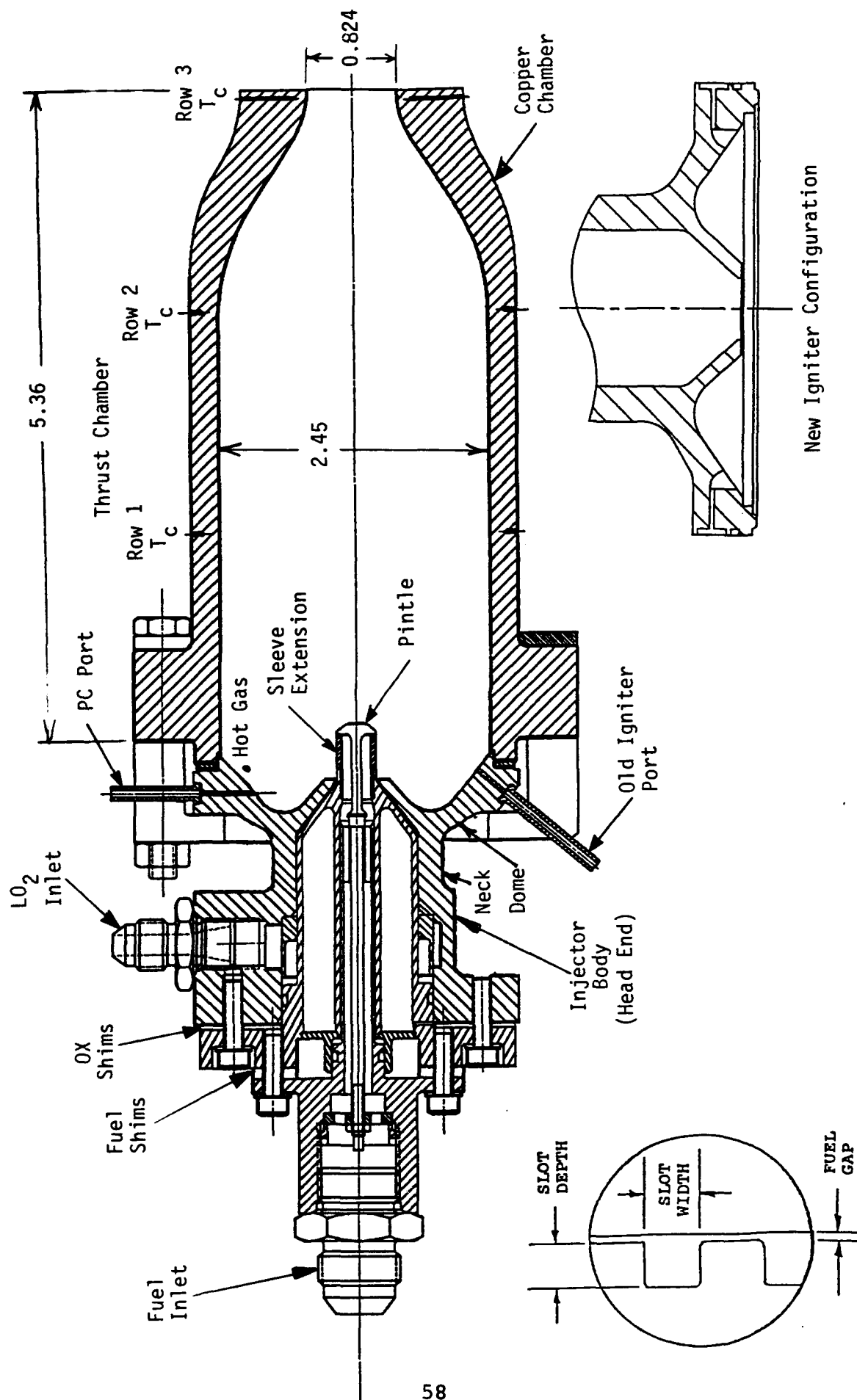
Figure 5-1. LO$_2$/Hydrazine Engine with Copper Chamber.

58

N₂O₄ IGNITER INLET

INJECTOR ASSEMBLY

CHAMBER PRESSURE PORT

-11 EXTENSION

-10 EXTENSION

-9 EXTENSION

N₂O₄ IGNITER INLET

INJECTOR BODY

PINTLE

SLEEVE

EXTENSIONS

COPPER THRUST CHAMBER
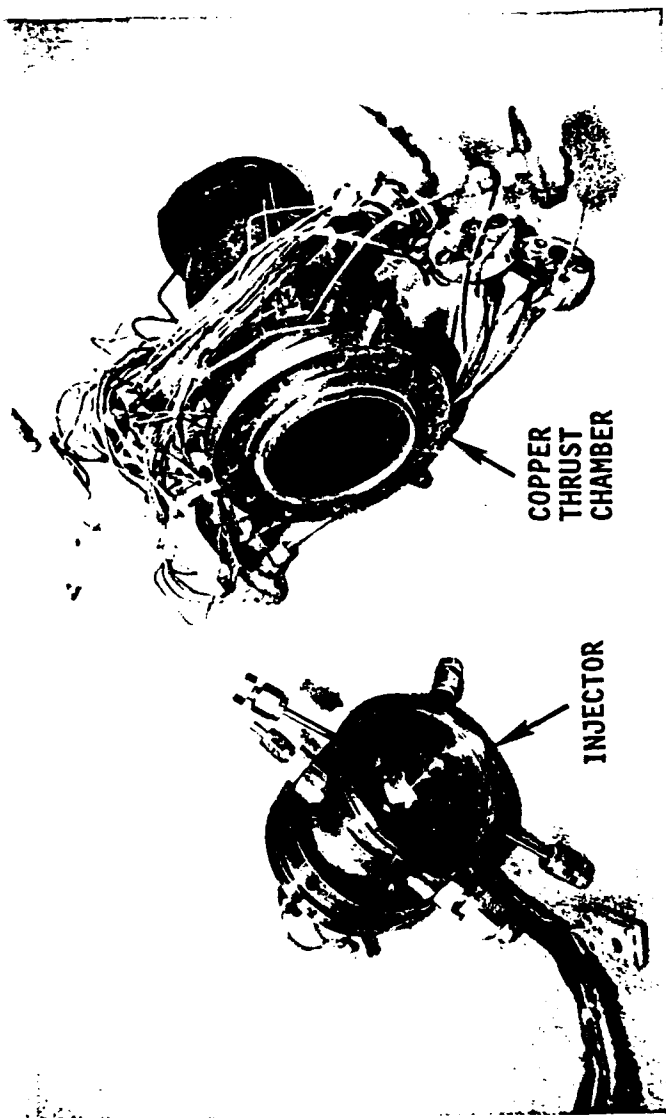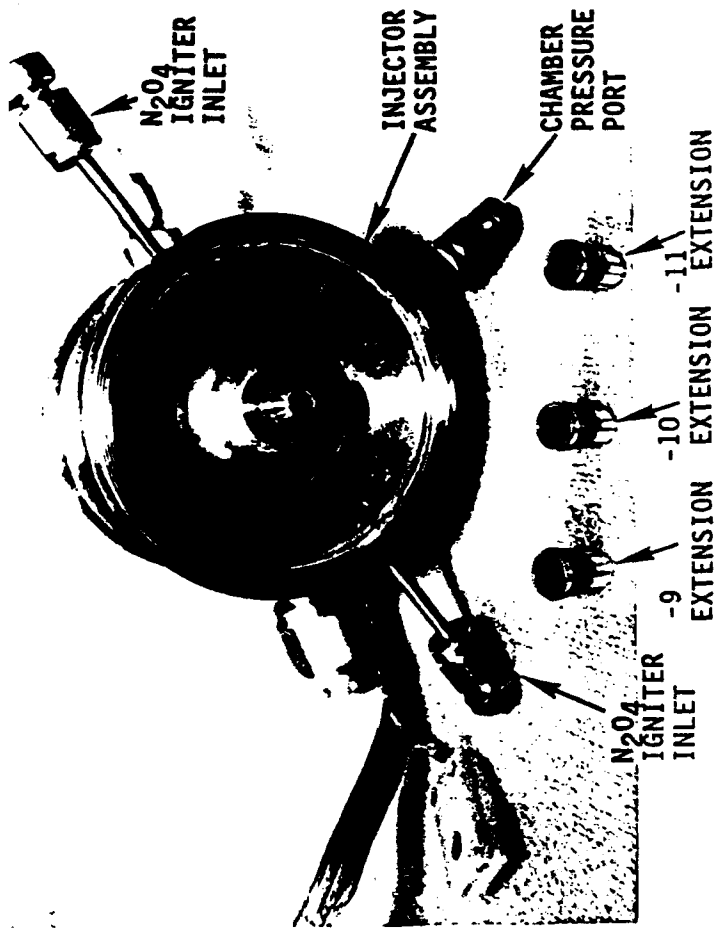
INJECTOR

Figure 5-2. Engine Hardware.

- Engine combustion performance characteristics
- Stable operation
- Engine thermal characteristics
- Injector characteristics
- Comparison of $LO_2/N_2H_4$ to hypergolic earth storable propellants
- Ignition characteristics with $N_2O_4$
- Hardware and system chill

Two test series were performed during the basic program. The first series addressed the differences between the $LO_2/N_2H_4$ propellant combination and the hypergolic propellant engines using the -8 fuel element. Also included in the first series was testing of the -7 fuel element, which is the baseline 200 lbf thrust fuel element (see table 4-1).

A second test series was performed, incorporating hardware modifications based on the initial test series results. Three new 200 lbf equivalent fuel elements were evaluated in this series, as was a modification to the injector pintle.


5.4.1.1 Test Facility

All hot fire testing of the SSRT engine in the basic program was performed at TRW's Capistrano Test Site (CTS) Facility in the HEPTS HA2A vacuum capsule. A facility schematic is shown in Figure 5-3. A mechanical pumping system maintained the test cell at less than 50 torr absolute pressure for all hot fire testing.

The fuel propellant tank was an 80 gallon hydrazine tank with an outer glycol jacket that allowed thermal conditioning of the propellant. Liquid oxygen propellant tankage included a 150 gallon run tank, fed from a 300 gallon $LO_2$ storage tank. Both $LO_2$ tanks were vacuum insulated. The $LO_2$ in the run tank was kept at its normal boiling point (-298F) by venting the tank to atmospheric pressure between tests. $LO_2$ propellant lines to the test capsule were insulated, and were chilled prior to a test by bleeding $LO_2$ from the run tank to the fire valve. The line downstream of the $LO_2$ fire valve and the injector were pre-chilled by liquid nitrogen prior to each test.

The igniter fluid was supplied by a small N2O4 tank and controlled by a cavitating venturi. Propellant line heaters were used on the fuel and igniter lines to prevent freezing of the propellants during engine start-up. All propellant lines were purged with GN2 during the start up and shutdown transients. All valve timing was controlled by an IBM PC based timer that allowed millisecond timing resolution of the valve command signals.
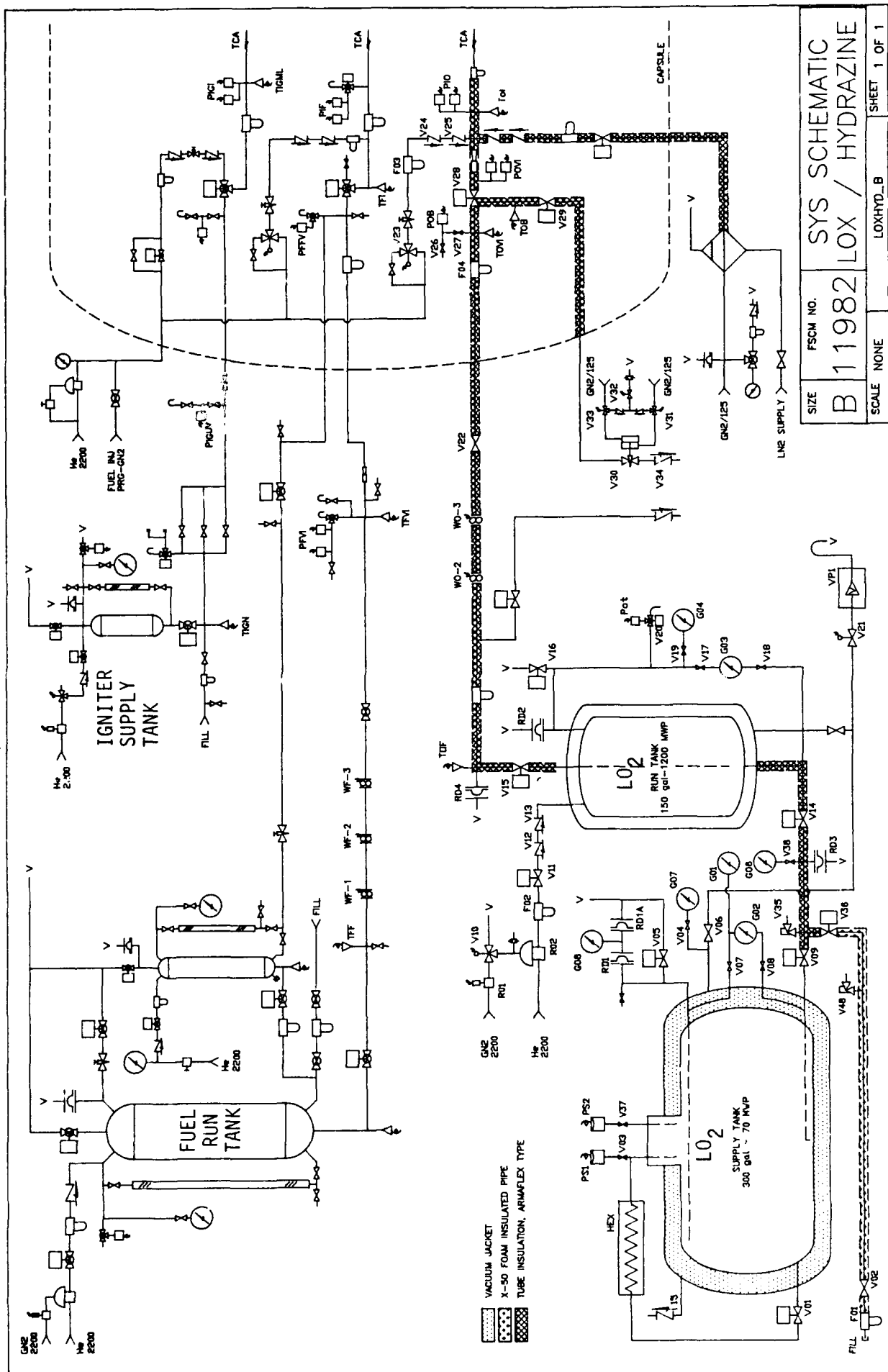
Figure 5-3. Test Facility Schematic.

## 5.4.1.2 Test Instrumentation and Data Recording

Performance evaluation of the SSRT engine was based on C* performance measurements. Redundant instrumentation was used on all performance related parameters, including propellant flow rates, chamber pressure transducers, and venturi inlet pressures. Cavitating venturis were used to control the flow rates to the engine. These venturis have been water flow calibrated. Three calibrated flowmeters in series were used to measure the fuel flow rate. The oxidizer flow rate was determined by use of a cavitating venturi.

Thermocouple instrumentation included 12 type K thermocouples brazed into the copper chamber. Also, 12 thermocouples were located at key locations on the injector to allow an assessment of the thermal characteristics of the injector head end. Other thermocouple instrumentation included propellant temperatures at the flowmeters, venturi inlets and engine inlets. An instrumentation list is presented in Table 5-1.

Critical temperature measurements such as chamber and injector dome temperatures were displayed on strip charts for real time monitoring during testing. Early shutdown of a test was determined by strip chart trends. Oscillograph recording of critical parameters was available for quick look and transient analysis of each test. All instrumentation was recorded on digital tape and printed in numeric format for data reduction analysis.

## 5.4.2 Test Summary of -8 Fuel Element

Initial hot fire testing of the SSRT engine was performed with the -8 fuel element. This extension was designed based on the TRW Dual Mode Liquid Apogee Engine (DM-LAE) fuel geometry. The -8 element was designed to match the fuel injection geometry and flow characteristics of the DM-LAE engine as closely as possible. This allowed a direct comparison of the operating trends of the non-hypergolic $LO_2/N_2H_4$ propellant combination verses the well characterized $N_2O_4/N_2H_4$ propellant combination utilizd by the DM-LAE engine. The nominal flow rate for this element was established at an equivalent thrust of 125 lbf to match the fuel injection characteristics of the DM-LAE engine.

Twenty-five tests were performed with the -8 element, ac-cummulating 306.5 seconds of hot fire duration. The test results for the -8 element are summarized in Table 5-2. Performance of the element was approximately 83% C* efficiency, compared to approximately 95% C* efficiency for the DM-LAE Engine. Many of the DM-LAE performance trends were non existent or not as clearly defined during testing of the SSRT engine with the -8 element.

TABLE 5-1
SSRT INSTRUMENTATION LIST

| ID | RANGE | RECORD/DISPLAY METHOD | | | PARAMETER |
|---|---|---|---|---|---|
| | | S/C | OSC | DVM | |
| PC-1 | 0-300 PSIA | X | X | X | CHAMBER PRESSURE |
| PC-2 | 0-300 PSIA | | | | CHAMBER PRESSURE |
| PIO-1 | 0-1000 PSIA | X | X | | OXID INLET PRESSURE |
| PIO-2 | 0-750 PSIA | | | | OXID INLET PRESSURE |
| PID | 0-500 PSIA | | | | OXID DISTRIBUTION PRESSURE |
| PIF-1 | 0-1000 PSIA | X | X | | FUEL INLET PRESSURE |
| PIF-2 | 0-750 PSIA | | | | FUEL INLET PRESSURE |
| POVI-1 | 0-1000 PSIA | | X | | OX VENTURI INLET PRESSURE |
| POVI-2 | 0-1000 PSIA | | | | OX VENTURI INLET PRESSURE |
| PFVI-1 | 0-1000 PSIA | | X | | FU VENTURI INLET PRESSURE |
| PFVI-2 | 0-1000 PSIA | | | | FU VENTURI INLET PRESSURE |
| WO-1 | 0.15-0.30 LBM/S | | X | X | OXID FLOWRATE |
| WO-2 | 0.15-0.30 LBM/S | | | | OXID FLOWRATE |
| WO-3 | 0.15-0.30 LBM/S | | | | OXID FLOWRATE |
| WF-1 | 0.20-0.40 LBM/S | | X | X | FUEL FLOWRATE |
| WF-2 | 0.20-0.40 LBM/S | | | | FUEL FLOWRATE |
| WF-3 | 0.20-0.40 LBM/S | | | | FUEL FLOWRATE |
| TOF | -350 to -200°F | | | | OXID FEEDLINE TEMP |
| TFF | 40-100°F | | | | FUEL FEEDLINE TEMP |
| TFI | 40-100°F | | | X | FUEL INLET TEMP |
| TOI | -350 to -200°F | | | X | OXID INLET TEMP |
| TOVI | -350 to 60°F | | | | OXID VENTURI TEMPERATURE |
| PIGT | 0-1000 PSIA | | | X | IGNITION TANK PRESSURE |
| PIGFV | 0-1000 PSIA | | | | IGNITION FIRE VALVE PRESS |
| PIGI-1 | 0-500 PSIA | X | X | | IGNITION INLET PRESSURE |
| PIGI-2 | 0-500 PSIA | | | | IGNITION INLET PRESSURE |
| TIGN | 40-100°F | | | | INGITION INLET TEMP |
| PA-1 | 0-50 TORR | | | X | CELL PRESSURE |
| PA-2 | 0-50 TORR | | | | CELL PRESSURE |
| POT | 0-1000 PSIA | | | X | OXID TANK PRESSURE |
| PFT | 0-1000 PSIA | | | X | FUEL TANK PRESSURE |
| TR-1 | 0-2000°F | X | | | CHAMBER/NOZZLE TEMPS |
| THRU | | | | | |
| TR-12 | 0-2000°F | X | | | CHAMBER/NOZZLE TEMPS |
| TI-1 | -300-1000°F | X | | | INJECTOR TEMPS |
| THRU | | | | | |
| TI-12 | -300-1000°F | X | | | INJECTOR TEMPS |
| TC-1 | 0-2500°F | X | | | TC PROBE TEMPS |
| THRU | | | | | |
| TC-16 | 0-2500°F | X | | | TC PROBE TEMPS |
| ACCEL | 0-100 Gs | | X | | HEA ACCELEROMETER |

*ALL PARAMETERS TO BE RECORDED ON DIGITAL TAPE.

# Table 5-2
## -8 Fuel Element Test Summary

| Test # HA2A- | Duration sec | O/F | Wt lb/sec | PC psia | C* ft/sec | Fuel Gap (df) | OX Gap (do) |
|---|---|---|---|---|---|---|---|
| 3992 | 5.0 | 0.717 | 0.3592 | 114.4 | 5443 | 0.0031 | 0.0083 |
| 3993 | 10.0 | 0.575 | 0.3126 | 84.8 | 4636 | 0.0031 | 0.0083 |
| 3994 | 10.0 | 0.550 | 0.3080 | 87.5 | 4856 | 0.0051 | 0.0083 |
| 3996 | 10.0 | 0.839 | 0.3601 | 111.4 | 5288 | 0.0031 | 0.0083 |
| 3998 | 10.0 | 0.786 | 0.3634 | 108.5 | 5124 | 0.0031 | 0.0063 |
| 3999 | 15.0 | 0.796 | 0.3641 | 112.8 | 5345 | 0.0031 | 0.0083 |
| 4000 | 15.0 | 0.776 | 0.3607 | 103.4 | 4926 | 0.0031 | 0.0103 |
| 4001 | 15.0 | 0.806 | 0.3674 | 106 | 4960 | 0.0042 | 0.0083 |
| 4002 | 15.0 | 0.832 | 0.4473 | 141.9 | 5490 | 0.0042 | 0.0083 |
| 4003 | 15.0 | 0.808 | 0.3674 | 109.1 | 5120 | 0.0024 | 0.0083 |
| 4004 | 14.8 | 0.830 | 0.4476 | 127.5 | 4912 | 0.0024 | 0.0093 |
| 4005 | 13.0 | 0.827 | 0.4498 | 129.2 | 4958 | 0.0042 | 0.0093 |
| 4006 | 15.0 | 0.782 | 0.3650 | 101.9 | 4798 | 0.0007 | 0.0093 |
| 4007 | 15.0 | 0.791 | 0.3634 | 105.7 | 5011 | 0.0007 | 0.0093 |
| 4008 | 15.0 | 0.789 | 0.3630 | 101.5 | 4805 | 0.0007 | 0.0093 |
| 4009 | 15.0 | 0.832 | 0.4475 | 125.6 | 4843 | 0.0007 | 0.0093 |
| 4010 | 15.0 | 0.799 | 0.3656 | 108.4 | 5112 | 0.0053 | 0.0062 |
| 4011 | 15.0 | 0.786 | 0.3628 | 109.5 | 5207 | 0.0082 | 0.0043 |
| 4012 | 8.9 | 0.787 | 0.3635 | 110.3 | 5215 | 0.0007 | 0.0043 |
| 4013 | 14.8 | 0.754 | 0.3544 | 105.6 | 5142 | 0.0031 | 0.0083 |
| 4014 | 15.0 | 0.780 | 0.3247 | 94.9 | 5029 | 0.0019 | 0.0083 |
| 4015 | 15.0 | 0.616 | 0.3653 | 106.9 | 5033 | 0.0019 | 0.0083 |
| 4016 | 15.0 | 0.841 | 0.4869 | 145.5 | 5185 | 0.0019 | 0.0083 |

Difficulties in obtaining single phase liquid oxygen flow to the injector caused poor repeatability of the test data, and resulted in no clear-cut performance trends with varying injector parameters. The most significant factor affecting performance was the amount of pre-chill to the injector and $LO_2$ run line bleed. Injector pressure drops and discharge coefficients on the oxidizer circuit varied by ±35% during testing and averaged 20% lower than the oxidizer Cd measured during water flow of the injector, indicating vapor generation and two phase flow conditions.

Incomplete fuel vaporization was evidenced by the chamber wall thermocouple data. Row 1 measurements showed a tendency to operate near the fuel saturation temperature, indicating liquid fuel impingement at the wall. Throat thermocouple data also corresponded to a low wall zone mixture ratio. Test durations for all -8 testing was limited by injector dome redline temperatures (500F) rather than chamber thermocouple redline (1000F).

The igniter for these tests was the same configuration tested in the 1990 IR&D program; a single $N_2O_4$ stream directed through the fuel spray pattern. This configuration caused a high heat load to one side of the dome during the igniter stage, resulting in a thermal maldistribution in the injector at the start of the test.

On test HA2A-4002, a reaction of fuel and $N_2O_4$ in the igniter line (located at 6 o'clock) caused the line to rupture. The engine was removed from the stand and a new igniter configuration was employed. The old igniter port was welded shut and two new ports, located 180 degrees apart (at 9 and 3 o'clock), were machined into the injector dome (see Figure 5-1 for both configurations). These igniter ports created a fine spray fan directed axially down the chamber, through the fuel spray pattern. The ignition sequence with this igniter configuration was improved, resulting in less thermal maldistribution to the injector during ignition. The original igniter would cause a thermal maldistribution of approximately 100F during the ignition stage, while the new configuration had a maximum maldistribution of approximately 30F. The igniter stage heat load to the injector was also reduced for the new configuration.

## 5.4.3 Test Summary of 200 lbf Elements

The remainder of the hot fire testing of the SSRT engine was conducted with fuel elements designed for 200 lbf equivalent flow rates. These elements( -7, -9, -10 and -11) all have equal slot flow areas, with the number of slots varying from 36 to 60. Performance was improved dramatically over the -8 fuel element, and test reproducibility and performance trend definition was also better. The higher oxidizer flow rate

65

allowed a colder oxidizer inlet temperature, resulting in fewer problems with vapor generation and two phase flow conditions. This was subtantiated by the 20% higher average oxidizer Cd measured during the -7 testing as compared to the -8 element testing, and by the lower oxidizer Cd variation of ±10% for the -7 compared to ±35% for the -8 element.


5.4.3.1  -7 Element Results

Fourteen tests were performed with the -7 element, accumulating 147.3 seconds of hot fire duration. The test data for the -7 element is summarized in Table 5-3. Performance of this element was in the 90% to 92% C* efficiency range. Although the performance was much more repeatable than with the -8 element, there was still some scatter that probably related to the injector and $LO_2$ line pre-chill conditions. Performance was relatively insensitive to flow rates and injector parameters, usually within the scatter of the data points. The -7 element performance verses total flow at fixed gap conditions is shown in Figure 5-4. The performance was essentially unchanged over the entire flow range tested. Performance verses mixture ratio for the same injector gaps is shown in Figure 5-5. A slight increase in performance with increasing mixture ratio is indicated, although the trend is within the data scatter.

The performance trends verses fuel gap and oxidizer gap is presented in Figure 5-6 and 5-7. Again, the trend was slight, indicating  maximum performance at a fuel gap of approximately 0.0020 inch and for an oxidizer gap of 0.0185 inch.

The injector gaps presented here are the gaps set prior to the test based on shim changes. However, differential thermal expansion between the fuel pintle and the oxidizer sleeve caused a post-chill growth of about 0.0040 inch in the fuel gap during the burn. Thus, a set fuel gap of 0.0020 inch resulted in an actual gap of approximately 0.0060 inch during the test. The magnitude of the change was determined by comparing hot fire fuel pressure drops to the water flow data on the fuel injector. A thermal analysis of the injector predicted a gap change of .0035 to .0040 inch based on the sleeve outer diameter being chilled to -280F (from 60F) prior to the run. The expansion of the fuel gap will be minimized in later hardware designs where the shim location is moved from its present location (shown in Figure 5-1) to the end of the sleeve near the fuel extension. This will greatly reduce the free length for thermal expansion.

The oxidizer gap also experienced a gap increase, although the magnitude of the change was more difficult to assess because of differences in injector body chill and $LO_2$ density from test to test. It was also likely that the oxidizer gap

# Table 5-3
## -7 Fuel Element Test Summary

| Test #<br>HA2A- | Duration<br>Sec | O/F | Wt<br>lb/sec | PC<br>psia | C*<br>ft/sec | Fuel<br>Gap (df) | OX<br>Gap (do) |
|---|---|---|---|---|---|---|---|
| 4017 | 11.4 | 0.809 | 0.5814 | 188.0 | 5617 | 0.0019 | 0.0163 |
| 4018 | 11.4 | 0.799 | 0.5802 | 189.1 | 5662 | 0.0019 | 0.0163 |
| 4019 | 11.2 | 0.803 | 0.5776 | 186.0 | 5594 | 0.0019 | 0.0143 |
| 4020 | 11.2 | 0.798 | 0.5814 | 190.2 | 5687 | 0.0019 | 0.0183 |
| 4022 | 12.0 | 0.822 | 0.5861 | 184.4 | 5471 | 0.0000 | 0.0183 |
| 4025 | 10.0 | 0.785 | 0.5733 | 184.8 | 5584 | 0.0034 | 0.0183 |
| 4026 | 10.0 | 0.788 | 0.5789 | 184.2 | 5513 | 0.0019 | 0.0213 |
| 4027 | 10.0 | 0.789 | 0.5773 | 187.0 | 5618 | 0.0019 | 0.0183 |
| 4028 | 10.0 | 0.808 | 0.6400 | 204.8 | 5556 | 0.0019 | 0.0183 |
| 4029 | 10.0 | 0.810 | 0.5824 | 190.2 | 5667 | 0.0019 | 0.0183 |
| 4030 | 10.0 | 0.828 | 0.5394 | 174.2 | 5593 | 0.0019 | 0.0183 |
| 4031 | 10.0 | 0.679 | 0.5673 | 181.2 | 5531 | 0.0019 | 0.0183 |
| 4032 | 10.0 | 0.942 | 0.5729 | 186.2 | 5644 | 0.0019 | 0.0183 |
| 4033 | 10.0 | 0.817 | 0.6009 | 194.0 | 5607 | 0.0019 | 0.0183 |
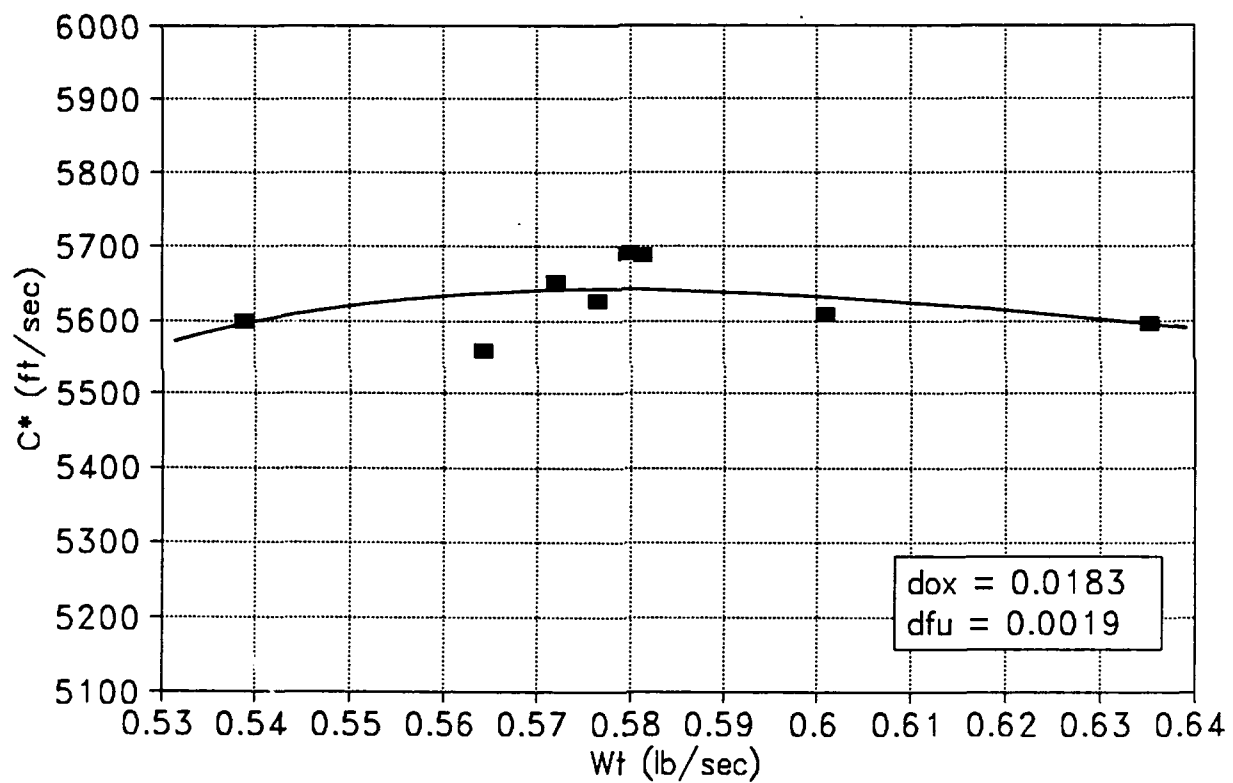
Figure 5-4. -7 element C* verses total flow rate
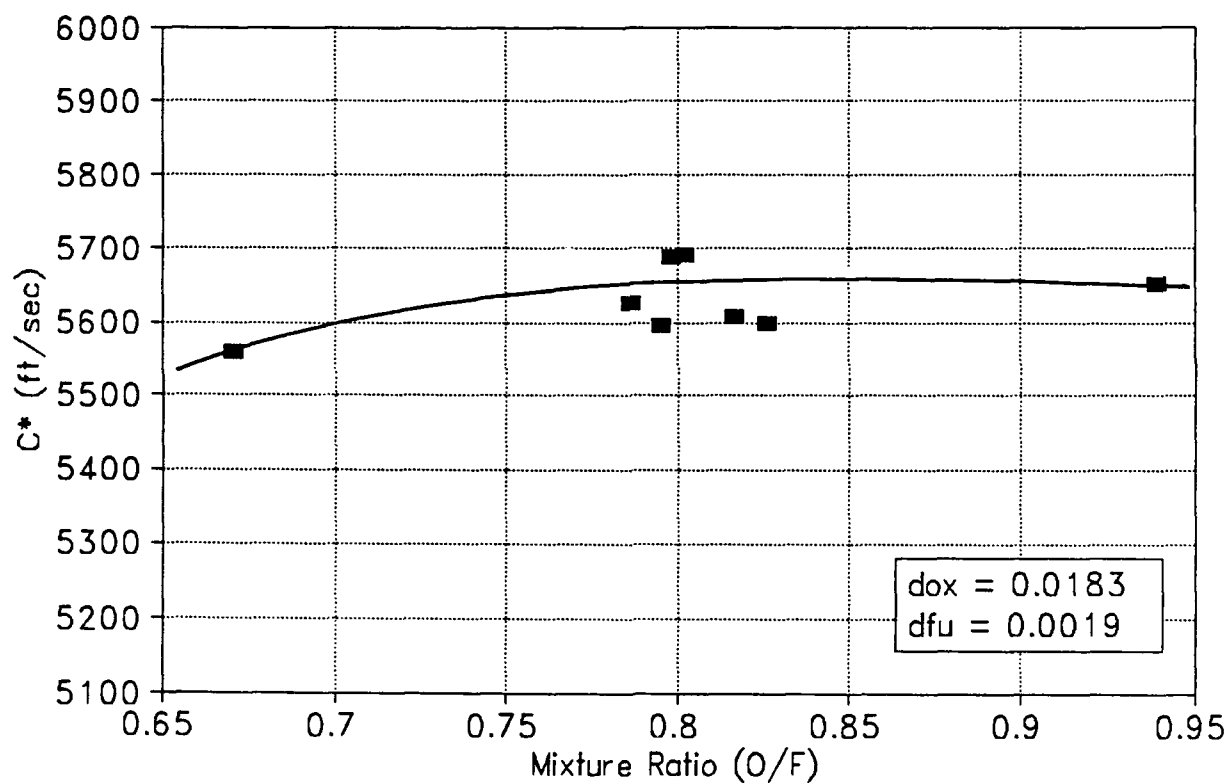
Figure 5-5.    -7 element C* verses mixture ratio
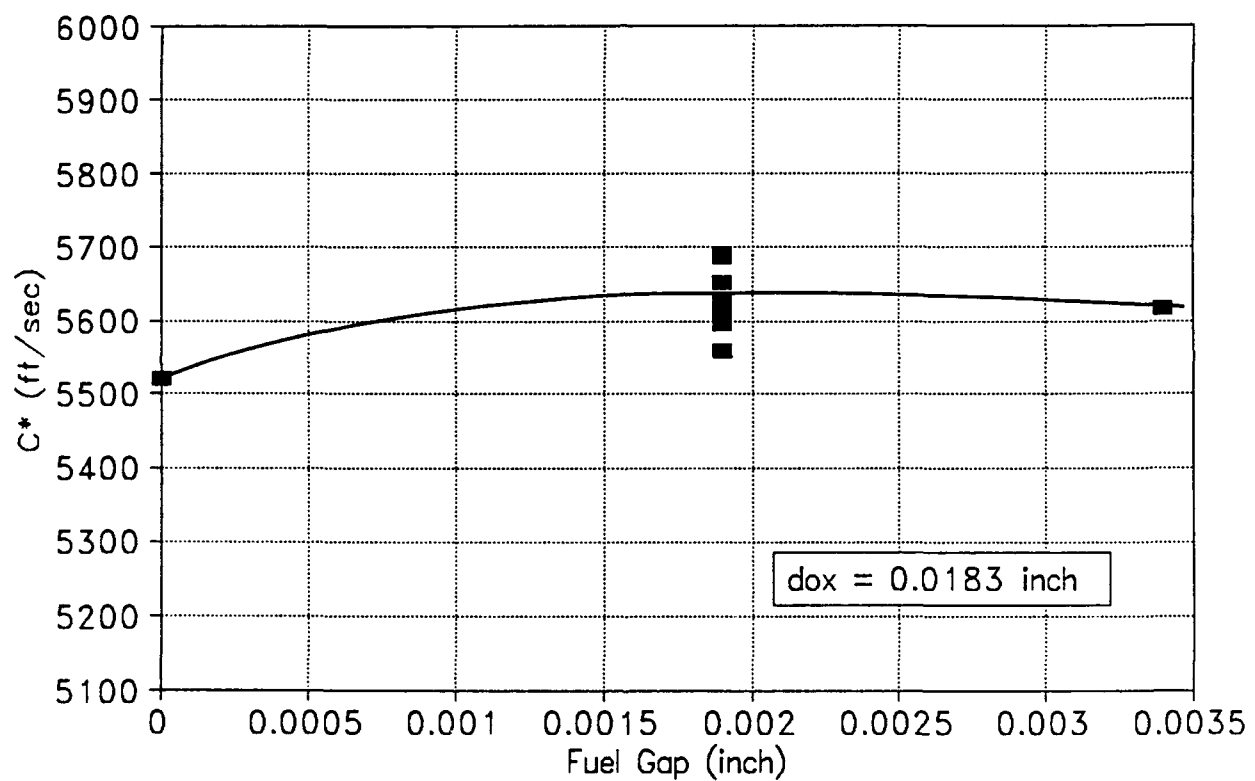
Figure 5-6. -7 element fuel gap performance trend

# SSRT Hot Fire Tests
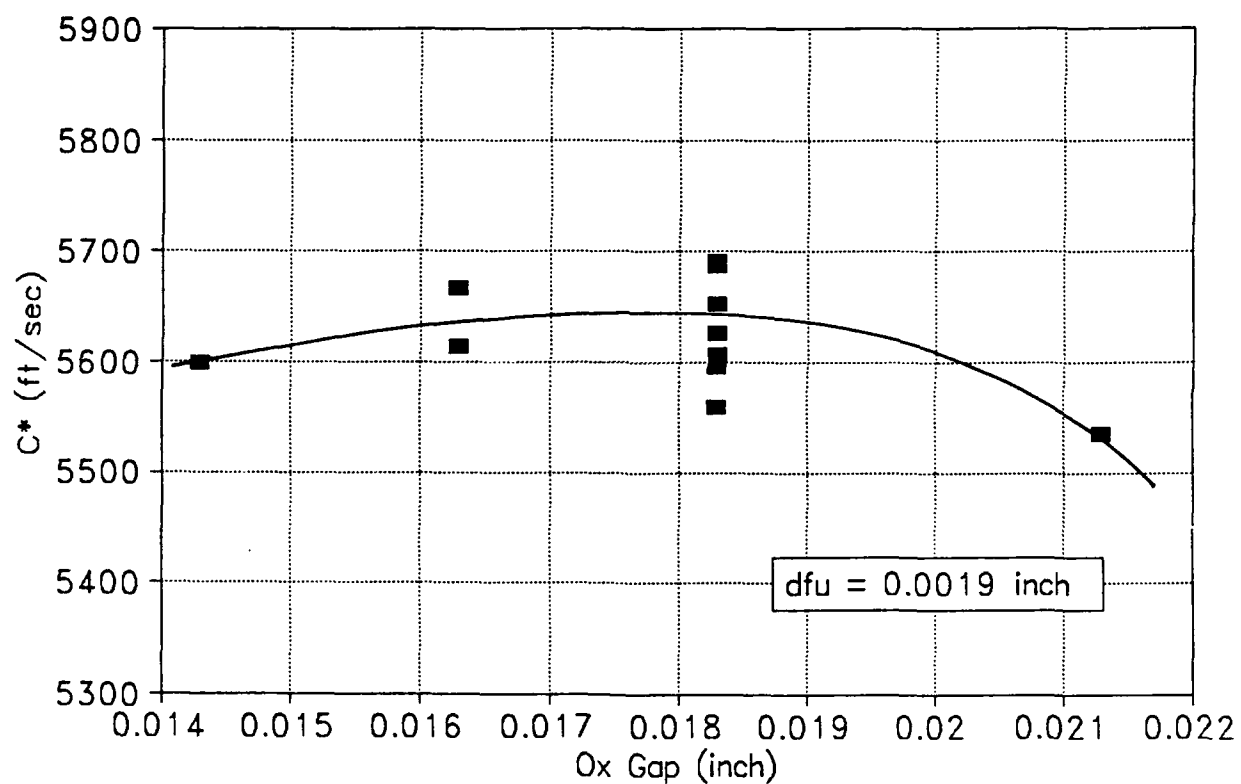## −7 Fuel Element



Figure 5−7.  −7 C* verses oxidizer gap

# SSRT Hot Fire Tests
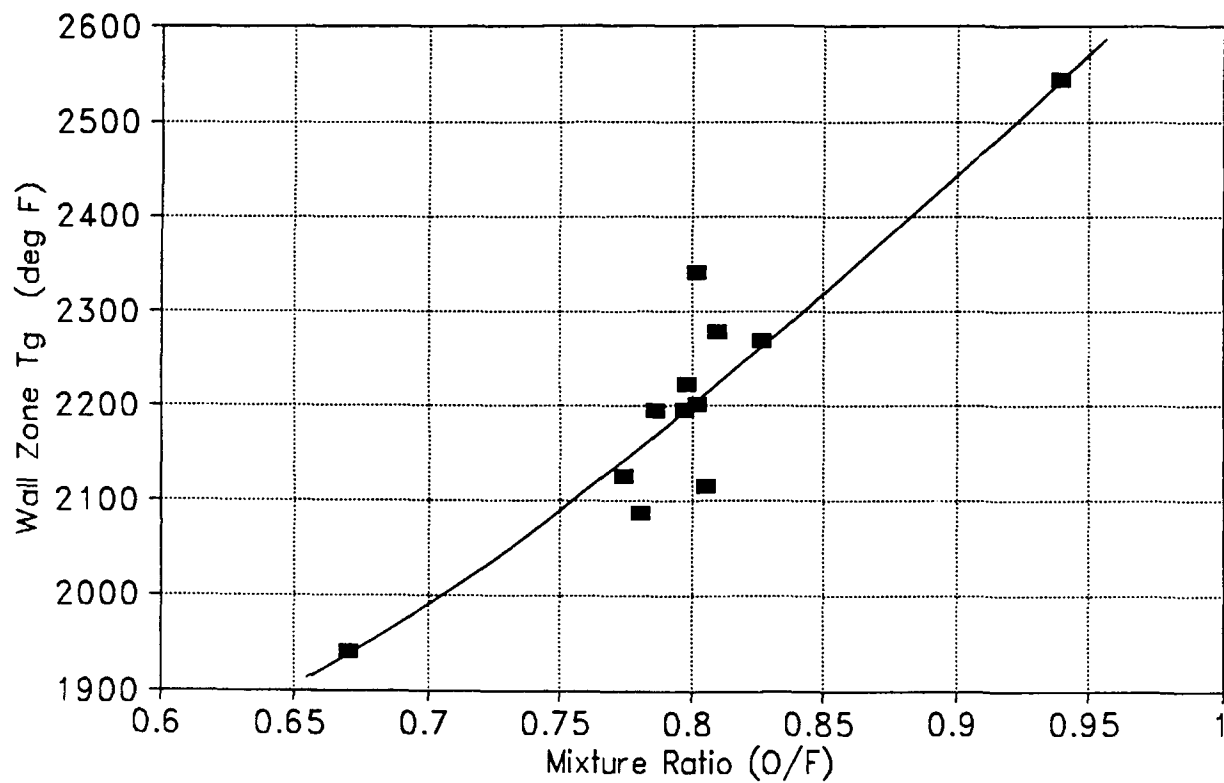## −7 Fuel Element,   Wt = 0.59



Figure 5−8.   Wall Zone Gas Temperature verses mixture ratio

was changing slightly during the test due to the injector body warming up while the injector sleeve remained at the $LO_2$ temperature. Comparing test data to water flow data of the oxidizer delta P indicates an average change in the oxidizer gap of about 0.0020 inch during injector chill, which agrees well with thermal analysis of the injector. With the dome cooling concepts incorporated the oxidizer gap change should be significantly reduced.

Chamber thermocouple data indicated a considerably higher heat load to the chamber for the -7 element compared to the -8. Throat thermocouples were reaching redline temperatures of 1000F in 11 to 12 seconds for the -7 element, while they were below 500F after 15 seconds duration for the -8 element. A trend of increasing chamber heating rate for higher mixture ratios is presented in Figure 5-8. A wall zone gas temperature of about 2500F was calculated by comparing the throat thermocouple data with predictions using the thermal model of the copper chamber. This corresponded to a wall zone mixture ratio of about 0.2, which indicated that steady state operation with a columbium chamber with a comfortable thermal margin is feasible.


5.4.3.2   Test Series Number 2: -9, -10 and -11 Results

After testing and data analysis of the -7 element was completed, three new elements, -9 through -11, were designed and built. These elements were based on the -7 geometry, with modifications to some of the geometrical parameters (see sections 5.3 and 4.1), with emphasis on increasing the fuel vaporization rate.

All previous testing of the SSRT engine demonstrated that the fuel element geometry was the primary factor in engine performance. For all fuel element geometries tested, the engine attained a certain level of performance, and only secondary changes in performance were observed by changing injector and flow parameters (aside from the detrimental effects of two phase flow in the oxidizer circuit). Based on this assessment, the test plan for the last three elements included a limited number of tests for each element. If the element tested didn't indicate increased performance in the range of parameters covered by these tests, the assessment was that no further gap or flow changes would make a significant improvement in performance for that injector geometry.

The hot fire testing performed with the -9, -10 and -11 elements are summarized in Table 5-4. The performance trend verses fuel gap for the three elements (-9, -10 and -11) is presented in Figure 5-9. This trend was similar to that demonstrated by the -7 element, although the -11 element did perform better at larger fuel gaps than the other elements. The -9 and -11 elements matched the -7 performance element

73

# Table 5-4

## -9 Fuel Element Test Summary

| Test # HA2A- | Duration Sec | O/F | Wt lb/sec | PC psia | C* ft/sec | Fuel Gap (df) | OX Gap (do) |
|---|---|---|---|---|---|---|---|
| 4034 | 10.0 | 0.808 | 0.5737 | 184.6 | 5511 | 0.0020 | 0.0185 |
| 4035 | 10.0 | 0.759 | 0.5738 | 187.6 | 5654 | 0.0020 | 0.0185 |
| 4037 | 10.0 | 0.819 | 0.5913 | 189.3 | 5538 | 0.0033 | 0.0185 |
| 4038 | 10.0 | 0.812 | 0.5895 | 192.3 | 5641 | 0.0007 | 0.0185 |
| 4039 | 10.0 | 0.802 | 0.5897 | 190.8 | 5595 | 0.0007 | 0.0140 |
| 4041 | 10.0 | 0.801 | 0.5894 | 185.7 | 5445 | 0.0007 | 0.0210 |

## -10 Fuel Element Test Summary

| Test # HA2A- | Duration Sec | O/F | Wt lb/sec | PC psia | C* ft/sec | Fuel Gap (df) | OX Gap (do) |
|---|---|---|---|---|---|---|---|
| 4042 | 10.0 | 0.783 | 0.5848 | 187.9 | 5555 | 0.0020 | 0.0185 |
| 4043 | 10.0 | 0.801 | 0.5883 | 187.6 | 5517 | 0.0034 | 0.0185 |
| 4044 | 10.0 | 0.795 | 0.5848 | 184.9 | 5470 | 0.0007 | 0.0185 |
| 4045 | 5.0 | 0.807 | 0.5913 | 193.2 | 5609 | 0.0020 | 0.0140 |

## -11 Fuel Element Test Summary

| Test # HA2A- | Duration Sec | O/F | Wt lb/sec | PC psia | C* ft/sec | Fuel Gap (df) | OX Gap (do) |
|---|---|---|---|---|---|---|---|
| 4046 | 10.0 | 0.791 | 0.5848 | 190.9 | 5647 | 0.0018 | 0.0185 |
| 4047 | 10.0 | 0.809 | 0.5917 | 194.9 | 5710 | 0.0033 | 0.0185 |
| 4048 | 10.0 | 0.798 | 0.5878 | 189.1 | 5572 | 0.0045 | 0.0185 |
| 4049 | 5.0 | 0.800 | 0.5932 | 198.9 | 5769 | 0.0033 | 0.0140 |
| 4050 | 6.2 | 0.808 | 0.5935 | 197.0 | 5708 | 0.0033 | 0.0160 |
| 4052 | 9.8 | 0.802 | 0.5881 | 187.9 | 5534 | 0.0033 | 0.0120 |
| 4053 | 8.6 | 0.651 | 0.5894 | 193.6 | 5672 | 0.0033 | 0.0140 |
| 4054 | 5.0 | 0.923 | 0.6062 | 202.1 | 5741 | 0.0033 | 0.0140 |
| 4055 | 6.2 | 0.821 | 0.5944 | 197.4 | 5723 | 0.0033 | 0.0140 |

# SSRT Hot Fire Tests
## MR=0.8,  Wt = 0.58
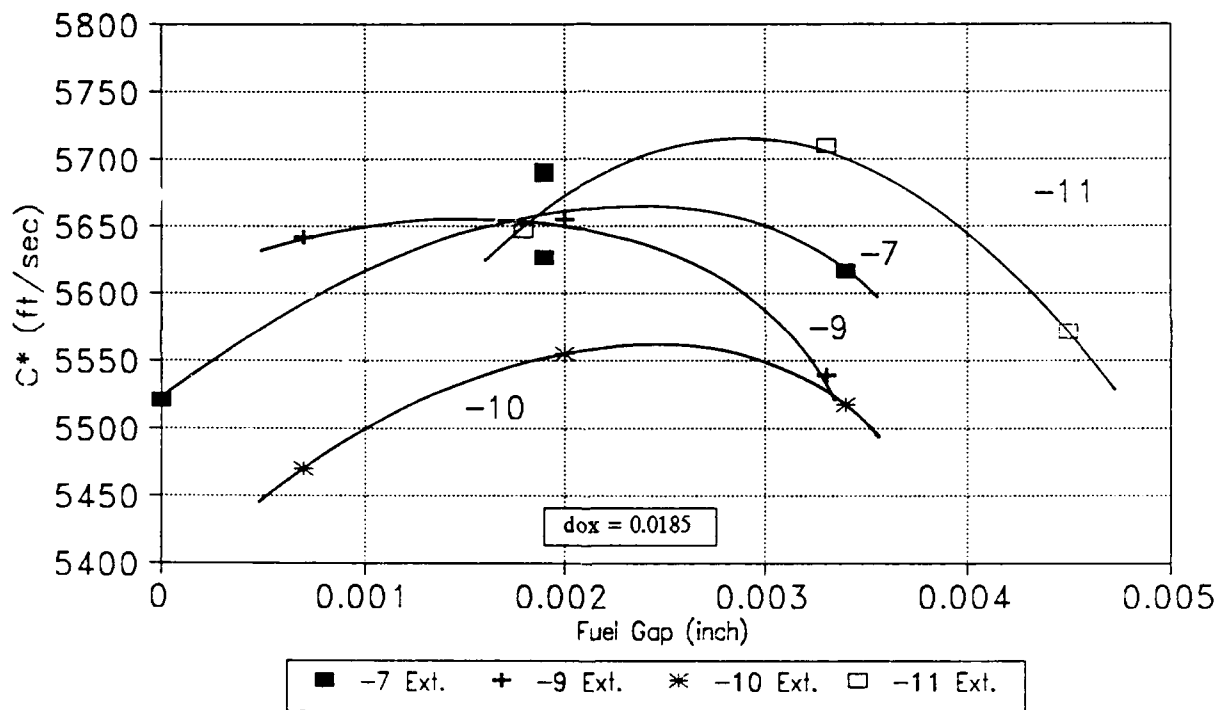


Figure 5-9.  C* verses fuel gap for 200 lbf elements

closely, but the -10 element operated at a lower performance level. This demonstrated that high slot aspect ratio was not the key to higher performance.

The performance of the elements verses oxidizer gap at the nominal flow conditions is shown in Figure 5-10. Once again the -9 element showed the same performance trend as the -7, preferring the 0.0185 oxidizer gap. The -10 and -11 elements demonstrated higher performance at smaller oxidizer gaps. The -11 element was tested at the 0.0120 inch oxidizer gap, but the performance decreased dramatically at this condition. Uneven injector dome heating and unsteady chamber pressure during this test indicated that there may have been a problem with the oxidizer injection distribution.

A mixture ratio survey was conducted with the -11 element at the 0.0033 inch fuel gap and the 0.0140 oxidizer gap. The results of this survey, Figure 5-11, indicated a trend of increasing performance with mixture ratio, similar to the -7 element. Performance verses injector momentum ratio is shown in Figure 5-12. A general trend of increasing performance with higher momentum ratio was observed for all the elements, with the exception of the test with highest oxidizer velocity (do = 0.0120) as discussed above.

Chamber heating rates for the -9 through -11 elements were very similar to the -7 element, but the injector dome heating rate was very rapid with the -11 element, especially at smaller oxidizer gaps. At a 0.0140 inch oxidizer gap and high mixture ratio, the injector dome reached the 500F red line temperature in about five seconds. The dome thermal distribution was uneven, with a higher heating rate on one side of the injector.


5.4.3.3   -11 Hybrid Results

The combination of relatively low wall zone mixture ratio and increasing performance trends at higher over all mixture ratios led to the conclusion that the core combustion zone of the engine was operating at a high mixture ratio. This assessment was also confirmed by the Priem model of the injector. A simple two-zone performance analysis indicated that if the wall zone was at a mixture ratio of 0.2, the core mixture ratio was approximately 1.3. Since the theoretical optimum mixture ratio for this propellant combination is approximately 0.73, the assessment was made that a significant increase in performance could be gained if more fuel could be directed into the core combustion zone, decreasing the core mixture ratio toward optimum. This would also result in increased performance at a lower over all mixture ratio.

Increasing the fuel flow to the combustion core zone was the reasoning behind the hybrid injector. A spare pintle was
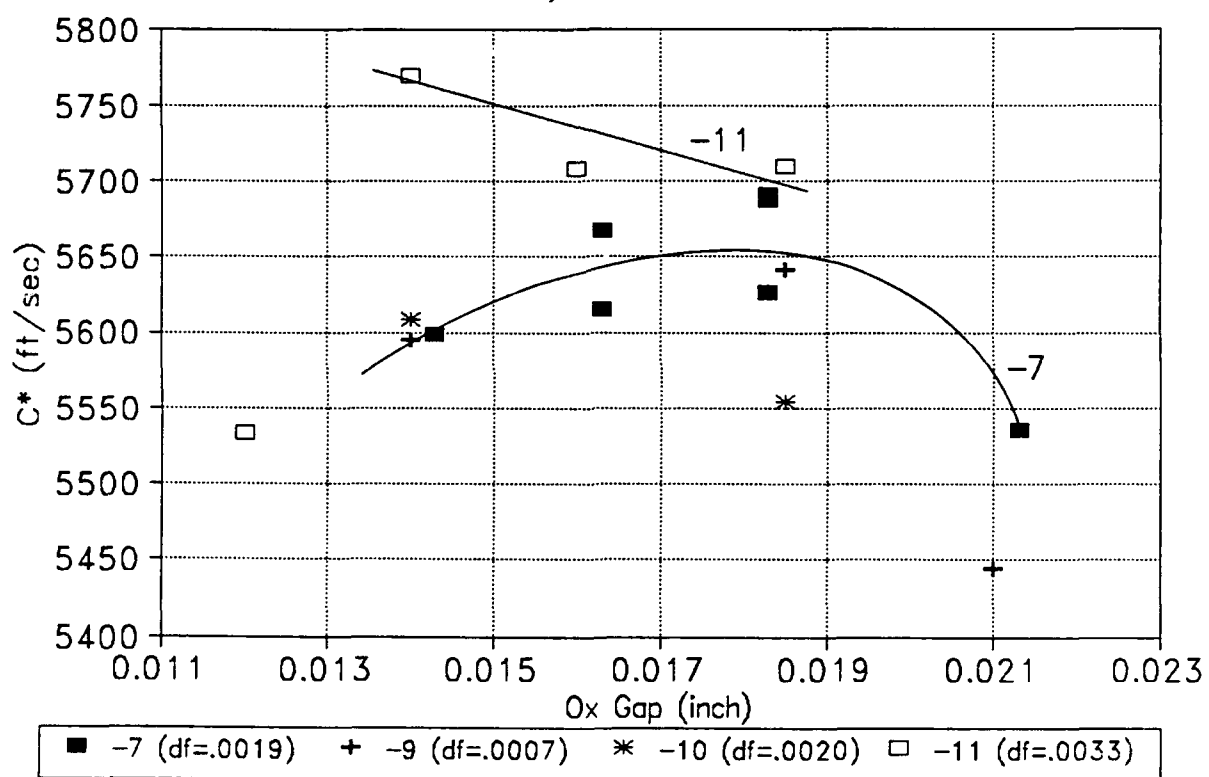
Figure 5-10.  C* verses oxidizer gap for 200 lbf elements
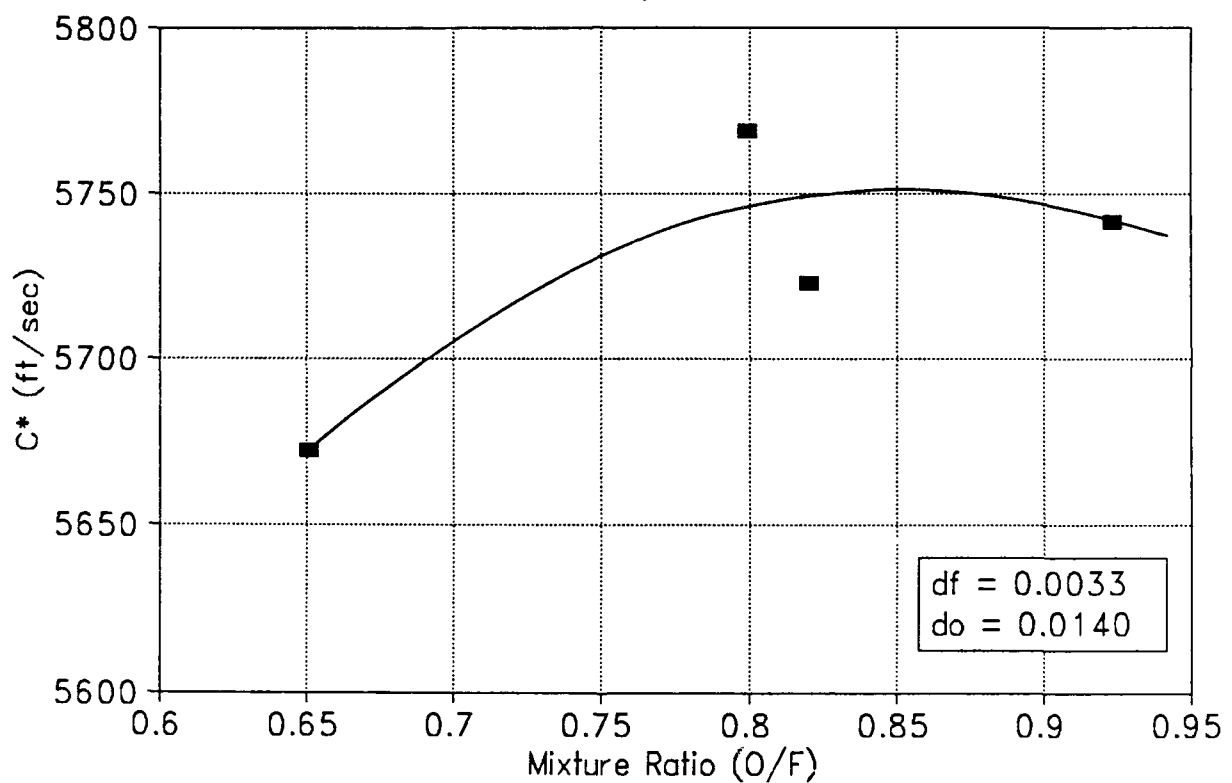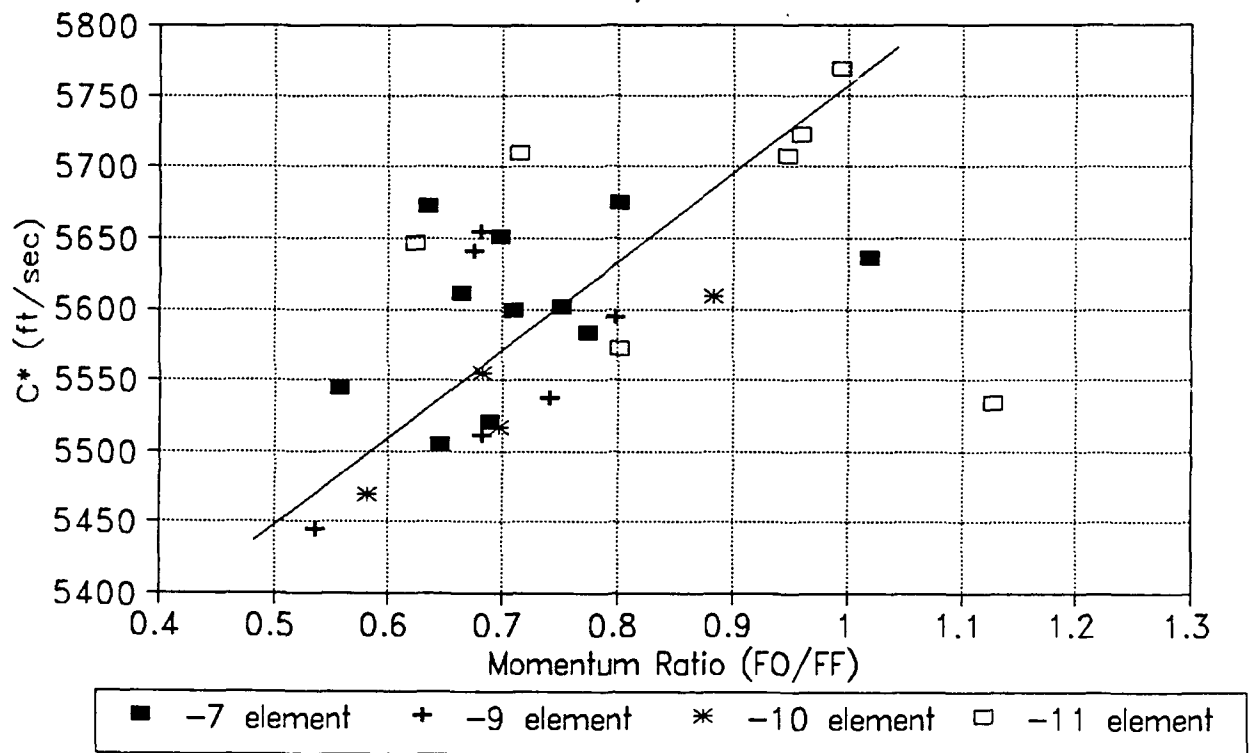
Figure 5-11.  -11 element C* verses mixture ratio

Figure 5-12. C* performance verses Momentum Ratio

modified by drilling three like-on-like doublets into the tip, yielding a hollow cone spray pattern oriented axially down the centerline of the chamber.  Figure 5-13 shows the pintle tip with the doublets installed.  The doublets were designed to direct about 10% of the total fuel flow into the core.  This pintle was tested with the -11 element, since this element gave the highest performance.

The performance summary for the -11 hybrid injector is presented in Table 5-5.  C* efficiencies over 95% of theroretical (ODK) were obtained, corresponding to a projected vacuum Isp of >340 lbf-sec/lbm.  However, as discussed below, problems with oxidizer injector delta P variations prevented a complete characterization of the injector.

The performance trend of the hybrid injector compared to the basic -11 element tests is shown in Figure 5-14.  At a mixture ratio of 0.8, performance of the two injectors was approximately equal.  As the mixture ratio was decreased by increasing the fuel flow rate, the performance of the hybrid injector increased, producing the highest performance at a mixture ratio of 0.70.  Decreasing the mixture ratio even further, however, caused variations in the oxidizer delta P that resulted in operation at a lower performance level.  The onset of this condition appeared primarily at low mixture ratios, even though the oxidizer flow conditions were essentially unchanged from other higher mixture ratio tests where the condition was not observed.

Post test examination of the oxidizer metering geometry revealed a contour downstream of the minimum area that could allow the oxidizer to diffuse to a lower velocity with attendant pressure recovery.  Apparently the attachment of the oxidizer to this surface was not complete, resulting in variations in the injection delta P.  All future SSRT injector hardware will incorporate  modifications to the oxidizer metering geometry to eliminate this condition.

The throat wall zone gas temperature verses momentum ratio for all of the 200 lbf elements is presented in Figure 5-15.  This was derived from the chamber thermal model.  The gas temperature increased with momentum ratio for all of the elements except for the hybrid injector, where the data was distorted by the oxidizer delta P variations discussed above.  The -7 element had the lowest gas temperatures at a given momentum ratio, even though it had equivalent or even higher performance than the -9 and -10 elements.

Dome and chamber thermocouple heating rates during testing with the hybrid injector were about 20% higher than with the -11 element testing.  This was expected, since the hybrid pintle diverted some of the fuel flow from the wall zone to the core, resulting in a higher wall zone mixture ratio.  It also created a higher effective momentum ratio (oxidizer to

## Table 5-5
### -11 Hybrid Element Test Summary

| Test # HA2A- | Duration Sec | O/F | Wt lb/sec | PC psia | C* ft/sec | Fuel Gap (df) | OX Gap (do) |
|---|---|---|---|---|---|---|---|
| 4056 | 5.4 | 0.794 | 0.5864 | 193.2 | 5672 | 0.0033 | 0.0140 |
| 4057 | 5.0 | 0.724 | 0.6201 | 207.9 | 5769 | 0.0033 | 0.0140 |
| 4058 | 7.8 | 0.796 | 0.5872 | 194.7 | 5732 | 0.0010 | 0.0140 |
| 4059 | 5.0 | 0.733 | 0.6214 | 207.0 | 5739 | 0.0010 | 0.0140 |
| 4060 | 6.6 | 0.712 | 0.6146 | 204.4 | 5743 | 0.0021 | 0.0140 |
| 4061 | 7.2 | 0.702 | 0.6388 | 216.2 | 5858 | 0.0021 | 0.0140 |
| 4062 | 7.4 | 0.674 | 0.6474 | 215.5 | 5764 | 0.0021 | 0.0140 |
| 4063 | 5.8 | 0.728 | 0.6375 | 214.5 | 5807 | 0.0021 | 0.0140 |
| 4064 | 8.8 | 0.685 | 0.6588 | 210.1 | 5531 | 0.0021 | 0.0140 |
| 4065 | 8.2 | 0.717 | 0.6424 | 204.9 | 5510 | 0.0033 | 0.0140 |
| 4066 | 6.2 | 0.720 | 0.5902 | 196.5 | 5737 | 0.0021 | 0.0140 |
| 4067 | 9.8 | 0.675 | 0.5931 | 193.4 | 5613 | 0.0021 | 0.0140 |

HYBRID PINTLE MODIFICATION
WITH THREE FUEL DOUBLETS

Ø0.020
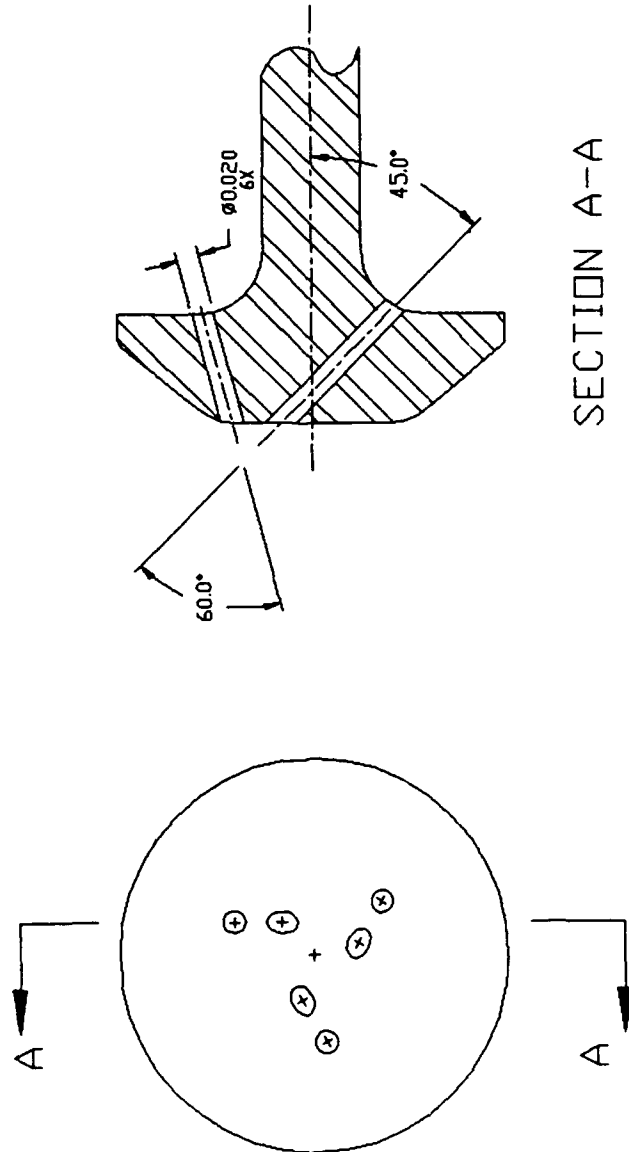6X

45.0°

60.0°

SECTION A-A
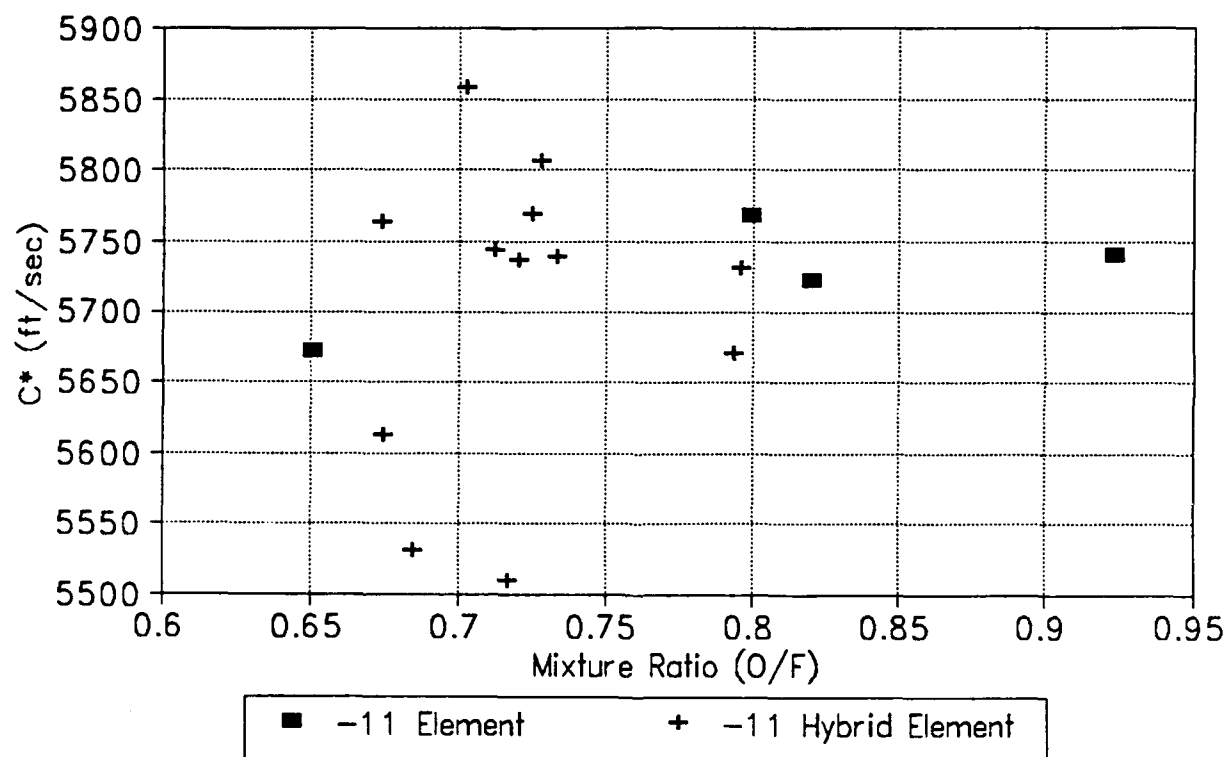
A

A

Figure 5-13. Hybrid Pintle.

Figure 5-14.  Hybrid injector compared to basic -11 injector

# SSRT Hot Fire Tests
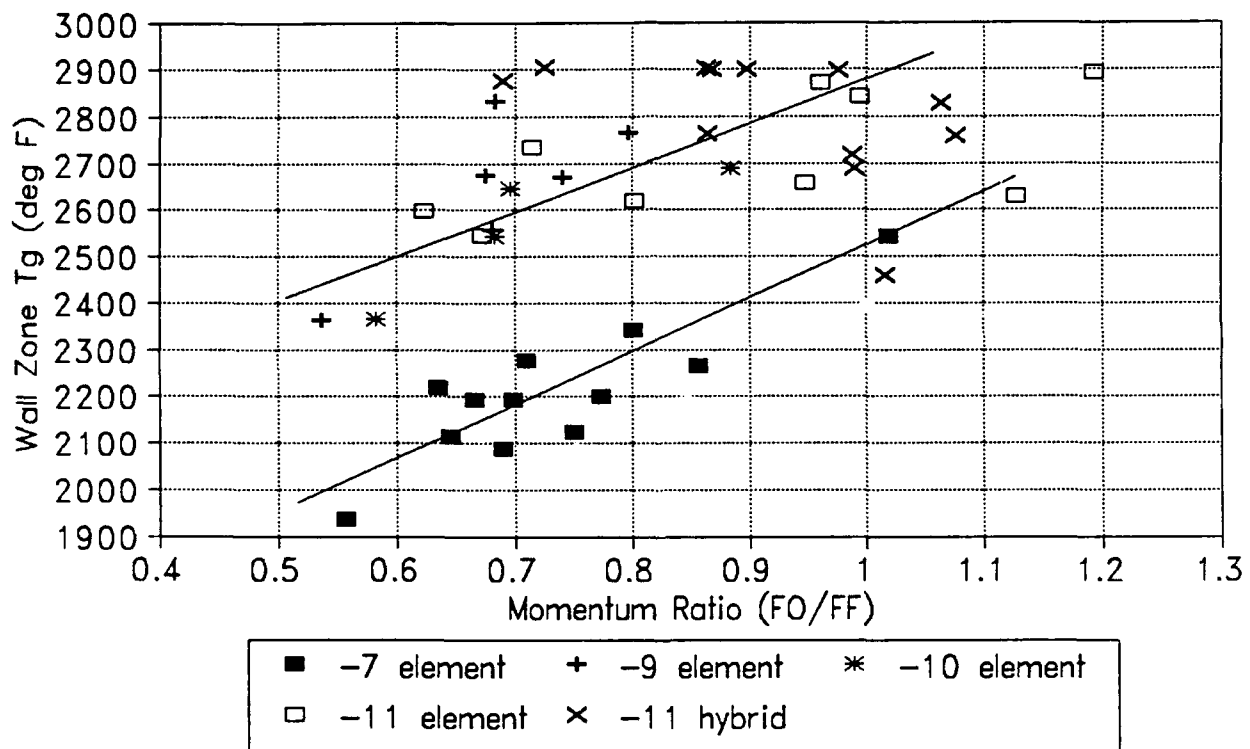## Chamber Thermal Environment



Figure 5-15.   Wall Zone Gas Temperature verses momentum ratio

fuel) at the primary impingement point, which caused a hotter dome heating condition.  As discussed in section 4, analysis of thermocouple data from the highest performing tests (HA2A-4061 and 4063) indicated that operation with a columbium thrust chamber at a maximum steady state temperature of 2500F is feasible.

The heat load to the injector during testing with the -11 hybrid element was too high to allow steady state operation of the engine in the current configuration (see section 4.2.1).  Analysis indicated that the oxidizer will experience film boiling in the injector, leading to an unacceptable thermal condition.  Additional work is needed with injector cooling concepts to reduce the heat load into the oxidizer main flow.

Post test hardware condition was excellent, with no signs of excessive heating or distortion.  The copper chamber was in excellent condition, with no signs of damage or erosion.


5.5 Test Conclusions

Overall, the exploratory test series of the SSRT was very successful.  A total of 76 tests was performed, accumulating over 700 seconds of hot fire duration.  The performance goal of a vacuum specific impulse (Isp) of >340 lbf-second/lbm ($\epsilon$ = 204) was demonstrated, while maintaining a wall environment compatible with long duration operation of a radiation cooled columbium thrust chamber.  The thermal load to the injector was defined, yielding information for the design of a thermally adequate injector in the next program option.  Reliable ignition and stable operation of the engine was demonstrated.

Testing of an injector fuel element geometry that yielded high performance with hypergolic propellants resulted in a lower level of performance with the $LO_2/N_2H_4$ combination. Significant differences in operating characteristics between the hypergolics and $LO_2/N_2H_4$ were observed.  Also, it was found that operation at lower flow rates (F = 125 lbf) resulted in difficulties in attaining single phase liquid oxygen flow to the engine.

Testing at the 200 lbf thrust equivalent flow rate allowed more control over the $LO_2$ inlet temperature, allowing single phase flow and improved injector cooling for short duration testing.  The results of the testing with five 200 lbf injector element configurations indicated that the fuel element geometry is the primary performance driver for this engine.  The engine was relatively insensitive to other injection parameters such as total flow and injection velocities, especially compared to the hypergolic engines.

85

The results of the testing indicated that an increased number of fuel slots resulted in highest performance. The smaller slots produced a finer drop size, resulting in better vaporization of the fuel.

Although significant accomplishments were achieved in this test series, additional development is required. A method of cooling the injector to allow steady state thermal operation of the engine is required. The impacts of the injector cooling approach on performance must be assessed. More extensive performance mapping of the injector is required, as well as the demonstration of long duration operation.

## 6.0 TEST PLANS

A preliminary logic plan was developed for Option 1 of the SSRT Program. This logic plan is shown in Figure 6-1.

### 6.1 Option 1

The major emphasis on the Option 1 program is evaluation of of the most promising methods of dome cooling for determination of the effectiveness of these concepts and their impact on performance and thrust chamber wall temperatures. A preliminary design of the injector integrating the cooling concept for generation of maximum performance will be accomplished at the conclusion of Option 1.

New injector hardware will be designed using a thermally isolated dome. This dome is designed to have the capability of using replaceable auxiliary sections incorporating thermal blockage and film cooling dome cooling concepts.

Pintle, sleeve, oxidizer gap and fuel gap changes are incorporated into the injector design similarly to the Basic program design. This injector is designed and manufactured to allow for wide flexibility of testing in a cost effective manner. In addition a study will be conducted to assess ignition methods so it can be incorporated into the preliminary design.

Testing will be accomplished in the same test cell as the Basic program tests (HA2A). The preliminary logic matrix is presented in Figure 6-2. The detailed test plan will be prepared upon completion of design. The test program is configured to obtain the data required to determine the dome cooling concept for integration into the Option 2 injector. The test program will utilize two injector elements and test varying oxidizer ($\delta_o$) and fuel ($\delta_f$) gaps and mixture ratio (O/F) and total flow ($W_T$). Analysis of the test data with correlations of performance and thermal considerations will be generated to allow an understanding for further design and test.

A preliminary design of an injector integrating the best cooling concept and the high performance mechanisms will be accomplished by the completion of the Option 1 program. The basis of the Option 2 detailed design will be provided by this preliminary design developed based on the test results of Option 1.

Figure 6-1.

SSRT PROGRAM LOGIC

OPTION 1
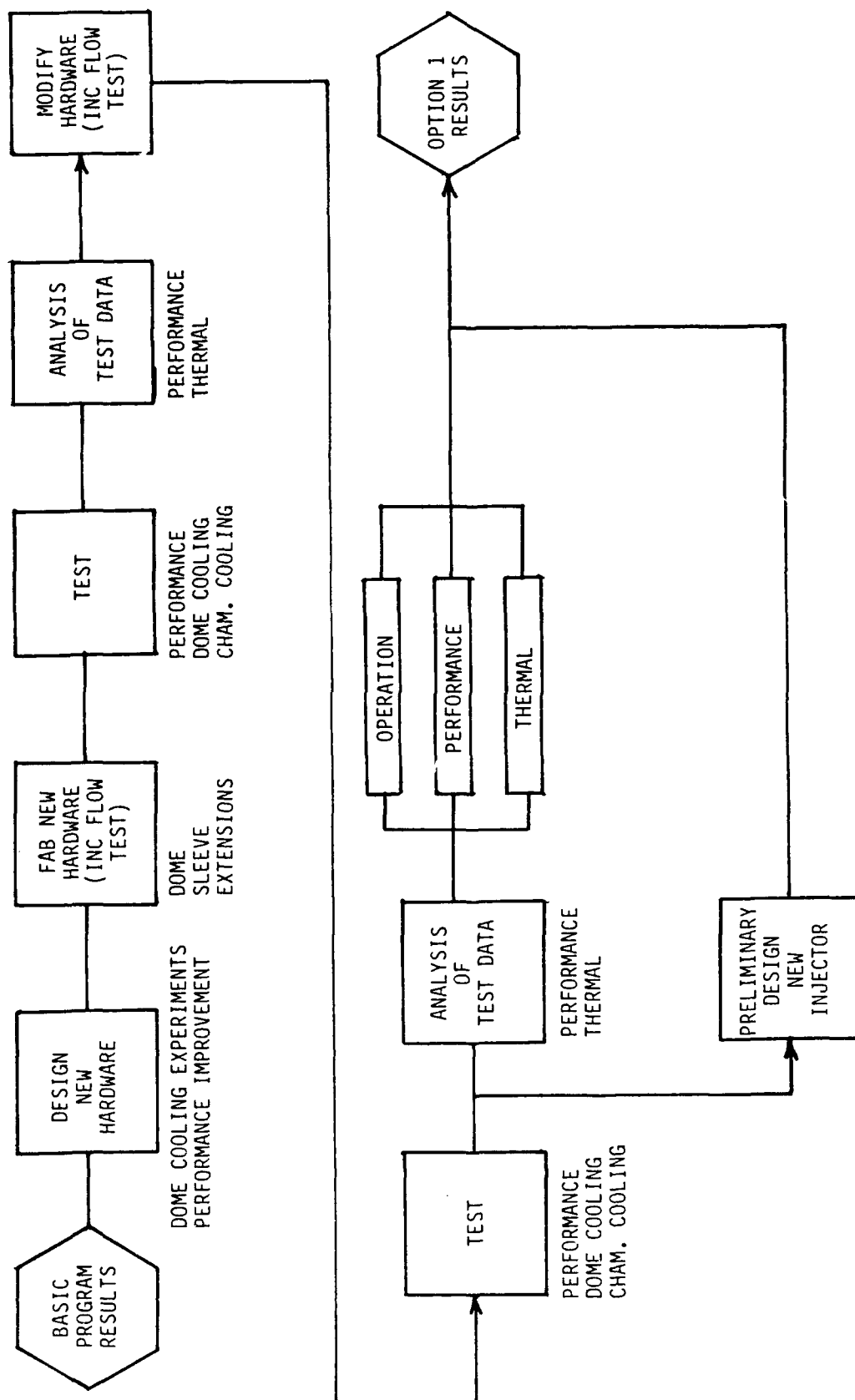
Figure 6-2.

OPTION 1 TEST LOGIC

(Preliminary)



OBJECTIVE: Determine dome cooling
concept for integration
into Option 2 injector.

RESULTS OF TESTS:

Performance - Effects of $\delta_o$, $\delta_f$, O/F,
$W_T$, % F.C. on various elements.

Dome Cooling - Dome Temps ($T_D$)
sensitivity to $\delta_o$, $\delta_f$, O/F, $W_T$,
% F.C.

Chamber Cooling - Chamber Temps ($T_C$)
sensitivity to $\delta_o$, $\delta_f$, O/F, $W_T$,
% F.C. to predict $T_{gas}$.
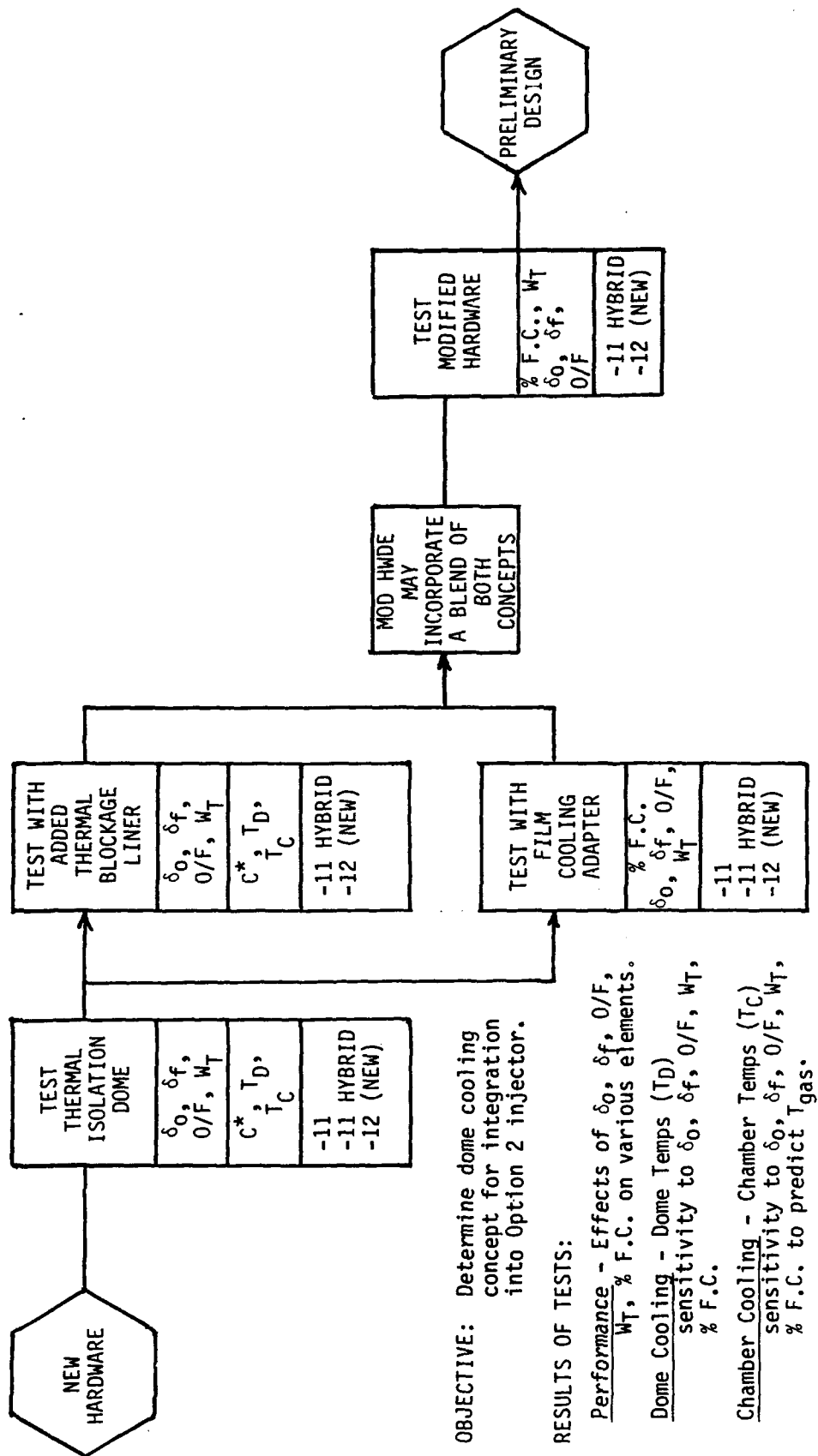
## 7.0 CONCLUSIONS

Several conclusions were reached as a result of completion of the basic SSRT program.

● The greatest potential usage for the Space Storable engine is utilization as an advanced dual mode apogee/perigee engine in a dual mode propulsion system for placement and maintenance of satellites in GEO. The best propellant combination to achieve this usage is $LO_2$-$N_2H_4$ as it provides the best system/engine capability including maximization of payload into orbit and achieved the best overall rating of the characteristics of the fuels evaluated.

● Thermal and performance analyses indicated that high performance of 340 lbf-sec/lbm ($\epsilon$ = 204) could be achieved with operation in a columbium thrust chamber.

● Testing confirmed the analyses. Six injector geometries indicated the need to redesign the injector dome to prevent two-phase $LO_2$. The testing demonstrated that high performance (95% $c^*$)(Isp $\geq$ 340 lbf-sec/lbm with $\epsilon$ = 204) could be achieved and that operation in a columbium thrust chamber is feasible. The use of a rhenium thrust chamber is another alternative which would allow even higher performance (approaching 97% $c^*$ to yield Isp $\rightarrow$ 350 lbf-sec/lbm).

## 8.0 RECOMMENDATIONS

The major recommendation based upon the basic program results is to continue the development of the $LO_2$-$N_2H_4$ Space Storable engine with Option 1. The emphasis on the Option 1 program is resolving the dome heating issues by incorporating dome cooling concepts and evaluation of these concepts by test to determine cooling capability and its impact on performance. Ignition concepts should also be studied to determine the concept to be incorporated into the integrated injector of Option 2. The output of the Option 1 program should be the preliminary design of the best cooling concept in the injector providing maximum performance.

The recommendations for the Option 2 and Option 3 programs are to complete development of the Space Storable engine to allow verification and qualification beyond Option 3. The recommendation for the Option 2 program is to develop the integral injector incorporating high performance and dome cooling and demonstrate its characteristics by test. The results of the Option 2 program are factored into Option 3. The recommendation for the Option 3 program is to develop a flight-type engine and demonstrate its characteristics by test prior to shipment to NASA-LeRC.

# REPORT DOCUMENTATION PAGE

Public reporting burden for this collection of information is estimated to average 1 hour per response, including the time for reviewing instructions, searching data sources, gathering and maintaining the data needed, and completing and reviewing the collection of information. Send comments regarding this burden estimate or any other aspect of this collection of information, including suggestions for reducing this burden, to Washington Headquarters Services, Directorate for information Operations and Reports, 1215 Jefferson Davis Highway, Suite 1204, Arlington, VA 22202-4302, and to the Office of Management and Budget, Paperwork Reduction Project (0704-0188), Washington, DC 20503.

| 1. AGENCY USE ONLY (Leave blank) | 2. REPORT DATE<br>12 May 1992 | 3. REPORT TYPE AND DATES COVERED<br>Final Contractor Report |
|---|---|---|

**4. TITLE AND SUBTITLE**
Space Storable Rocket Technology
Final Report - Basic Program

**5. FUNDING NUMBERS**
WU-
Contract NAS 3-26246

**6. AUTHOR(S)**
Melvin L. Chazen     A. Ramon Casillas
Thomas Mueller     David Huang

**7. PERFORMING ORGANIZATION NAME(S) AND ADDRESS(ES)**
TRW Space & Technology Group
Applied Technology Division
One Space Park
Redondo Beach, CA

**8. PERFORMING ORGANIZATION REPORT NUMBER**
E-    None

**9. SPONSORING/MONITORING AGENCY NAMES(S) AND ADDRESS(ES)**
National Aeronautics and Space Administration
Lewis Research Center
Cleveland, Ohio 44135-3191

**10. SPONSORING/MONITORING AGENCY REPORT NUMBER**
NASA CR- 189131

**11. SUPPLEMENTARY NOTES**
Project Manager - Mr. James A. Biaglow
Space Propulsion Technology Division
NASA-Lewis Research Center

**12a. DISTRIBUTION/AVAILABILITY STATEMENT**
Unclassified - Unlimited
Subject Category

**12b. DISTRIBUTION CODE**

**13. ABSTRACT (Maximum 200 words)**

The Space Storable Rocket Technology Program (SSRT) was conducted for NASA-LeRC by TRW to establish a technology base for a new class of high performance and long-life bipropellant engines using space storable propellants. The results of the initial phase of this systematic multi-year program are described. Task 1 evaluated several characteristics for a number of fuels to determine the best space storable fuel for use with $LO_2$. The results of this task indicated that $LO_2$-$N_2H_4$ is the best propellant combination and provides the maximum mission/system capability-maximum payload into GEO of satellites. Task 2, Preliminary Design, developed two models-performance and thermal. The performance model indicated the performance goal of specific impulse $\geq$ 340 seconds ($\epsilon$ = 204) could be achieved. The thermal model was developed and anchored to hot fire test data. Task 3, Exploratory Test, consisted of design, fabrication and testing of a 200 lbf thrust test engine operating at a chamber pressure of 200 psia using $LO_2$-$N_2H_4$. A total of 76 hot fire tests were conducted demonstrating performance > 340 seconds ($\epsilon$ = 204) which is a 25 second specific impulse improvement over the existing highest performance flight apogee type engines.

**14. SUBJECT TERMS**
Rocket engines, Satellite propulsion, Bipropellant engines, Space storable, High performance engines, Long life engines.

**15. NUMBER OF PAGES**

**16. PRICE CODE**
A05

| 17. SECURITY CLASSIFICATION OF REPORT | 18. SECURITY CLASSIFICATION OF THIS PAGE | 19. SECURITY CLASSIFICATION OF ABSTRACT | 20. LIMITATION OF ABSTRACT |
|---|---|---|---|
| Unclassified | Unclassified | Unclassified | SAR |

NSN 7540-01-280-5500

Standard Form 298 (Rev. 2-89)
Prescribed by ANSI Std. Z39-18
298-102

**TRW Applied Technology
Division**
Space & Technology Group

One Space Park
Redondo Beach, CA 90278
310 812 4321

SN 56372
25 June 1992
SSRT-022

National Aeronautics and Space Administration
Lewis Research Center
21000 Brookpark Road
Cleveland, Ohio  44135

Attention:    Mr. James Biaglow, MS SPTD-1
              Project Manager

Subject:      Contract NAS 3-26246
              Space Storable Rocket Technology (SSRT)
              Basic Program Final Report Errata

Dear Mr. Biaglow:

Enclosed is page 45a of the Final Report for the SSRT Basic
Program which was omitted from the report.  This page is
being distributed to the receivers of the Final Report.

Sincerely,

*Melvin L. Chazen*

Melvin L. Chazen
Program Manager - SSRT

MC:sc
CC:  Saundra R. Hill, 01/1040

TRW Inc

initial effective gas temperature was the same as of test -4000 (1650°F) but the steady-state value decreased to only 1300°F (Figure 4-10). Local film coefficients on the gas side were the same as for test -4000. Resulting heat flows are shown in Figure 4-11. For a 400°F dome (~ 10 secs. into the run, Figure 4-8), the $LO_2$ would have to remove 1.7 Btu/sec in the present injector design. The $LO_2$ was able to absorb only ~ 0.5 Btu/sec due in part to film boiling over a considerable cooling area.

- **High Performance.** Test number, HA2A-4061, with a different injector element and at a higher pressure than -4000 and -3999, had high performance (95.1% C*). Measured vs. calculated dome and neck temperatures for this case are shown in Figure 4-12 and 4-13 respectively. The imposed gas temperature is shown in Figure 4-14. Reflecting an improved ignition design, the initial temperature was 1300°F for -4000 and -3999). Steady-state gas temperature, however, doubled to 2600°F. Gas-side film coefficients for zones 1 and 2 (see Figure 4-3) were an order of magnitude higher then over the rest of the area, but approximately the same as those used for zone 1, tests -4000 and -3999. Corresponding heat flows are shown in Figure 4-15. For a dome temperature of 400°F (about 4 secs. into test), the $LO_2$ would have to absorb 4 Btu/sec to stabilize the temperatures. The onset of film boiling was clearly seen in the sharp decrease in the heat absorbed by the $LO_2$ at 7 seconds.

The above results indicated boiling of $LO_2$ in the injector passage will be difficult to prevent in the present configuration. Therefore, preliminary investigations were conducted to identify various methods of avoiding film boiling. Table 4-2 presents these concepts including advantages and disadvantages/concerns. Further evaluation of the best of these concepts and critical experiments will be conducted in Option 1 to assess their capabilities prior to incorporation into the design.

4.2.2   Thrust Chamber Thermal Analyses

Thermal analyses were conducted to assess the wall temperatures of the thrust chamber using the high performance tests with the -11 hybrid element. The results are shown in Figures 4-16 and 4-17 which indicate a wall zone combustion gas temperature of 2900°F. Using a columbium thrust chamber coated with R512E silicide coating, the maximum temperature is 2444°F (outside) and 2573°F (inside) which is slightly upstream of the throat. The throat temperatures are 2553°F